The role and dynamics of DNA catenation in sister chromatid cohesion

Alejandro Mateos Martín

New College

University of Oxford

Thesis submitted for the degree of Master of Science by Research in Biochemistry

Supervisor: Dr Madhusudhan Srinivasan

Thesis word count: 23,771

Graphical Abstract

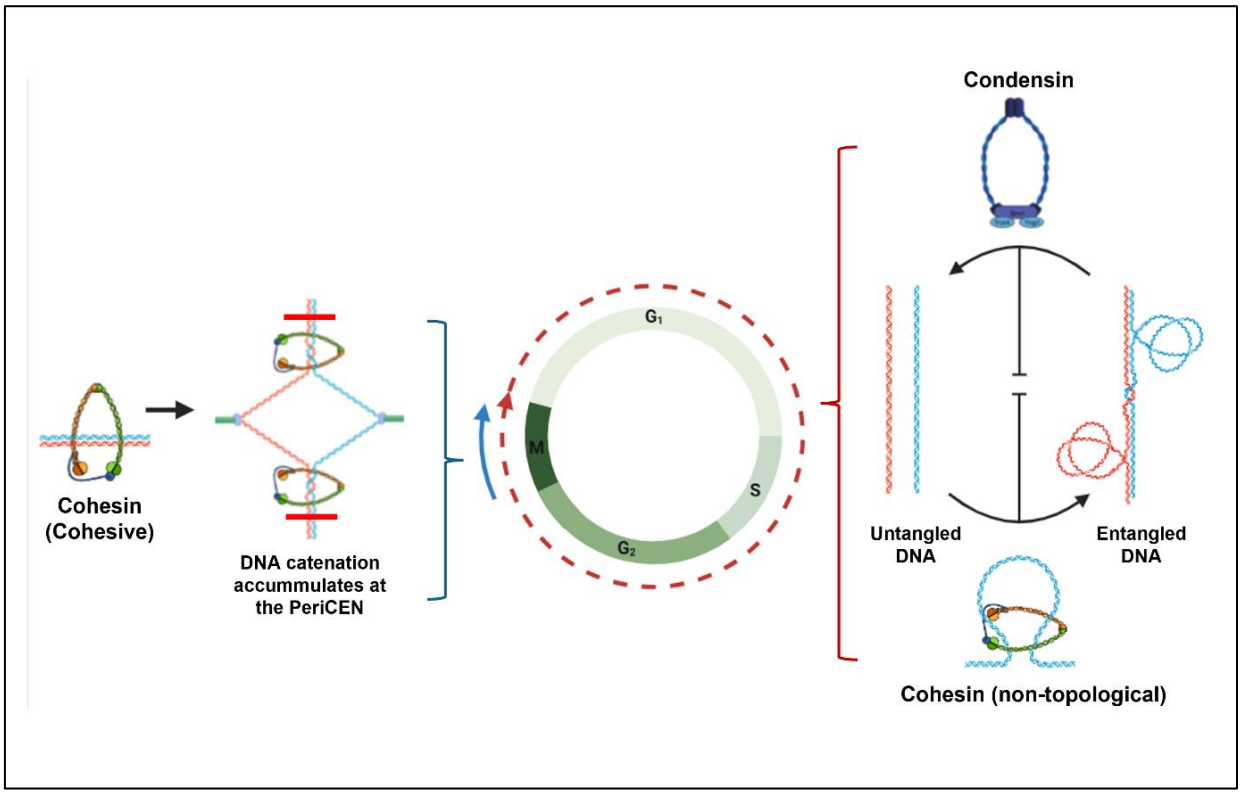

Abstract

Cohesion is the fundamental activity that tethers eukaryotic sister chromatids from S phase until mitosis. The Structural Maintenance of Chromosomes (SMC) complex, known as cohesin, mediates this process by co-entrapping sister chromatids within its ring-like structure. Sister chromatids are also extensively entangled through DNA catenation, which involves physical interlinks created during DNA replication and protected by

cohesin. Unresolved DNA catenation in mitosis leads to anaphase bridges and segregation errors. Nevertheless, the role of DNA catenation and the mechanism by which cohesin safeguards it remain uncertain. Additionally, DNA catenation co-accumulates alongside cohesin at pericentromeres borders under spindle forces in metaphase, but the underlying mechanism has never been investigated. Elucidating whether DNA catenation is implicated in sister chromatid cohesion and what molecular phenomena drive its function and dynamics is critical for fully understanding chromosome segregation. Our lab recently found that cohesin is unable to withstand spindle forces when DNA catenation is artificially removed in metaphase-arrested cells. By measuring cohesion in cells lacking functional cohesin, I find that DNA catenation can noticeably hold sister chromatids without spindle forces but fails to do so when these are present. Moreover, I demonstrate that the ability of cohesin to stably co-entrap sister chromatids is essential for retaining DNA catenation at pericentromeres under spindle forces, but not for protecting DNA catenation from topoisomerase 2. The latter function is antagonised by condensin-directed topoisomerase 2 activity across the cell cycle. The fine balance of topoisomerase 2 activity set by cohesin and condensin is shifted towards decatenation when the protein is truncated at its C-terminus, revealing a key regulatory feature residing in this region. Overall, this project reveals the crucial role of DNA catenation in maintaining sister chromatid cohesion, providing unprecedented insights into its regulation and turnover via a coordinated SMC mechanism.

Acknowledgements

I am deeply grateful to Dr Madhusudhan Srinivasan for his supportive supervision and attentiveness, which ensured my smooth and steady learning throughout the year. Without him, none of my work would have been possible. I must also acknowledge the help I received from Dr Aditi Kaushik as a key part of my training, whose previous work served as the foundation of my project. I would finally like to thank all members of the Srinivasan lab, especially my bench partners, Dr Maurici Brunet, Dr Aditi Kaushik, Andres, Yushi, and Alba, for the laughs we shared and the thoughtful discussions that arose during those long days in the lab. The professional and cheerful environment we created made my research experience something I will never forget.

Declaration and contributions

I generated all the data presented in this thesis between September 2024 and September 2025, which represents the entirety of my research project. The two-dimensional gels shown in Figure 10B and Figure 11 were done together by me and Alba Ayats Fraile, a visiting PhD student. I also created all the figures presented here unless otherwise stated, and acknowledged any tools and sources used. When other lab members created a yeast strain or a DNA plasmid employed in my experiments, they are also acknowledged.

Contents

Abbreviations

ABC-ATP-binding cassette

AID-Auxin-inducible degradation

APC-Anaphase-promoting complex

ATP-adenosine triphosphate

Cdc20-Cell division cycle 20

Cdk1-Cyclin-dependent kinase 1

Chip-Seq-Chromatin immunoprecipitation followed by sequencing

Cre-Causes Recombination

CTCF-CCCTC-binding factor

CTD-C-terminal domain

Ctf-Chromosome transmission fidelity

DDK-Dbf4-dependent kinase

DMSO-Dimethyl sulfoxide

DNA-Deoxyribonucleic acid

dNTP-Deoxynucleotide triphosphate

E. coli- Escherichia coli

Eco1-Establishment of cohesion 1

EDTA-Ethylenediaminetetraacetic acid

Esco1/2-Establishment of sister chromatid cohesion N-acetyltransferase ½

FACS-Fluorescence-associated cell sorting

FPC-Fork protection complex

g-gravitational force

GAL-Galactose

Gcn5-General control non-repressed 5 protein

GFP-Green fluorescent protein

GHKL-Gyrase-Hsp90-Histidine Kinase-MutL

G0 phase-Gap 0 phase

G1 phase-Gap 1 phase

G2 phase-Gap 2 phase

G2/M- Gap 2 phase-Mitosis interphase

HAWK-HEAT repeat-containing proteins associated with kleisins

HEAT-Huntingtin-EF3-PP2A-TOR1

HeLa-Henrietta Lacks

Hi-C: High-throughput chromosome conformation capture

HRP-Horseradish peroxidase

Hos1-Histone deacetylase 1

HphMX-Hygromycin

KanMX-Kanamycin

Kb/Kbp-Kilobases/Kilobasepairs

kDa-Kilodalton

KITE-Kleisin Interacting Tandem winged-helix (WH) Elements

Leu-Leucine

LoxP-Locus of X-over P1

LYS-Lysine

MET-Methionine

MOPS-Morpholine-propanesulfonic

M phase-Mitosis

NaCl-Sodium Chloride

NatMX-Natamycin

NIPBL-Nipped-B-like protein

NLS-Nuclear localisation signal

nM-Nanomolar

nm-Nanometer

NP-40 Nonyl phenoxypolyethoxylethanol

N-terminus-Amino terminus

OD_{600}/OD_{595}-Optical density at 600/595nm

PBCV-1-Paramecium Bursaria Chlorella Virus 1

PBS-Phosphate-buffered saline

PBST-Phosphate-buffered saline + 0.05 Tween®20

PCR-Polymerase chain reaction

Pds5/1-Precocious dissociation of sisters 5/1

PEG-Polyethylene glycol

Phos/Sorb-Phosphate sorbitol

PMSF-PhenylMethylSulfonyl Fluoride

Rad21/61-Radiation-sensitive protein p21/65

Rpm-Revolutions per minute

RSC-Remodelling the structure of chromatin

Scc1-Sister chromatid cohesion 1 protein

S. cerevisiae-Saccharomyces cerevisiae

SDS-Sodium dodecyl sulfate

SV40-Simian vacuolating virus 40

Smc-Structural maintenance of chromosomes

SSC-Saline-sodium citrate

SOK1-Supressor of kinase 1

S phase-Synthesis phase

Spc42-Spindle pole body component 42

TAD-Topologically associating domain

TAE-Tris-acetate-EDTA

TBE-Tris-borate-EDTA

Td-tandem dimer

TE-Tris-acetate

tetO-tetracycline operator

TetR-Tet-repressor protein

TEV-Tobacco etch virus

Trp-Tryptophan

TOPRIM-Topoisomerase-primase

TY-Tryptone-yeast extract

URA-Uracil

w/v-weight by volume

Wapl-Wings apart-like protein homolog

WHD-Winged-helix domain

WT-Wild type

YEP-Yeast extract + peptone

YEPD-Yeast extract + peptone + 2% glucose

YEPgal-Yeast extract + peptone + galactose

YEPR-Yeast extract + peptone + 2% raffinose

Introduction

1.1 The cell

The most basic form of life, from which all living organisms originate, is the cell (Cooper, 2000). Cells appeared on Earth around 3.8 billion years ago, allowing a long time for their evolution into the living beings of the present day. Based on their structure and composition, cells can be classified into two divisions. Eukaryotic cells are highly sophisticated and contain a nucleus and functionally diverse membrane-bound compartments called organelles. In contrast, prokaryotic cells lack dedicated intracellular compartments and are functionally simpler. Despite their differences, they share DNA as the fundamental molecule that governs all the key aspects of the cell.

1.2 DNA and cellular heredity

The structure of DNA resembles that of a pair of intertwined laces, with two individual strands that interact through the complementarity of their nucleotide sequences (Watson & Crick, 1953). The message encoded in these sequences supplies the instructions for producing the proteins that carry out the wide range of activities of the cell. As such, the cell's genetic code must be passed on to subsequent generations to maintain the

production of functional cells. To add a layer of complexity, most eukaryotic genomes are divided into independent double stranded DNA-protein bodies called chromosomes, which vary in number between species (Bendich et al., 2000). Accurate handling of these molecules thus represents an elemental aspect of a cell's life cycle, and errors in this process are often the basis of developmental disorders and cancer (Jallepalli & Lengauer, 2001).

Cell reproduction happens through the splitting of a mother cell into two identical clones that carry the same genetic information, which poses the problem of ensuring the maternal DNA is evenly divided into the two arising progeny cells (Alberts et al., 2002). Luckily, the double-stranded structure of DNA provides an excellent solution to this. During a cell's division cycle, the strands of its DNA are separated to serve as templates for the replication of its genome. The newly arising DNA strands become paired with the template strands, creating two identical copies of each chromosome called sister chromatids. This mechanism allows them to be pulled apart and transported to the opposite ends of the dividing cell, so when it splits into two different ones, each receives a complete copy of the maternal genome (Anjur-Dietrich et al., 2021). The genome of the daughter cells is then replicated before the next division round. This coordinated series of events through which genetic integrity is preserved, cells grow and reproduce is called the cell division cycle.

1.3 The mitotic and meiotic cell division cycles

There are two types of cell division cycles in eukaryotic cells. The mitotic cell cycle produces two identical daughter cells and coordinates one round of DNA replication with one round of division (Mclntosh, 2016). In contrast, meiosis is characterised by two subsequent cell division events that generate genetic variability between the four arising cells and underpins the mechanism of sexual reproduction (Marston & Amon, 2004).

Certain cell types in higher organisms, such as neuronal cells, are unable to multiply, an ability lost through the differentiation process (Cooper, 2000). However, this is not the case for all types of differentiated cells. Cell differentiation is the mechanism through which non-specialised cells, including stem cells, alter their transcriptional landscape to acquire new morphological and functional properties characteristic of a specific tissue. As a result, cell differentiation is essential to build the organs of complex organisms such as humans.

The initial descriptions of the cellular processes that segment a cell's life into different phases were made by Walther Flemming in the late 19th century (Flemming et al., 1882; Uzbekov & Prigent, 2022). Despite the limitations in imaging technology at the time, he was able to track the timely movement and conformation changes of intracellular components, including chromosomes, that led to cell division. The next century saw the development of innovative techniques that allowed a more precise study of the cell cycle when the currently accepted G1, S, G2, Mitosis/Meiosis and

G0 phases were proposed. While the G1, S, G2, and G0 phases are shared between the mitotic and meiotic cell cycles, meiotic cells undergo Meiosis I and Meiosis II consecutively before returning to G1, both subdivided into the same stages as Mitosis but presenting noticeable differences (Gottlieb et al., 2023).

1.3.1 Interphase

The first phase of a new cell division cycle is G1 (Cooper, 2000). During this phase, cells do not undergo massive morphological changes other than a substantial increase in size, but rather set the stage for genome replication. This requires synthesising proteins composing the replisome and regulatory proteins that collaboratively decide whether to continue into the S phase or stall indefinitely in G0 until environmental conditions become favourable (Johnson, 1992). For G1 progression to occur, the cell's growth rate must be optimal and the genome safe and intact. In the case of a haploid yeast such as *S. cerevisiae*, two mating types exist: a and α (alpha) (Sieber et al., 2023). Therefore, G1 can also be halted by the presence of pheromones released by a cell of opposite mating type. The result of mating is the fusion of the two compatible cells into a diploid cell carrying two homologous copies of each chromosome (homologous chromosomes). Once mating is completed, the cell resumes its progression through the cell cycle and is able to enter Meiosis I following G2.

S phase represents the stage where pre-assembled replication proteins recruit further factors required for replication initiation (Takeda & Dutta, 2005). Ineffective or externally compromised replication triggers signals that halt progression through S phase and promote DNA stabilisation and repair, or apoptosis.

Completion of DNA synthesis marks the beginning of the second gap phase or G2 (Fischer et al., 2018). At this point, human cells (naturally diploid) and diploid yeast cells have 2 replicated sets of each chromosome, each composed of 2 sister chromatids. G2 is characterised by the production of mitotic factors and an increased rate of cell growth and membrane component biosynthesis, particularly lipids, an essential preparation step for cell division (Icard et al., 2019). During G2, cells carrying damaged DNA are arrested, ensuring its repair before committing to cell division in Mitosis or Meiosis (Wang et al., 2009).

1.3.2 Mitosis, Meiosis and Cytokinesis

The Mitosis, Meiosis I and Meiosis II, are subdivided into five stages, namely prophase, prometaphase, metaphase, anaphase and telophase (O'Connor, 2008). The terms I and II will now be used to refer to stages of Meiosis I and Meiosis II, respectively. Stages mentioned without these terms refer to mitotic stages.

As cells enter prophase and progress through cell division, their chromatin becomes highly condensed and compact, forming visible chromosomes. The

assembly of the mitotic/meiotic spindle and its fibres at opposite ends of the dividing cell also occurs during prophase. Recombination between homologous chromosomes also happens during prophase I, altering their composition through the mutual exchange of genetic markers (Sansam & Pezza, 2015).

Prometaphase encompasses the destruction of the nucleus, resulting in the formation of small nuclear particles that contain the DNA (O'Connor, 2008; Nature Education, 2014). The spindle microtubule fibres then travel the intracellular space from the poles towards the kinetochores, a centromeric protein assembly that serves as their docking point on the sister chromatids. By applying pulling forces, the spindle checks whether the microtubule-kinetochore interactions have the correct orientation: if each spindle pole attaches the chromatid oriented towards it, also known as bipolar attachment or biorientation. This control point is called the Spindle Assembly Checkpoint (SAC). When biorientation happens, the force generated on opposite spindle poles is neutralised, creating tension at kinetochores and stabilising the chromosomes and allowing their alignment at the centre of the metaphase plate in the dividing cell. The checkpoint is then passed, allowing progression from metaphase. During metaphase I, homologous chromosomes lie in parallel across the metaphase plate, and each of them (with its two sister chromatids) becomes attached to one spindle pole (Marston & Amon, 2004).

Anaphase/Anaphase I then commences, breaking the cohesion between sister chromatids or homologous chromosomes and drawing them toward opposite spindle poles, an event coordinated by the microtubule network (O'Connor, 2008; Nature Education, 2014; Marston & Amon, 2004). The chromosome condensation built up until metaphase is then lost, and the chromatids or homologous chromosomes localise to the poles to be encased by the newly established nuclei in Telophase or Telophase I, respectively (O'Connor, 2008; Nature Education, 2014; Gottlieb et al., 2023).

Finally, during Cytokinesis, the contractile ring separates the cytoplasm into two independent cell membranes. These are repaired at the cleavage point by the insertion of new membrane (O'Connor, 2008; Nature Education, 2014). As a result, following mitosis, two identical daughter cells are generated. Conversely, following Meiosis I, the two daughter cells will have genetic differences dictated by the extent of homologous recombination in Prophase I (Gottlieb et al., 2023; Sansam & Pezza, 2015). Following Meiosis I, meiotic cells enter Meiosis II, the stages of which closely resemble the mitotic stages described above. The outcome of Meiosis is the creation of four genetically distinct daughter cells. One alternative to the conventional, open, mitotic pathway in budding yeast (and also other organisms) is closed mitosis, in which the mitotic stages do not involve the collapse of the nuclear envelope (Boettcher & Barral, 2013; Sazer et al., 2014). Instead, the spindle bodies assemble and operate inside the nucleus, attaching sister kinetochores and pulling the chromatids to opposite nuclear poles (Mori et al., 2020). The nucleus then divides into two nuclei, preserving the integrity

of the nuclear envelope without its rupture. The cell finally undergoes division, ensuring each of the daughter cells receives one nucleus. A summary of the eukaryotic cell division cycle is shown in Figure 1.

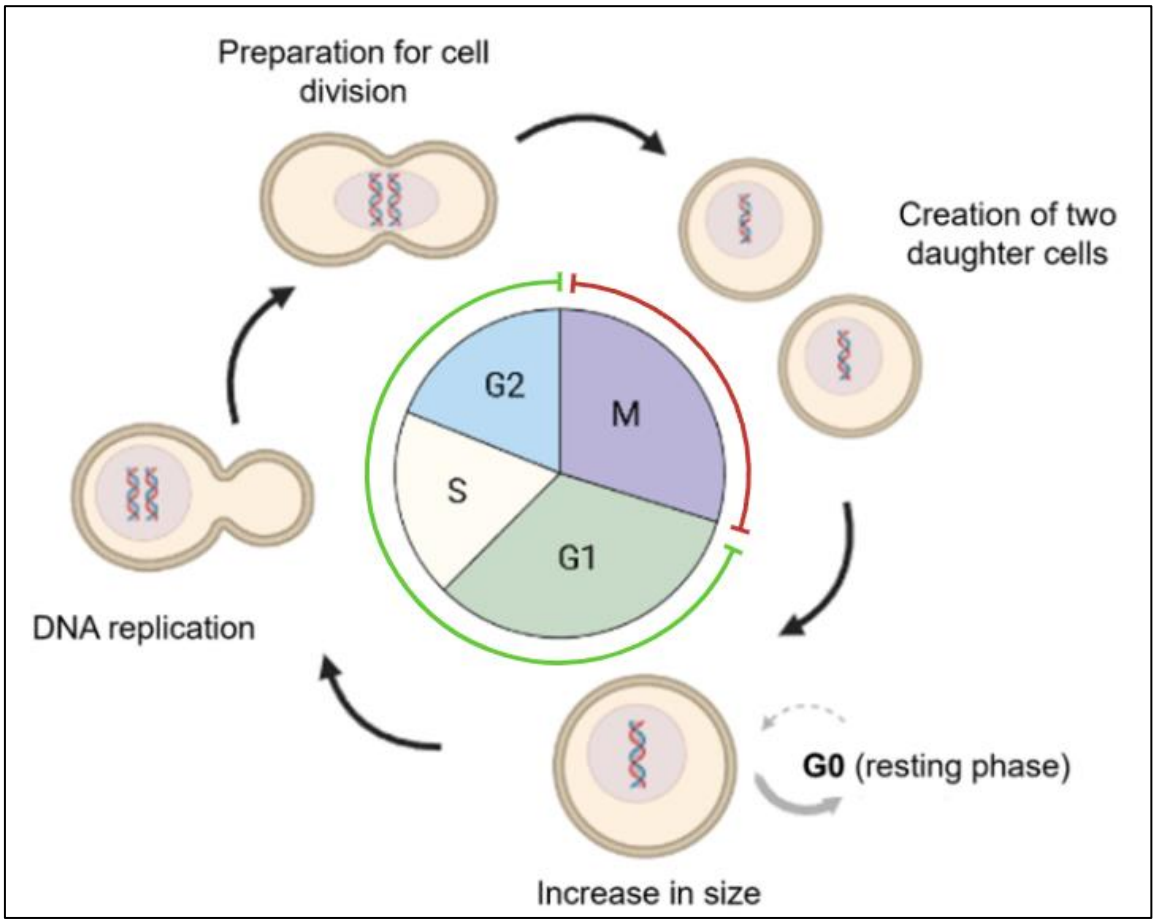

Figure 1. The eukaryotic cell division cycle is divided into interphase (G1, S and G2) (green) and mitosis/meiosis (red). Schematic of the cell division cycle showing the distinct phases that compose it, with their respective lengths represented by the area of the circle they occupy. Adapted from Rosenberg & Rosenberg, 2012.

1.4 Sister chromatid cohesion and segregation

Chromatin in cells experiences a constant shift between distinct higher-order structural configurations tailored to specific cellular events, such as DNA repair, transcription and cell division (Delvaux de Fenffe, 2025). The third, due to its complexity and length, requires a timely cycle of activities to control the evolution of chromosomal morphology throughout the different phases. The first major structural change occurs following DNA replication in S phase, with the establishment of cohesion, a force that physically sticks the newly replicated sister chromatids together (Guacci et al., 2009; Tanaka et al., 2000). This force is maintained until the sister chromatids are ready to split at the beginning of anaphase. The fundamental feature of cohesion is that it allows sister chromatids to withstand the spindle forces occurring in metaphase, creating the tension required for the cell to sense that biorientation has taken place (Uhlmann, 2001; Tanaka et al., 2000). Once this tension is sensed, anaphase kicks off and cohesion is destroyed, allowing sister chromatids to segregate to opposite poles (Figure 2A). Prematurely losing cohesion would result in a random spatial assortment of chromatids, impeding the cell from distinguishing which chromatids are sisters and should be directed to opposite poles (Nasmyth et al., 2000). It is for this reason that defective cohesion, whether by mutation or other factors, is often the cause of segregation errors and aneuploidy (Figure 2B).

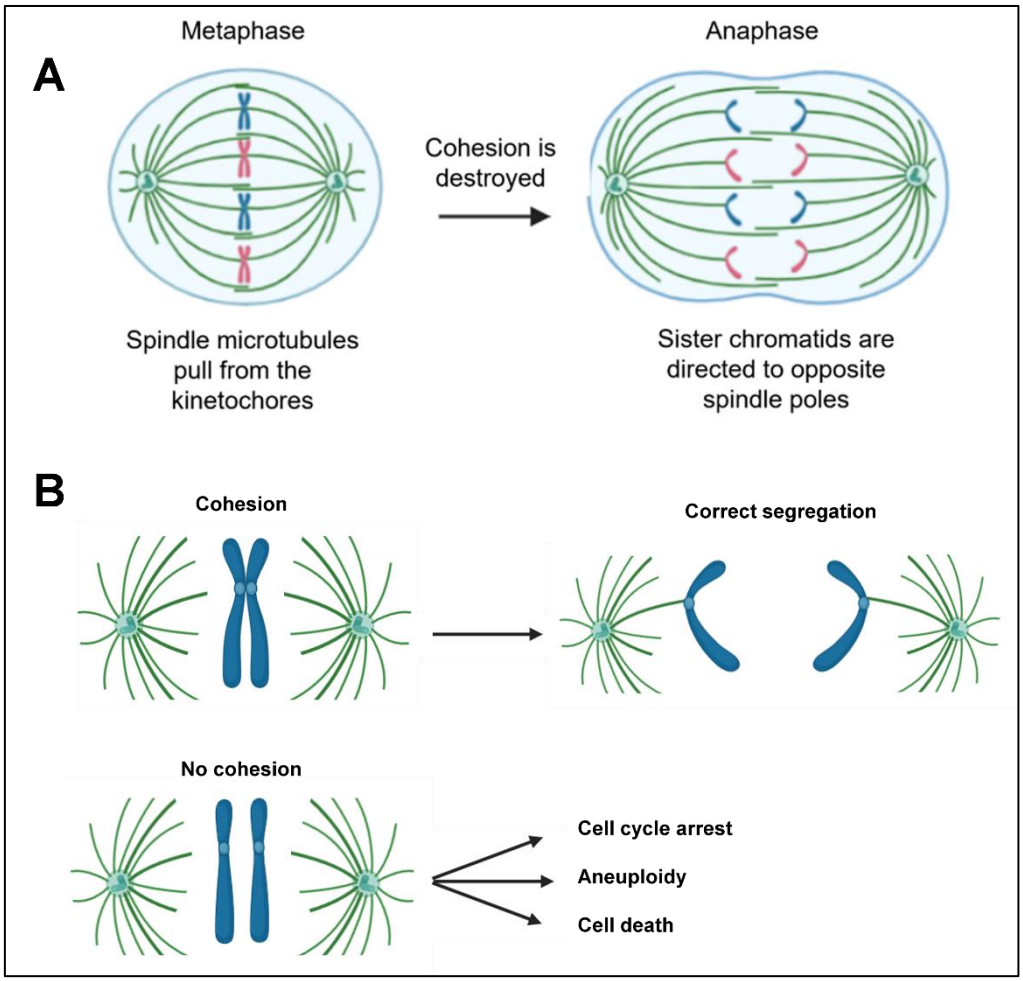

Figure 2. The implication of cohesion in sister chromatid segregation. A The metaphase to anaphase transition. During metaphase, microtubules from the mitotic spindle apparatus extend to, and attach sister chromatids at the kinetochores. The spindle microtubules then start pulling sisters apart, aligning them at the metaphase plate and generating tension. The spindle assembly checkpoint is then satisfied, and cohesion is destroyed to allow anaphase onset and the segregation of sister chromatids to opposite spindle poles. **B** Schematic of the outcomes of chromosome segregation. Cohesion between sister chromatids ensures their faithful segregation towards opposite spindle poles and prevents catastrophic cellular events.

1.5 SMC complexes

Structural Maintenance of Chromosomes (SMC) complexes are central to regulating the dynamic structure of chromosomes across cellular life (Hoencamp & Rowland, 2023). Three main complexes comprise this protein family in eukaryotes: cohesin, condensin and SMC5-SMC6. All consist of a heterodimer of SMC proteins, Smc1/Smc3 for cohesin, Smc2/Smc4 for condensin and Smc5/Smc6 for Smc5/6 complexes. The two monomers of each heterodimer are engaged directly in a head-to-toe orientation through their dimerisation domain at the apices of their hairpin-like structured coiled-coils, resulting from their antiparallel nature (Hoencamp & Rowland, 2023; Gligoris et al., 2014; Haering, 2004). They are additionally linked indirectly through a kleisin subunit, which forms a junction at the interface of their ATPase domains. The individual ATPase domain of each SMC protein is created by the tight juxtaposition of the amino and carboxyl ends. The ATPase or head domains of the SMC subunits also come in contact in the presence of ATP, dimerising to form an ATP-binding cassette (ABC) -like ATPase, which, together with the hinge domain resulting from the dimerisation of the coiled coils, plays an essential role in the assembly and function of SMC complexes (Hirano & Hirano, 2006). A remarkably similar structure to eukaryotic SMC complexes is found in their prokaryotic counterparts, such as MukBEF, MksBEF and SMC-ScpAB (Bürmann & Löwe, 2023). However, the SMC proteins of prokaryotic complexes form a homodimer (Morozova et al., 2024).

Both eukaryotic and prokaryotic SMC complexes exhibit functional diversity. Cohesin is a main player in the maintenance of sister chromatid cohesion from S phase until anaphase and also in the three-dimensional structuring of the genome (Guacci et al., 2009; Michaelis et al., 1997), condensin mediates the condensation and progressive resolution of meiotic and mitotic chromosomes from prophase until metaphase (Hirano & Mitchison, 1994; Hirano et al., 1997; O'Connor, 2008) and Smc5/6 has roles in driving faithful DNA replication and repair as well as preventing DNA damage (Peng & Zhao, 2023). Prokaryotic MukBEF, MksBEF and SMC-ScpAB function analogously to eukaryotic condensin by promoting the condensation and segregation of bacterial chromosomes (Zhou, 2022; Mäkela & Sherratt, 2020; Morozova et al., 2024). Except for sister chromatid cohesion, all the aforementioned SMC functions are thought to be mediated by their ability to extrude loops of DNA.

Interestingly, whereas the accessory proteins for cohesin and condensin belong to the HEAT repeat protein Associated With Kleisins (HAWK) superfamily, the Smc5/6 and prokaryotic ones belong to the Kleisin Interacting Tandem winged-helix Elements (KITE) superfamily (Palecek & Gruber, 2015; Wells et al., 2017).

1.5.1 Kleisins, KITEs and HAWKs

Kleisin proteins are a core component of SMC complexes that mediate the physical linkage between the outer regions of an SMC head and an SMC

coiled-coil, creating their characteristic trimeric structure with a central channel (Schleiffer et al., 2003; Bürmann & Löwe, 2023). As a result, kleisin proteins are essential to functionalize SMC complexes into active tethers and extruders of chromatin segments (Schleiffer et al., 2003; Bürmann & Löwe, 2023). For example, cleavage of Scc1 results in the abolishment of cohesion and loop extrusion by cohesin (Davidson et al., 2019; Uhlmann et al., 1999). The bridging activity of kleisins depends on the integrity of their amino and carboxyl end regions, which are functionally and structurally homologous across species and serve as the anchor points between the SMC ATPase heads (Hoencamp & Rowland, 2023; Bürmann et al., 2013; Zawadzka et al., 2018; Gligoris et al., 2014). Members of this protein superfamily include Brn1 (yeast)/hCAP-H/H2 (human), Scc1 (yeast)/Rad21 (human), Nse4, ScpA, MukF and MksF, found in condensin, cohesin, Smc5/6, SMC-ScpAB, MukBEF and MksBEF, respectively (Schleiffer et al., 2003; Wang et al., 2018; Fennell-Fezzie et al., 2005).

Kleisin proteins serve as recruitment platforms for KITE and HAWK proteins through their non-conserved linker core found between the head and coiled-coil binding interfaces (Schleiffer et al., 2003; Bürmann & Löwe, 2023). While some members of these two families are permanent subunits of SMC complexes (e.g. MukE), others are only transiently associated (e.g. Pds5) and provide temporal fine-tuning of their activities (Wells et al., 2017; Palecek & Gruber, 2015).

KITEs are winged-helix repeat-rich proteins that assemble into functional dimers before interacting with SMC-bound kleisins (Palecek & Gruber, 2015). They are found in prokaryotic MukBEF and MksBEF as MukE, SMC-Scp-AB as ScpB and eukaryotic Smc5/6 as Nse1/Nse3. KITE proteins have been implicated in regulating the ATP-binding-hydrolysis cycle of these complexes and enhancing their chromosomal organisation activities (Bürmann & Löwe, 2023; Vondrova et al., 2020; Gloyd et al., 2011). Taking MukB as an example, it has been shown that the rate of condensation is increased upon interacting with MukE (Wang et al., 2006; Gloyd et al., 2011). Furthermore, MukB is incapable of segregating chromosomes when it does not form the classical trimeric SMC-kleisin complex with its KITE subunit.

HAWK proteins are composed of HEAT (Huntingtin-EF3-PP2A-TOR1) repeat elements that provide protein-protein binding interfaces necessary to form large molecular scaffolds (Neuwald & Hirano, 2000; Andrade et al., 2001; Wells et al., 2017). In this manner, HAWK proteins such as Ycg1 and Ycs4, and Scc2, Scc3 and Pds5, are able to interact with the kleisin subunit of the eukaryotic SMC complexes condensin and cohesin, respectively (Wells et al., 2017). Ycg1 targets condensin to pericentromeres to promote chromosome biorientation and other highly catenated loci to mediate sister chromatid resolution (Wang et al., 2024). Conversely, Ycs4 plays a key role in stimulating ATP-hydrolysis-driven loop extrusion by condensin, substrate detection and specificity and promoting the displacement of non-productive cohesin from chromatin (Sarkar et al., 2021). Pds5 and Scc2 are only transiently associated with cohesin's Scc1, whereas Scc3 is permanently

associated with Scc1 as part of the ring (Petela et al., 2018; Chao et al., 2015; Muir et al., 2016; Hartman et al., 2000; Losada et al., 2000). Scc2 stimulates the ATPase activity of cohesin's heads and is necessary for loading and loop extrusion (Petela et al., 2018; Chao et al., 2015; Davidson et al., 2019). On the other hand, Pds5 and Scc3 mediate cohesion and cohesin turnover, but Pds5 additionally limits loop extrusion by cohesin (Sutani et al., 2009; Ruiten et al., 2022; Yu et al., 2022; Losada et al., 2000; Wells et al., 2017; Brunet Roig et al., 2014).

1.6 Loop extrusion

SMC complexes have been shown to possess loop-extruding activity through ATP-hydrolysis under variable experimental conditions (Figure 3). However, their extruding mechanisms differ slightly, as is the case for the topological association with DNA these complexes adopt during the process (Davidson et al, 2019; Ganji et al., 2018; Pradhan et al., 2023). Additionally, cohesin and condensin operate as monomers, whereas Smc5/6 extrude DNA as a homodimer. SMC complexes could expand loops by allowing the non-topological/pseudo-topological passage of DNA through the tripartite ring or via a mechanism independent of DNA passage, a matter that is still discussed to this day (Banigan & Mirny, 2020).

Evidence of cohesin's involvement in loop generation across mitotic chromosome arms in budding yeast comes from Hi-C and Pile-up plot analyses (Dauban et al., 2020). Additionally, several experiments have shown

that AID-mediated depletion of cohesin in G1 results in the same architectural pattern across arms as cells arrested prior to cohesin loading, poor in intrachromosomal interactions and loop structures. Therefore, the presence of cohesin is essential to stabilise existing loops. Interestingly, most of these loops, removed by cohesin depletion, map to sites of convergent transcription where cohesin is known to concentrate (Dauban et al., 2020; Lengronne et al., 2004). These sites are known to accumulate positively supercoiled DNA, which has been directly linked to facilitating cohesin-mediated chromosomal compaction (Sun et al., 2013; Guo et al., 2021).

Through loop extrusion, cohesin is able to physically connect distant loci, providing transcriptional fine-tuning by bringing promoters and enhancers or silencers into functional proximity (Kagey et al., 2010; Schoenfelder & Fraser, 2019). Loop extrusion also creates Topologically Associated Domains (TADs), which represent chromosomal regions enriched in loops that contact each other more frequently than loops belonging to other TADs (Dixon et al., 2012; Wutz et al, 2017). Both individual loops and TADs are restricted in size and space by the transcription factor CTCF, serving as an insulator that organises local and higher-order chromatin structure. Importantly, cohesin mediates loop extrusion independently of its ability to entrap DNA (Davidson et al., 2019; Nagasaka et al., 2023; Srinivasan et al., 2018).

It has also been possible to observe condensin-mediated loop formation by single-molecule live imaging (Ganji et al., 2018). This mechanism in yeast is

promoted by positively supercoiled DNA, not only by actively facilitating it but also by attracting high concentrations of condensin molecules (Kim et al., 2022). These are able to extrude loops upon stably associating with DNA. If present, local plectonemes serve as preferential docking points for condensin, further enhancing the extrusion process. Nevertheless, the outcome of condensin-mediated loop extrusion is increased local supercoiling, which generates a positive feedback cycle for further extrusion.

The exact mechanism for the extrusion of DNA loops is not fully clear. For instance, there is evidence that cohesin and condensin can extrude chromatin loops past obstacles 5-fold larger than the ~35nm diameter of their lumen when ring opening is abolished through the crosslinking of their three interfaces (Pradhan et al., 2022; Davidson et al., 2019; Anderson et al., 2002; Haering et al., 2002). This challenges the previously postulated pseudo-topological mechanism through which cohesin pulls DNA bidirectionally through its lumen to expand loops (Pradhan et al., 2022; Davidson et al., 2019). It also indicated that the loops may be extruded without passing through the lumen via DNA-protein contacts on the outer surface of the ring. Moreover, experiments in bacteria have recently led to the proposal of an interesting model which recapitulates principles of a topological mechanism (Diebold-Durand et al., 2017; Marko et al., 2019). This model explains that a DNA segment is first pulled through a transient cavity delimited by the juxtaposed, ATP-free ATPase heads and the connecting kleisin extending underneath them. The subsequent binding of ATP would promote the separation of the coiled coils, thereby releasing the

hinge and creating a larger Smc-Smc-head lumen (Diebold-Durand et al., 2017; Marko et al., 2019). The bending of the DNA segment region immediately adjacent to this lumen into the complex would lead to the extrusion of this segment into a loop. This loop would be stabilised within the complex through internal contacts with the ring, both near the exposed hinge and around the initial kleisin-head cavity, while simultaneously allowing its expansion unidirectionally. ATP hydrolysis would then be followed by the unlocking of the contiguous Smc-Smc-kleisin lumen by the disruption of the ATPase head engagement (Diebold-Durand et al., 2017; Marko et al., 2019). Accordingly, the loop would spring outwards, and the DNA would be pushed back into the kleisin-head cavity to produce a net forward translocation of the SMC complex. Importantly, the broader conformational states and compartmentalisation explained by this model are compatible with the known eukaryotic and prokaryotic SMC complexes.

Different SMC complexes may extrude DNA loops through distinct mechanisms or alternate between them. Nevertheless, the concert of loop extrusion by the different SMC complexes is an essential aspect of the dynamic nature that defines the eukaryotic and prokaryotic genomes.

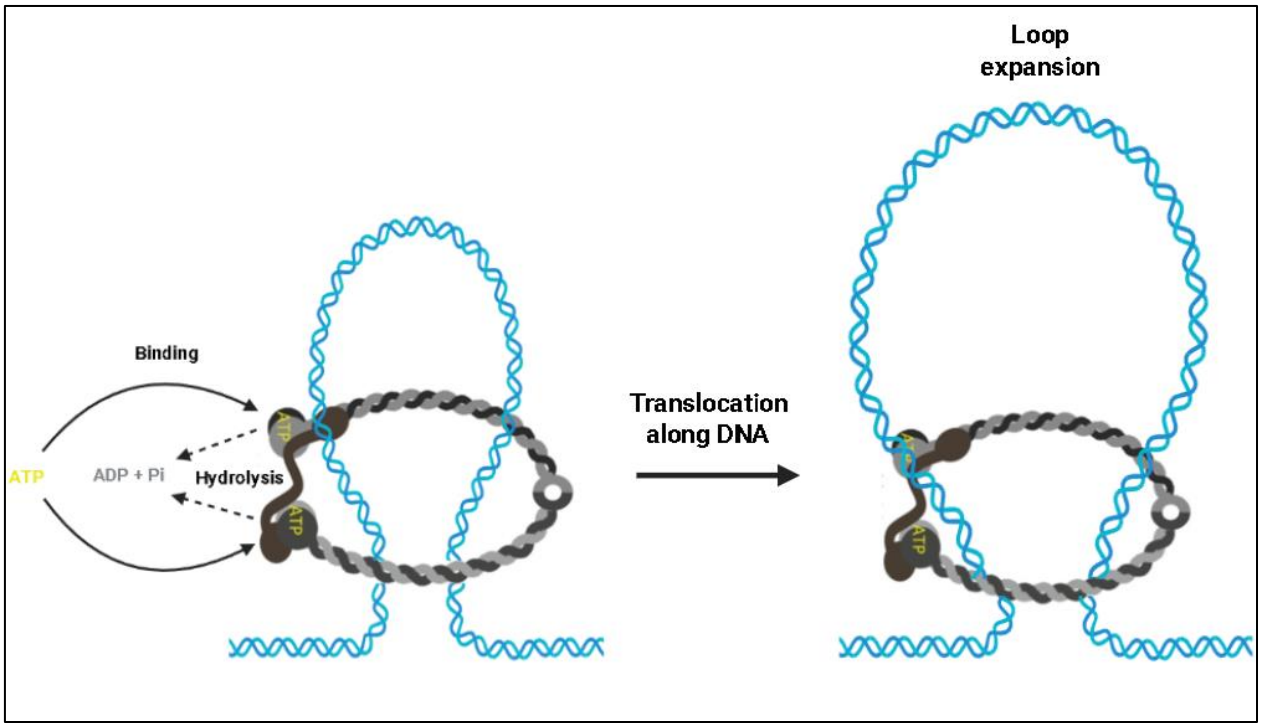

Figure 3. Loop extrusion by SMC complexes. Schematic representation of the loop extrusion process, mediated via non-topological/pseudo-topological association to DNA. ATP binding and hydrolysis power the expansion of extruded loops as DNA is reeled inside the SMC ring through translocation. Image of SMC complex taken from Gligoris et al., 2016.

1.7 The cohesin ring

Cohesin's kleisin subunit Scc1 engages Smc3's and Smc1's ATPase domains through its N- and C-terminal domains, respectively, circularising the structure into its characteristic ring shape (Figure 4). Initial evidence that pointed to cohesin as a primary mediator of cohesion included fluorescence microscopy experiments showing that mutations in the ring resulted in prematurely split chromatid regions (Straight et al., 1996). Additionally,

researchers noticed that the onset and withdrawal of the forces tethering sister chromatids coincided with cohesin binding and turnover on DNA, respectively (Michaelis et al., 1997). The requirement of Scc1 cleavage by separase for segregation was also an initial hint that this would release trapped sister chromatids (Uhlmann et al., 1999). Later on, as cohesin's morphology was described and more was being unearthed about its influence on chromosome dynamics, the ring model was put forward, and to this day, it remains widely accepted (Haering et al., 2002). This model explains that cohesin entraps sister chromatids following DNA replication to provide cohesion (Haering et al., 2002; Haering et al., 2008). Supporting it are also experiments showing catenated sister minichromosomes in yeast cells that depend on the crosslinking of all three of cohesin's interfaces prior to the denaturation of the complex (Haering et al., 2008; Gligoris et al., 2014).

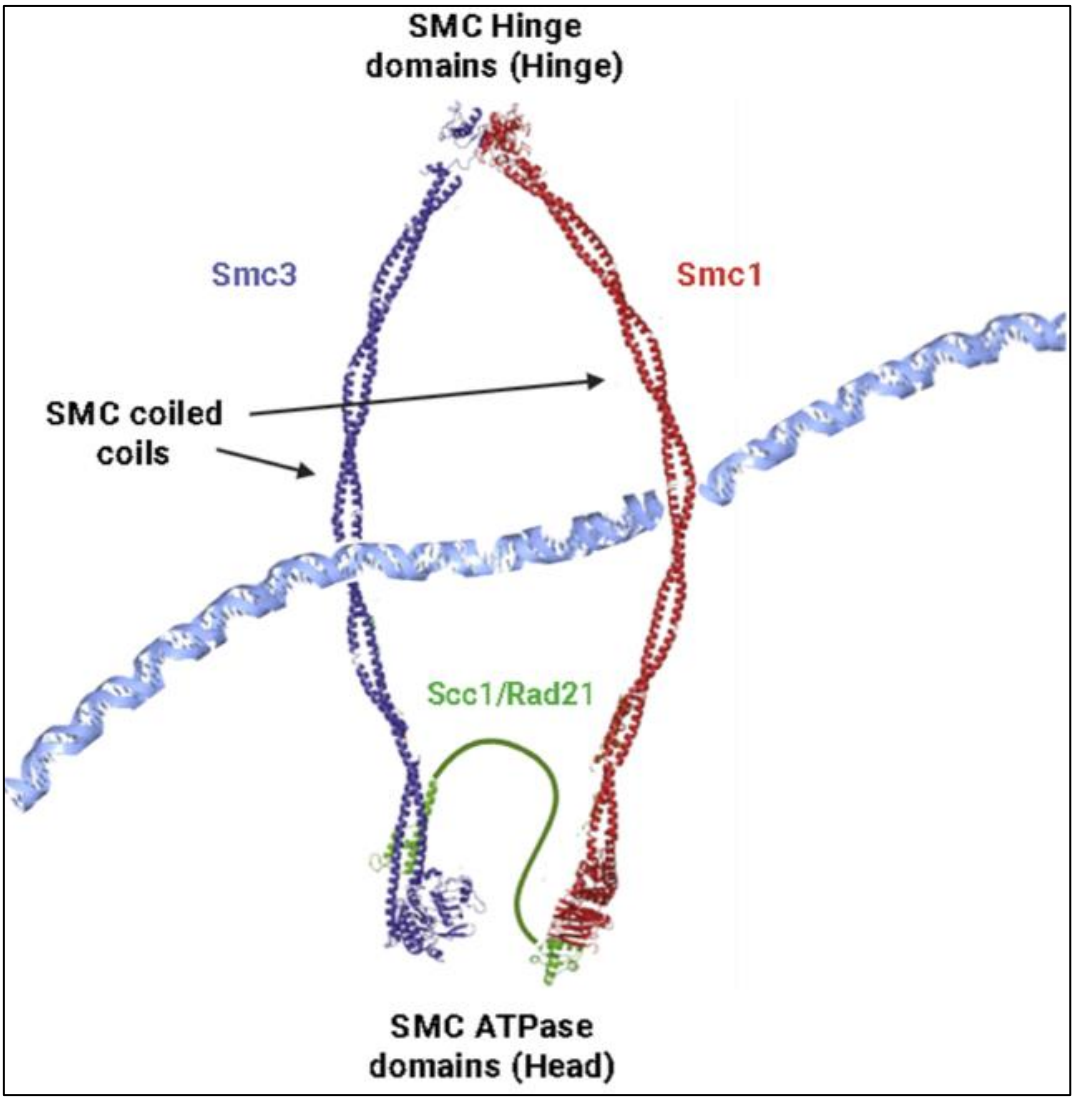

Figure 4. Structure of cohesin topologically entrapping DNA. Simplified structure of the cohesin ring formed by Smc3, Smc1 and Scc1 (Rad21 in humans) topologically encircling a DNA molecule. The hinge domain forms the V-shaped structure of the SMC heterodimer, and the SMC ATPase domains are connected through the kleisin subunit. Made using Biorender and CCP4MG. DNA structure taken from PDB ID: 7W1M (Zhang et al., 2023). Adapted from Gligoris et al., 2016.

1.7.1 Cohesin removal in mitosis

Cohesin is cleaved at its Scc1 subunit at the onset of anaphase to allow sister chromatid segregation. Central to this event is the anaphase-promoting complex (APC), a multisubunit ubiquitin ligase complex activated by Cdc20 or Hct1 association (Fang et al., 1998). Once biorientation is confirmed, APC triggers the degradation of cyclin B, necessary for the metaphase-to-anaphase transition, and securin proteins such as *Saccharomyces cerevisiae* (*S. cerevisiae*) Pds1 (Irniger et al., 1995; Cohen Fix et al., 1996; Yamamoto et al., 1996). Securin proteins inhibit separase, the cysteine protease responsible for Scc1 cleavage (Uhlmann et al., 2000). Therefore, degradation of securin releases the active site of separase, abolishing its inhibition and allowing it to cleave the cohesin ring. Thus, APC activation is essential for removing cohesin in vertebrates and budding yeast, serving as the key determinant of cohesion destruction. Additionally, vertebrate cells possess the prophase pathway, responsible for dissociating the bulk of cohesin from chromosome arms in a separase-independent manner and allowing its recycling onto chromosomes from telophase onwards (Waizenegger et al., 2000).

1.7.2 Regulators of cohesin

There is a series of factors that modulate the multiple functions of cohesin and its dynamics on chromosomes. Firstly, *S. cerevisiae* Eco1, orthologous to vertebrate Esco1 and Esco2, is a multimeric Gcn5-related N-acetyltransferase with 2 globular domains, one providing specificity for Eco1

targets, and another housing its catalytic activity at the C-terminus (Onn et al., 2009; Zhang et al., 2008; Chao et al., 2017). Its role in sister chromatid cohesion establishment was initially seen in budding yeast carrying the *eco1-1* thermosensitive allele that attenuates its acetyltransferase activity, showing increased rates of cohesion loss prior to anaphase (Tóth et al., 1999). Eco1 acetylates Smc3 at K112 and K113 within the head domain of cohesin during S phase to lock it around sister DNAs (Lengronne et al., 2006; Zhang et al., 2008). The deacetylation of these residues happens in anaphase, concomitantly with the destruction of cohesion and is mediated by the Hos1 deacetylase in budding yeast (Li et al., 2017; Xiong et al., 2010).

Another known regulator of cohesin is Wapl (Wpl1/Rad61 in yeast), universally recognised as the cohesin release factor for its ability to disengage cohesin from DNA (Kueng et al., 2006). This function is likely mediated by opening the Smc3-Scc1 (Smc3-Rad21 in humans) interface, a process thought to release cohesin-entrapped chromatids (Beckouët et al., 2016). Importantly, this release mechanism is prevented by Eco1-dependent acetylation of Smc3 at K112 and K113. In humans, Wapl is a key player in the prophase pathway, whereas *S. cerevisiae* Wpl1 has been suggested to steadily disrupt existing cohesion from its onset, possibly also counteracting cohesion establishment during replication (Lopez-Serra et al., 2013; Sutani et al., 2009). Interestingly, Wpl1 deletion causes increased chromosomal compaction, indicating a role in restricting condensation (Lopez-Serra et al., 2013; Dauban et al., 2020). Therefore, a second function of Wpl1-mediated

displacement of unacetylated cohesin may be to counterbalance excessive chromosome condensation, disengaging actively loop-extruding, non-topologically associated cohesin molecules. This is consistent with the fact that mammalian and yeast cells show increased loop size in the absence of Wapl/Wpl1 (Wutz et al., 2017; Dauban et al., 2020). Because the lethality of *eco1*Δ in yeast cells can be rescued by *wpl1*Δ, it has been suggested that the main purpose of Smc3 acetylation in budding yeast is to inhibit Wpl1 to allow cohesion onset (Rowland et al., 2009; Sutani et al., 2009). However, deacetylation of Smc3 by Hos1 in budding yeast is necessary to complete the turnover of cohesin from DNA following separase cleavage (Li et al., 2017). This process is Wpl1-independent and proceeds via the disintegration of the cohesin head domain, thereby fully opening the ring. This supports a cohesion-promoting mechanism involving Eco1-dependent modulation of Smc3 unrelated to Wpl1 (Guacci et al., 2014). Shortly after Smc3 acetylation, Cdk1 promotes Eco1 degradation without affecting cohesion integrity (Lyons & Morgan, 2012). Thus, Eco1 serves no purpose beyond S phase following the acetylation of Smc3 (Tóth et al., 1999).

Scc1 serves as a recruitment platform for the HEAT repeat protein Associated With Kleisins (HAWK) protein Pds5 in budding yeast, homologous to vertebrate Pds5A and Pds5B (Hartman et al., 2000; Muir et al., 2016). The multifunctionality of Pds5 is evidenced by its involvement in both promoting and destroying cohesion (Sutani et al., 2009). The latter in budding yeast is mediated by its ability to recruit Wpl1, thereby promoting the removal of unacetylated cohesin from DNA. Interestingly, depletion of

Pds5 in G1, G2 and mitosis causes a massive decrease in K112 and K113 acetylation levels, suggesting a direct role in the cohesion establishment reaction (Chan et al., 2013). Pds5, therefore, functions in concert with Eco1 to generate cohesion in S phase, possibly by serving as a bridge to interact with Smc3 or triggering a structural change in its head domain. Because this phenotype is notably reversed in the absence of Hos1, it likely also supports the maintenance of acetylation marks by limiting the activity of this protein. Pds5 is also involved in building the 3D architecture of chromosomes by regulating loop formation (Ruiten et al., 2022; Yu et al., 2022). Interestingly, Pds5 depletion causes greater defects in loop length and localisation than Wpl1 depletion in yeast (Wutz et al., 2017; Dauban et al., 2020). The distinct phenotype implies that, in addition to collaborating with Wpl1, Pds5 acts through an additional unrelated mechanism. This could involve its role as a positive regulator of cohesion, providing limits for loop extension in the form of topologically embraced cohesin molecules that encase loops into separate domains.

Scc1 constitutively exists in a complex with S. Cerevisiae Scc3, another HAWK protein orthologous to human SA1/2 that binds Scc1 through its C-terminal domain (Losada et al., 2000; Wells et al., 2017). Scc3 is essential for loading and maintaining cohesin associated with DNA, but also cooperates with Pds5 and Wpl1 to promote its removal in interphase (Brunet Roig et al., 2014). Scc3 is also required for cohesin turnover at anaphase following separase-mediated cleavage, as it enhances the deacetylation of Smc3 necessary to disengage the ATPase heads (Brunet

Roig et al., 2014). Additionally, studies in vertebrate cells have described SA2 phosphorylation as a crucial step of the prophase pathway (Hauf et al., 2005).

One last HAWK protein, Scc2 (NIPBL in humans), binds the cohesin complex through its kleisin subunit and is essential for cohesin loading onto DNA and its active movement along it (Petela et al., 2018; Chao et al., 2015). In addition, through in vitro reconstitution, it has been possible to elucidate the requirement of Scc2 for cohesin to extrude DNA loops and allow their retention on chromatin (Davidson et al., 2019). All these roles are mediated by its capacity to promote ATP hydrolysis by cohesin's head domains through its hook-shaped C-terminal domain (Petela et al., 2018). Loading of cohesin by Scc2 requires that the latter interacts with Scc4 (MAU2 in humans) to form the Scc2-Scc4 kollerin complex (Lopez-Serra et al.,2014). Scc4 contains several tetratricopeptide repeats that bind the RSC complex to access chromatin (Lopez-Serra et al., 2014; Muñoz et al., 2019). Therefore, RSC also plays a key role, serving as a landing platform for Scc2/Scc4 and remodelling local chromatin structure into a suitable site for cohesin loading through its nucleosome displacement activity. Consistent with this argument is the fact that inactivating mutations in RSC and Scc2/Scc4 produce comparable cohesin loading and cohesion defects. Once Scc2/Scc4 is recruited, cohesin is deposited at these sites of low structural complexity. The majority of cohesin loading onto DNA happens at *CEN* sites within centromeres and along chromosome arms (Tanaka et al., 1999; Fernius et al., 2013). The former is regulated through the post-translational

modification of the kinetochore complex Ctf19 (Hinshaw et al., 2017). When the Dbf4-dependent kinase (DDK) targets this complex for phosphorylation, this event allows the recruitment of Scc2/4, forming a scaffold that ultimately loads cohesin across centromeric *CEN* sequences.

1.7.3 Cohesin association with DNA

Mutations in Smc1 and Smc3 ATPase domains that abolish ATP hydrolysis leave cohesin only able to associate weakly with *CEN* sites upon ATP binding-induced head association, an event necessary for cohesin to bind DNA (Hu et al., 2010; Hu et al., 2016). These results resemble the effect produced by mutating the kollerin loading complex, supporting the idea that both the binding of ATP at the Smc Nucleotide-Binding Domains (NBDs) and its subsequent hydrolysis are essential to form stable cohesin-chromatin interactions (Arumugam et al., 2003). Smc1's NBD must, in fact, be occupied by ATP to form the classic tripartite ring structure, as it allows Scc1 association with the Smc subunits and the subsequent head engagement. The hydrolysis reaction that follows at both Smc heads could allow loading in a non-topological manner or by triggering the entrapment of an individual DNA molecule (Srinivasan et al., 2018). The former mechanism is supported by experiments showing how cohesin with a mutationally compromised hinge is prevented from locking around single or sister DNAs while largely preserving its dynamics on chromosomes. The latter may proceed through a transient opening of the Smc3-Smc1 hinge interface,

providing an entry gate for DNA that can then be topologically captured (Collier & Nasmyth, 2022; Gruber et al., 2006). If true, this model could explain why stable entrapping interactions with chromatin are only possible upon ATP hydrolysis.

1.7.4 The DNA entry and exit gates of cohesin

The Scc1-Smc3 interface represents the proposed exit gate for cohesin to release entrapped DNA molecules in the absence of Scc1's cleavage (Chan et al., 2012; Gligoris et al., 2014; Beckouët et al., 2016). This idea comes from the fact that expressing Smc3 and Scc1 as a single polypeptide rescues the viability of eco1-depleted cells while maintaining cohesin-concatenated minichromosomes even upon the overexpression of *wpl1* (Chan et al., 2012). In contrast, the hinge interface has been suggested to allow DNA passage for entrapment, as its chemical locking severely disrupts cohesin's ability to associate with chromosomes or tether sister DNAs (Gruber et al., 2006). Importantly, this feature is not seen in Scc1-Smc1/3 ATPase fusions.

1.7.5 Cohesin behaviour under spindle forces

Due to its capacity to move through loop extrusion and be pushed along DNA, cohesin tends to reposition and concentrate in regions spatially distant from loading sites (Lengronne et al., 2008). This is particularly

evident in centromere-loaded cohesin during sister centromere separation in metaphase. In this regard, ChiP-Seq and single particle-tracking experiments have shown that cohesin is enriched along a 50 kb domain of chromatin that spans the centromere and regions across both chromosome arms (Weber et al., 2004; Blat & Kleckner, 1999; Tanaka et al., 1999). This distribution pattern relies on the kinetochore subcomplex Ctf19 of *S. cerevisiae* (Fernius et al., 2013; Hinshaw et al., 2017). Microtubule pulling forces in metaphase displace cohesin from *CEN* loading sites outwards of the centromere (Figure 5) (Weber et al., 2004; Tanaka et al., 2000). This remodels the enrichment pattern, creating a 15-20kb cohesin-depleted region along centromere flanking chromatin, delimited on both ends by high concentrations of cohesin (He et al., 2000; Weber et al., 2004. This region that retains a high density of cohesin until metaphase is called the pericentromere (Paldi et al., 2020). The most prominent, centromere-proximal hotspot of cohesin accumulation on each arm, created under spindle microtubule forces, defines a pericentromere border, displaying an array of 3 genes with a conserved configuration. Two are oriented towards the centromere and one towards the arms, creating a characteristic convergent transcription site where spindle tension-induced cohesin sliding halts (Figure 5) (Paldi et al., 2020; Lengronne et al., 2004). Consistent with this, interfering with centromeric loading by disrupting Ctf19 function and altering the arrangement of genes at borders results in the loss of cohesin at these sites (Paldi et al., 2020). The latter also causes the emergence of alternative, more distal borders, increasing the size of pericentromeres and

the region of chromatin separated by the spindle microtubules. Therefore, pericentromeres largely determine the region that splits under microtubule forces in metaphase, with differences across chromosomes conferred by cohesin accumulating at other naturally occurring border-like gene groups.

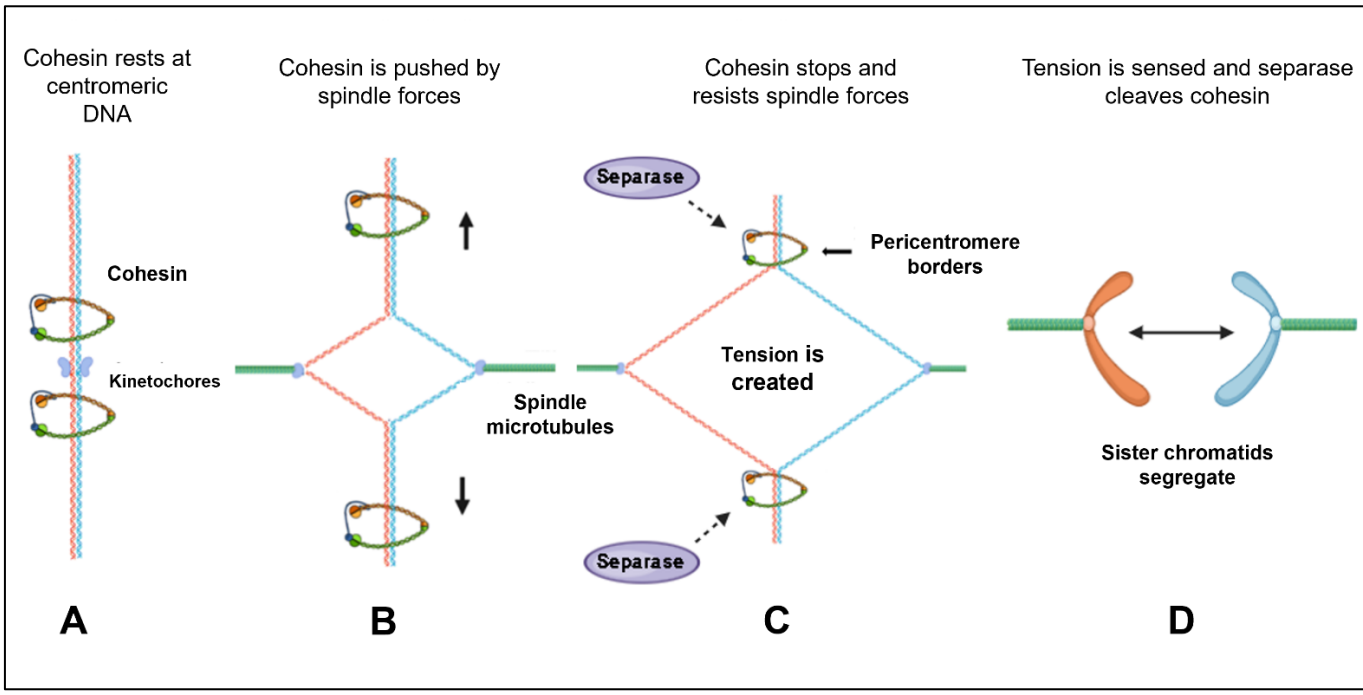

Figure 5. Interplay between cohesion and spindle forces in the creation of tension. **A** From S phase to metaphase, sister chromatids are held by cohesin mainly at and around centromeres. **B** Metaphase onset triggers spindle microtubule attachments to sister kinetochores. Here, sister chromatids begin to be pulled apart, starting at the centromeric DNA. This causes cohesin to slide down the chromosome arms. **C** Cohesin stops sliding at pericentromere borders, where it counteracts spindle forces to prevent further separation of sister chromatids. This opposing action of cohesion and the spindle forces creates tension and triggers the activation of separase. **D** Separase cleaves cohesin, allowing sister chromatids to segregate to opposite spindle poles.

1.8 Cohesion as the foundation of faithful chromosome segregation

The segregation of sister chromatids during anaphase results from the combined effect of cohesion loss and the contraction of the mitotic spindle. However, without bipolar attachment of chromosomes, there would be no way to ensure the equal distribution of chromosomal DNA between cells. Cohesin accumulating at borders offers a solution to this, as it limits the physical dissociation of sisters, ultimately allowing them to remain tethered despite being partially separated across pericentromeres in metaphase (Paldi et al., 2020; Tanaka et al., 2000). The cohesion generated here withstands and counterbalances the microtubule pulling forces. It is only after the tension generated by this opposing action of cohesion to the spindle is sensed that biorientation is confirmed. This leads to the alignment of chromosomes at the metaphase plate and the eventual separase-mediated cleavage of cohesin, with the encompassing destruction of cohesion (Figure 5) (Nasmyth et al., 2000). Cohesion thus provides the fundamental proofreading mechanism that ensures biorientation, preventing premature splitting of sister chromatids and co-localisation to the same spindle pole. Nevertheless, how cohesin is able to withstand such forces and whether the underlying or surrounding topology of DNA plays a role is unknown.

1.9 DNA topology

DNA's lengthy and flexible nature allows it to adopt distinct functional topologies and three-dimensional configurations, often as a byproduct of essential cellular processes and the physical constraints of the nuclear environment (Deweese et al., 2008). Topological DNA structures can only be reversed by disrupting DNA's continuity and not by mechanical stretching (Dröge & Cozzarelli, 1992). For instance, this can happen through the enzymatic cleavage of the DNA strands. Catenation, knots, torsion and plectonemes are DNA features of particular significance due to their capacity to alter the spatial and functional properties of intracellular chromatin (Baxter & Aragón, 2010; Rodríguez-Campos, 1996; Portugal & Rodríguez Campos, 1996; Ma et al., 2017).

1.9.1 Topoisomerase enzymes

There are two primary types of topoisomerases in budding yeast: type I and type II (Wang, 1980; Liu et al., 1980; Liu et al., 1979). Topoisomerase I (also topoisomerase 1), classified as type IB, catalyses the cleavage of a single DNA strand (nicking), allowing the end of the broken strand unattached by the enzyme to swivel around the intact strand to relieve the accumulated torsional stress (Capranico et al., 2017; Wang, 1985). Following relaxation, the broken strand is religated. Conversely, topoisomerase II (also topoisomerase 2), a type IIA, cleaves both DNA strands, allowing the passage of another duplex before religating the ends, making it capable of relieving torsional stress by acting at DNA crossovers (Wang, 1985). Thus,

type I and type II topoisomerases facilitate a mechanism to relax supercoiled DNA of either directionality. This function is of particular importance, since transactions along DNA, such as loop extrusion by condensins or helix unwinding by the replication and transcribing machineries, unavoidably create torsional stress through the supercoiling of DNA (Kim et al., 2022; Schvartzman et al., 2019; Gilbert & Allan, 2014). In the case of the latter two, DNA is overwound (positively supercoiled) ahead of the fork while it is simultaneously underwound (negatively supercoiled) behind it. This is translated into increasingly harder to unwind DNA segments ahead of the fork and the formation of supercoiled DNA loops called plectonemes to compensate for the extra tightness. These plectonemes provide DNA crossovers that attract type II topoisomerases for relaxation (Timsit et al., 1998). In the absence of the relaxation activity of topoisomerases, positively supercoiled DNA can inhibit DNA replication and transcription termination (Nudler, 2013). Conversely, negatively supercoiled DNA, which also creates compensatory plectonemes, facilitates the unwinding of the helix and is therefore helpful in such situations, but must still be carefully regulated to avoid the disruption of other cellular processes (Bates & Magnan, 2015; Dabney et al., 2013; Naughton et al., 2013).

Yeast topoisomerase II is homodimeric with a jaw shape and contains several domains shared between the two monomers (Martínez-García et al., 2013; Corbett & Berger, 2003). The GHKL (Gyrase-Hsp90-Histidine Kinase-MutL) and Transducer domains form the ATP hydrolysis centre and sit at

the N-gate of the enzyme (Schmidt et al., 2012; Lotz & Lamour, 2020). The DNA-gate is composed of the TOPRIM (topoisomerase-primase), WHD (winged-helix domain) and Tower coiled-coil domains. A subsequent coiled coil domain also forms the C-gate (Figure 6B). Finally, there is an intrinsically disordered C-terminal domain (CTD) shared between the two monomers (Dougherty et al., 2021). The CTD experiences high post-translational modification, which helps regulate its substrate selection, localisation, catalytic activity and interactions with other protein factors. According to the clamp model, an intact gate segment first enters the clamp through the N-gate, anchoring to the cleavage-rejoining centre at the DNA-gate (Roca & Wang, 1992). A second DNA transport segment can then follow the same path and be trapped by the bridging of the ATP hydrolysis centres once they bind an ATP molecule. Subsequently, the catalytic centre of the enzyme produces a double-strand break on the gate segment, allowing passage for the intact transport segment upon hydrolysis of one ATP molecule (Worland & Wang, 1989). Finally, the C-gate serves as the exit point, first for the transport segment, and following religation, for the gate segment, releasing the newly generated topoisomer (Roca & Wang, 1994; Roca et al., 1996). The enzyme then hydrolyses the last bound ATP molecule to return to its original state (Baird et al., 1999; Baird et al., 2001). Therefore, the activity of topoisomerases is essential to maintain a physiological balance of catenated, knotted and supercoiled species in intracellular chromatin (Liu et al., 1980).

1.9.2 DNA knots

DNA knots are naturally occurring cis-topological entanglements found throughout chromatin *in vivo* (Valdés et al., 2017). Evidence for this in eukaryotes comes from studies on chromatinized plasmids rather than chromosomal DNA. In terms of the latter, contact map studies have not been able to identify DNA knots, a finding often attributed to the low resolution of the technique (Schmitt et al., 2016; Denker & Laat, 2016; Valdés et al., 2017). It is nevertheless possible that they may form within smaller DNA segments, a question that remains unanswered. In bacteria, knotting can be induced *in vivo* in plasmids by inactivating DNA gyrases and topoisomerases, but knots also arise spontaneously during DNA replication behind the fork (Shishido et al., 1987; Sogo et al., 1999). Biochemical reconstitution on plasmid DNA has shown that unremoved knots pose a physical obstacle to DNA-acting enzymes, hindering transcription and nucleosome formation (Rodríguez-Campos, 1996; Portugal & Rodríguez Campos, 1996). However, evidence of their function is lacking. Just as with DNA catenation, the activity of type IIA topoisomerases is directly involved in generating and removing knots, but how it is regulated in space and time also remains unclear (Figure 6A) (Liu et al., 1980). Interestingly, the local topological state of DNA adjacent to topoisomerase II substrates influences its knotting and unknotting rates. *In vitro*, compacted DNA, whether achieved by supercoiling, condensation or other factors, promotes knotting, whereas simpler topological states and naked DNA favour the opposite (Valdés et al., 2019). An interesting aspect of knotting

dynamics is the correlation between knotting probability and DNA length (Valdés et al., 2017). Whereas *in vitro* the extent of knotting grows indefinitely at a constant rate with bigger plasmids, *in vivo*, this only occurs to a maximum of 4 kb. Past this size threshold, plasmids experience knotting probability gains increasingly more subtly the longer they are. The fact that there is a threshold indicates a potential regulatory mechanism or a series of them that exist in cells to prevent the formation of excessive genomic obstacles with catastrophic consequences (Valdés et al., 2017; Rybenkov et al., 1997; Fernández et al., 2014; Sen et al., 2016; Piskadlo et al., 2017). In this regard, condensin has recently been found to promote the resolution of knots by topoisomerase 2 in plasmids (Dyson et al., 2020). However, the interplay between this activity and cohesin and other SMC complexes is not known.

1.9.3 DNA catenation

DNA catenation refers to the physical intertwining between two different DNA molecules and is an unavoidable consequence of DNA replication (Hudson & Vinograd, 1967). DNA catenation was first observed in HeLa cells as interlocked circular DNAs (catenanes) employing caesium chloride-ethidium bromide density gradients of mitochondrial DNA extracts (Hudson & Vinograd, 1967). Later experiments described topoisomerase II as the enzyme responsible for their turnover and generation (Baldi et al., 1980; Kreuzer & Cozzarelli, 1980). Additionally, DNA catenation also arises from

the rotation of the advancing replication fork (precatenanes) (Bermejo et al., 2012; Olof & Alexander, 1980). The budding yeast Fork Protection Complex (FPC) negatively regulates this event to prevent excessive intertwining of replicated DNA and genotoxic stress (Schalbetter et al., 2015). However, structurally complex regions that suppress topoisomerase II activity require the extra unwinding energy provided by fork rotation, albeit at the expense of transferring the topological stress onto the newly replicated DNA in the form of precatenanes. These can then be resolved by topoisomerase II (Figure 6A). A number of these catenations survive until mitosis, and are only resolved following Scc1 cleavage in anaphase, the reason for which has remained elusive (Baxter & Aragón, 2010). Furthermore, inactivation of topoisomerase 2 after S phase results in unresolved anaphase bridges and errors in segregation, indicating their resolution is necessary to complete mitosis.

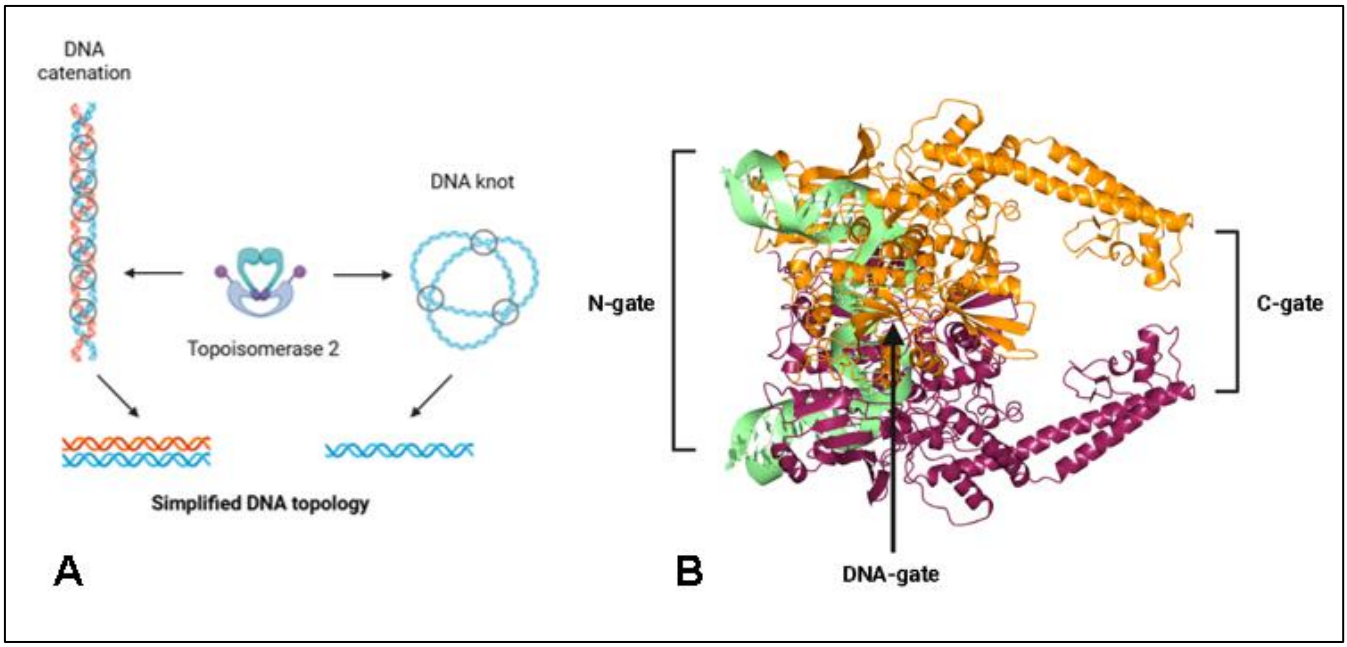

Figure 6. The interplay between topoisomerase 2 and DNA topology. A DNA knots and catenation are resolved by topoisomerase 2. **B** Structure of human topoisomerase IIA in complex with DNA bound to the gate segment at the DNA-gate (C-terminal domain not shown). The N-gate in this conformation is closed (PDB ID: 2RGR, Dong et al, 2007). Each monomer of the enzyme is represented with a different colour. Made using Biorender and CCP4MG.

1.9.3.1 DNA catenation is a key feature of chromosome structure

DNA catenation links sister chromatids along the length of their arms but has been observed through fluorescence microscopy at a significantly higher density at and around centromeric DNA (Bauer et al., 2012). Supporting this, our lab recently revealed that around 30% of DNA in this region remains catenated in yeast cells arrested at the G-to-M interphase (G/M) (unpublished data). This catenation depends on the presence of cohesin, as depletion of Scc1 results in a dramatic decrease in the fraction of

catenated DNA. Cohesin, therefore, is required to maintain sister chromatid intertwining by preventing topoisomerase 2 cleavage, supported by the fact that co-inactivation of both enzymes rescues the phenotype to nearly WT levels of intertwining.

Several lines of evidence suggest that DNA catenation is not a mere byproduct of DNA replication, but instead is a key feature of interphase and mitotic chromosome structure. In this respect, DNA catenation is necessary for the maintenance of the three-dimensional shape of chromosomes and their condensation status (Bauer et al., 2012). More recent work in mammalian cells has elucidated the highly coordinated mechanism for their turnover in anaphase (Chu et al., 2022). As sisters separate under spindle forces, their intertwining progressively elongates, promoting their resolution by topoisomerase 2. This is thought to contribute to the timely segregation of chromatids and to ensure their regulated movement during the late stages of mitosis. Notably, sister chromatid decatenation by topoisomerase 2 in mitosis has been shown to depend on condensin, although the molecular details of this mechanism and how it interplays with cohesin are not well understood (Charbin et al., 2013).

1.9.3.2 Implication of DNA catenation in sister chromatid segregation

Due to the need to resolve it before segregation and the fact that cohesin ensures its maintenance on chromosomes, it has been hypothesised that DNA catenation could provide an alternative mechanism of cohesion (Murray

& Szostak, 1985). However, previous studies have shown that the artificial cleavage of Scc1 in metaphase allows sister DNAs to disjoin, arguing that cohesin provides the sole force against the mitotic spindle (Oliveira et al., 2010). To complicate matters further, plasmid dimers held together by cohesin remain in a dimeric form after being subjected to spindle tension despite dramatically losing DNA catenation (Farcas et al., 2011). In contrast, our lab has recently made a revolutionary discovery that changes the paradigm of what is known about cohesion. Our lab showed that pericentric sister loci in metaphase-arrested cells lose cohesion at a rate of ~50% when treated with ectopically overexpressed topoisomerase 2 from the Paramecium Bursaria chlorella virus (PBCV-1) (unpublished data) (Figure 7C). This enzyme exhibits exceptionally high decatenation activity in vivo and is capable of rescuing segregation defects caused by unresolved chromosomal DNA catenation (D'Ambrosio et al., 2008; Lavrukhin et al., 2000). This finding was later extended to show that catenated minichromosomes in G2/M-arrested cells are fully decatenated shortly after the enzyme is overexpressed (unpublished data). Importantly, PBCV-1 did not interfere with cohesin's capacity to co-entrap sister minichromosomes, as determined through differential sedimentation of minichromosome species extracted from metaphase-arrested cells followed by treatment with PBCV-1 topoisomerase 2 and agarose gel electrophoresis (unpublished data). This showed that PBCV-1 topoisomerase 2 resolves dimer fractions resulting from catenation but not from cohesin-mediated interlinking (unpublished data).

These results indicate that the loss of cohesion arises due to the decatenation of the sister chromatids.

Moreover, previous experiments from our lab have revealed that DNA catenation follows the same pattern as cohesin, accumulating at pericentromere borders under spindle tension (unpublished data) (Figure 7A). Interestingly, this feature is compromised when Pds5 is degraded in metaphase-arrested cells, which results in a dramatic loss of catenated DNA at pericentromere borders (Figure 7B). Inactivation of Pds5 has been shown to abolish sister DNA co-entrapment by cohesin, thereby resulting in a complete cohesion loss, which could be the reason for such a severe phenotype (Srinivasan et al., 2018). In contrast, the degradation of Pds5 in G2/M-arrested cells does not cause a meaningful decrease in the fraction of catenated DNA at centromeres (unpublished data). Collectively, these findings suggest that while Pds5 is essential to retain catenation at pericentromere borders under spindle forces, it is not necessary to protect them from topoisomerase 2.

If DNA catenation were mediating cohesion, its co-localisation with cohesin under tension would explain why spindle microtubules can separate sister centromeres but fail to do so past pericentromere borders. The combined action of cohesin and DNA catenation might therefore underpin the molecular glue that tethers sister chromatids and prevents their premature separation. Cohesin could therefore mediate cohesion through sister DNA

intertwining, or in addition to it, a question that has thus far remained unresolved.

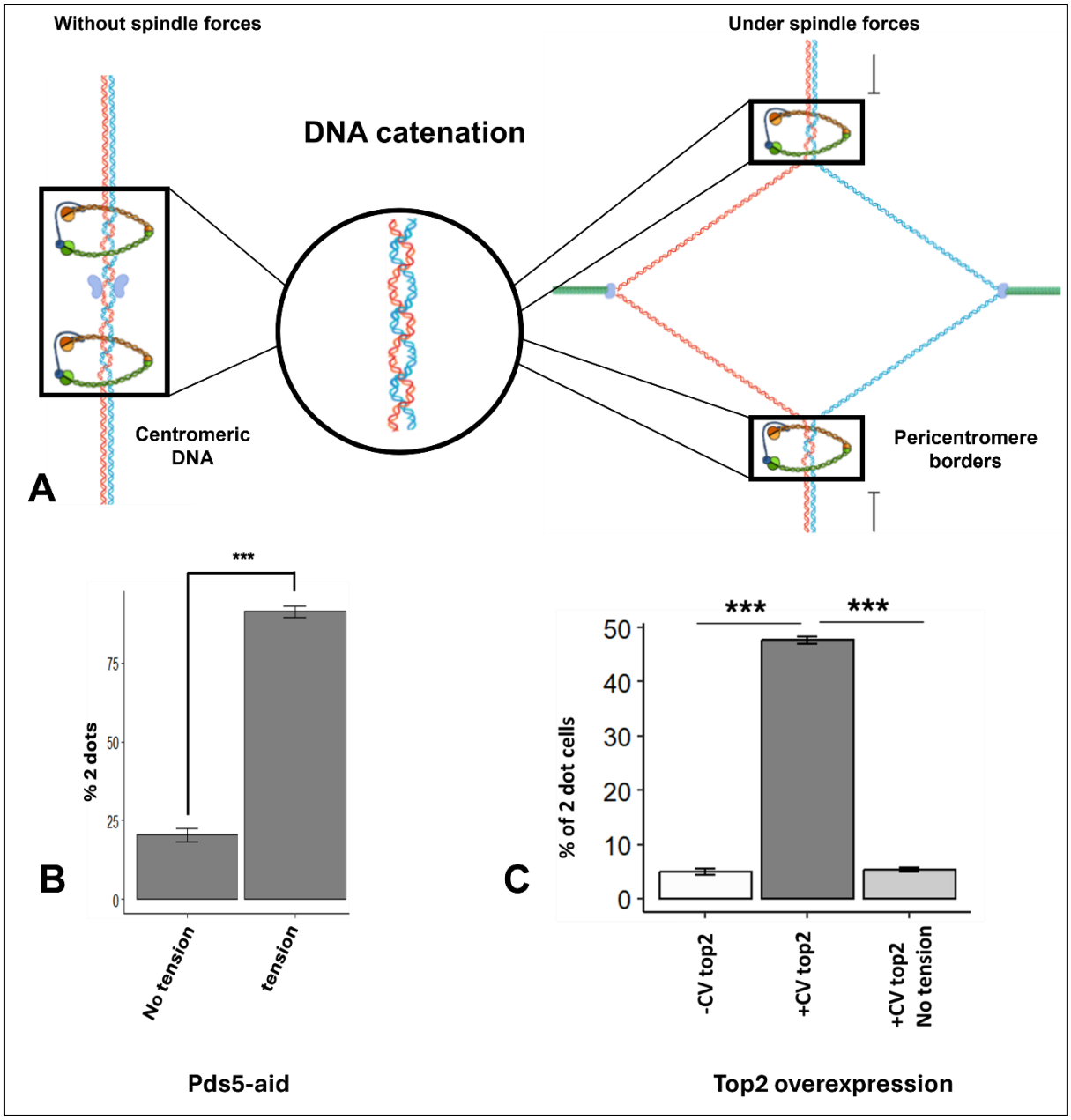

Figure 7. DNA catenation is redirected to pericentromere borders under tension. A Schematic showing the location of chromosomal DNA catenation (left) without spindle forces and (right) under spindle forces. **B** Bar chart comparing the percentage of sister loci near the pericentromere border split without tension

(G2/M) and under tension (Metaphase) in cells depleted of Pds5 following cell cycle arrest (Data not published). **C** Bar chart comparing the percentage of split sister loci near the pericentromere border in cells expressing (middle and right) and not expressing (left) PBCV-1 topoisomerase 2 under tension and without tension. Graphs **B** and **C** were made by Dr Aditi Kaushik.

1.10 Aims of the project

1st aim

Cohesin is known to provide cohesion to sister chromatids to withstand spindle forces until bipolar attachment is ensured. However, the mechanism mediating this function is not completely understood. DNA catenation could potentially be involved in resisting spindle forces to maintain cohesion, but this has never been addressed in real chromosomes and studies using plasmids have failed to provide a reliable conclusion.

The finding that triggering the artificial decatenation of sister chromatids results in their separation makes a strong case for catenation as a direct mediator of cohesion. Hence, I planned to follow up on this finding by assaying the ability of DNA catenation to hold sister chromatids in the absence of functional cohesin. Firstly, this would confirm or refute the idea that DNA catenation can provide cohesion. Secondly, it would reveal whether this role is dependent on cohesin. For this matter, I created a strain carrying the thermosensitive alleles *scc1-73* and *top2-4*, which allow the inactivation of cohesin and topoisomerase 2 at the restrictive

temperature by interfering with protein folding, respectively. These cells accumulate DNA catenation despite lacking functional cohesin, offering a chance to observe whether and to what extent these structures can hold sister chromatids together. By tracking tagged sister loci using fluorescence microscopy, it is possible to assess whether cohesion has been lost at different points of the cell cycle.

2nd aim

As previously described, cohesin safeguards DNA catenation from topoisomerase 2, but how this is regulated at the molecular level is unknown. Additionally, cohesin performs loop extrusion and provides cohesion by interacting with DNA through different topological mechanisms. It is challenging to study loop extrusion by cohesin, as no mutations have been found that only abolish this activity without compromising its dynamics on DNA. I therefore focused on understanding whether cohesin-mediated cohesion is involved in protecting DNA catenation.

Our lab recently revealed that cells depleted of Pds5 retain nearly WT levels of DNA catenation at centromeres in G2/M. Pds5 depletion abolishes cohesion, as it is essential for its maintenance. This result indicates that non-cohesive cohesin is still able to prevent DNA catenation resolution. I therefore sought to validate this finding by studying whether this effect is seen in the G1 phase, when cells naturally lack cohesion, as sister DNAs have not yet been generated. More specifically, this effect was studied in the late G1 phase, as Scc1 is not detected on chromatin until then

(Uhlmann & Nasmyth, 1998). Since DNA catenation does not exist in G1, DNA knots were employed as a model to study DNA catenation in this phase. For this purpose, I designed an episomal CEN plasmid incorporating the centromere sequence of budding yeast chromosome 2 and 9.3kbp into the right arm (CEN2 plasmid), which was used for all the DNA knotting assays. The capacity of cohesin to prevent knot resolution was studied in a newly created strain carrying this plasmid and the thermosensitive allele *scc1-73*.

3rd aim

The condensin SMC complex is necessary to complete chromosome segregation, which has been linked to its capacity to promote topoisomerase-2-mediated resolution of DNA knots and catenation. However, how this activity is regulated is not well understood. Moreover, how cohesin and condensin modulate topoisomerase 2 activity to orchestrate the topological changes in the DNA has never been studied before. Thus, I expanded the findings from the G1 knot assays by studying the interplay between cohesin and condensin in regulating DNA catenation. For this purpose, I employed the strain mentioned above, in addition to one carrying the thermosensitive allele *smc2-8,* which also incorporated the 9.3kbp CEN2 plasmid. This assay assesses the impact of inactivating condensin and cohesin on the catenation state of the CEN2 plasmid *in vivo,* providing quantitative insights into the mechanism underlying this phenomenon.

4th aim

DNA catenation, like cohesin, relocalizes to pericentromere borders under spindle forces in metaphase. Nevertheless, how it is able to stop at these sites and whether cohesin, through any of its functions, is involved is unknown. If catenation were mediating cohesion, it is plausible that the capacity of cohesin to provide cohesion by co-entrapment of sister chromatids could serve to stop the sliding of DNA catenation. This could allow them to accumulate at the same site and collaboratively resist spindle forces. This idea is consistent with the fact that abolishing cohesin entrapment by degrading Pds5 when sister chromatids are under tension results in the loss of DNA catenation from pericentromere borders. However, it is also possible that the phenotype is driven by the lack of Pds5 per se. As a result, I decided to expand this finding by experimenting with a newly created *eco1Δwpl1Δ* strain, in which cohesin, unlike the previous one, can co-entrap sister DNAs. I first evaluated the presence of DNA catenation at the pericentromere of chromosome 4 under spindle forces in this strain by gel electrophoresis and Southern blotting. Cohesion in this genetic background has been measured at centromeric (*TRP1*) and distal arm (*LYS4*) loci, revealing a significant cohesion defect in both G2/M and metaphase-arrested cells (Guacci & Koshland, 2012). I therefore planned to follow up by measuring cohesion under spindle forces closer to the pericentromere border, at the *SOK1-TRP1* intergenic region, from now on referred to as PeriCEN. Next, I compared the result with the amount of local DNA catenation maintained. Bearing in mind the results from the Pds5-depletion assay, this setup allowed me to determine whether the phenotypes seen

are caused by the absence/presence of cohesin-mediated cohesion or the proteins involved.

5th aim

PBCV-1 topoisomerase 2 is fully functional and highly active in all the properties of eukaryotic type 2 topoisomerases. Interestingly, it is the smallest type 2 topoisomerase known to date, extending only 1,061 amino acids in length (Lavrukhin et al., 2000). This is partly due to the lack of a C-terminal extension, which is present in all yeast and human topoisomerase 2. If this feature contributes to its capacity to resolve sister chromatids in yeast cells, this could be replicated in eukaryotic topoisomerase 2 lacking a functional C-terminal domain. This domain spans a region starting around residue 1177 and ending at the final residue 1428 of the *S. cerevisiae* enzyme (Schmidt et al., 2012).

I therefore set out to investigate whether expressing two truncated versions of *S. cerevisiae* topoisomerase 2 at residues 1166 and 1220 had a meaningful effect on sister chromatid cohesion. The former truncation has been shown to retain decatenation activity *in vitro* to wild-type levels, while failing to complement *TOP2* deletions and *top2-4* mutations in yeast, likely due to the disruption of its nuclear localisation (Caron et al., 1994). Conversely, the latter decatenates DNA both *in vivo* and *in vitro* and allows minimal cell survival in *top2-4* and *TOP2Δ* yeast strains. For this experiment, I cloned each of the truncated proteins into a plasmid vector under the control of the *GAL1* promoter, allowing their overexpression upon the

addition of galactose to the culture. As in our previous PBCV-1 topoisomerase assay, I measured sister chromatid cohesion under spindle forces at the PeriCEN. If the truncated proteins have lost the regulation of their decatenation activity, high rates of cohesion loss should be observed. This would point to the C-terminal domain of topoisomerase 2 as a key intermediary of the cohesin-dependent protection of chromosomal DNA catenation.

2. Results

It has long been speculated that DNA catenation could provide sister chromatid cohesion in addition to cohesin. However, the idea that cohesin drives cohesion has partly shifted the focus away from DNA catenation and its role in the process. Current evidence indicates that persistent DNA catenation contributes to the formation of anaphase bridges and erroneous sister chromatid segregation, yet its role in tethering sister chromatids remains unaddressed (Uemura et al., 1987). To this end, I employed a set of methodologies that allow the quantification of catenated DNA and sister chromatid cohesion of yeast chromosomes *in vivo* as the cornerstone of all the experiments performed here. The quantification of DNA catenation can be performed by agarose gel electrophoresis followed by Southern blotting

of DNA extracted from fixed cells. The DNA employed for analysis here was either in a circular DNA loop-out form (loop-out), in which regions of chromosomes are excised and circularised, or in plasmid form.

Chromosomal DNA loop-outs can be performed by using the Cre-lox recombination system (Sternberg & Hamilton, 1981; Hoess et al., 1982; Abremski & Hoess, 1984). This consists of employing two 34-bp-long LoxP DNA sequences flanking the region of interest, which serve as target sites for the Cre recombinase. This protein cleaves and circularises the DNA, forming a circular DNA loop-out (Figure 8A). Therefore, by overexpressing Cre under the *GAL1* promoter, it is possible to obtain large amounts of looped-out DNA, which can be in dimeric form if the original chromosomal DNA was catenated, or in monomeric form if it was uncatenated. Loop-outs in this study were performed on chromosome 4 at pericentromere borders (~3.5kbp loop-out) and on chromosome 3 at the CEN locus (5kbp loop-out) (Figure 8B).

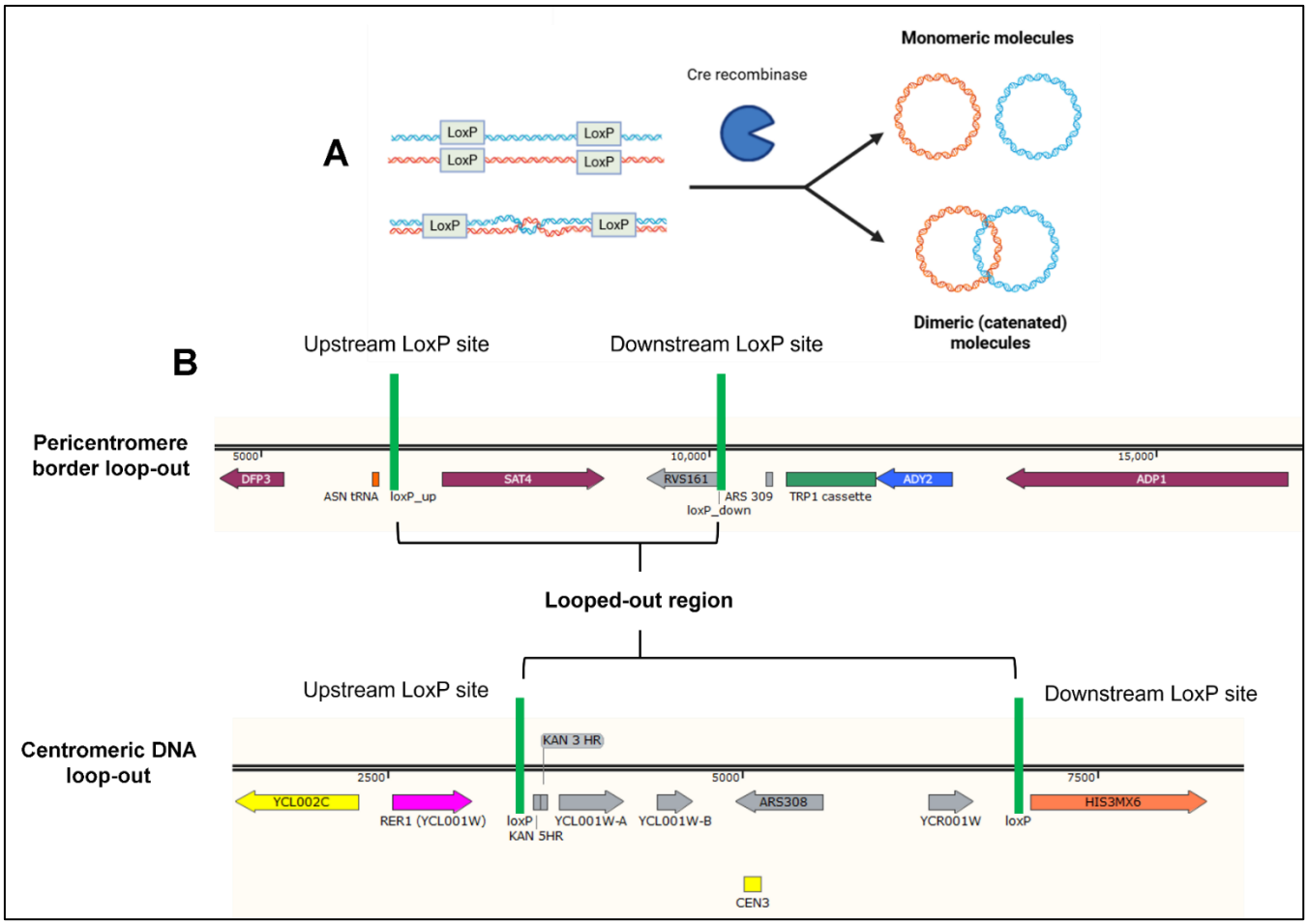

Figure 8. The Cre-LoxP system. A Schematic diagram of the Cre-LoxP system. LoxP sites are inserted into the DNA. Once the Cre recombinase is expressed, the DNA flanked by LoxP sites becomes circularised, creating monomeric or dimeric molecules. **B** Maps of pericentromere border loop-outs (top) and centromeric loop-outs (bottom) performed in this study.

Both one-dimensional and two-dimensional gel electrophoresis can be employed to analyse DNA topoisomers, which provide different insights. While the former allows a direct comparison of catenated vs uncatenated DNA by means of differentially migrating bands, the latter shows the knotted fraction of the samples. One-dimensional gel electrophoresis allows

the measurement of band intensity as a readout of the DNA fraction of a specific weight. Since catenated circular DNA molecules migrate twice as slowly as uncatenated monomers, this method allows the unambiguous separation of the different DNA forms.

The method of choice to measure cohesion *in vivo* was the fluorescence microscopy tracking of GFP-tagged chromosomal loci, extensively used in the field for the same purpose. By visualising the intracellular position of and distance between sister DNA loci, one can infer whether cohesion has been lost at this site. If a single GFP dot is observed within a cell, sister loci remain tethered, whereas if two dots are seen, sister loci have split, and cohesion has been lost. The percentage of cells under determined conditions (tension/no tension) that present 1 GFP dot gives a readout of the degree of cohesion preserved in the genetic background studied. Note that the region of choice to study DNA catenation in all the assays described here was the pericentromere border.

2.1 DNA catenation is insufficient to hold sister chromatids under spindle tension

Following our conclusion that cohesin cannot fully resist spindle forces without DNA catenation, I aimed to test the capacity of catenated chromatids to resist these forces in cells lacking functional cohesin. As shown in previous studies, thermal inactivation of topoisomerase 2 using the *top2-4* allele leads to the accumulation of DNA catenation on

chromosomes (Charbin et al., 2013). For this experiment, I also used the *scc1-73* temperature-sensitive allele of cohesin that prevents the formation of a complete cohesin ring by disrupting the Scc1-Smc1 interface at the restrictive temperature. Combining *top2-4* with *scc1-73* allows the co-inactivation of topoisomerase 2 and cohesin, which, according to previous data, should lead to the maintenance of preformed catenation. Thus, any cohesion these cells may have would be entirely mediated by DNA catenation.

Our lab recently showed that budding yeast carrying the *scc1-73* allele displays split centromeric sister loci at a rate of 44% under a G2/M arrest at the restrictive temperature, whereas the incidence in double *scc1-73 top2-4* mutants decreases to 17% (unpublished data). The capacity of DNA catenation to hold sister loci without cohesin prompted us to investigate this effect when sister chromatids are subject to spindle forces in metaphase. Since spindle forces redirect DNA catenation to pericentromere borders, I decided to study the splitting of sister loci located in this region. Two budding yeast strains carrying either *scc1-73* alone or combined with *top2-4* were employed. Fluorescence microscopy was used to measure cohesion as previously described; thus, these strains also carried a GFP-tagged PeriCEN sister loci and a TdTomato red tag on Spc42, a protein composing the spindle body. While the GFP tag allows the scoring of local cohesion, the red tag can help facilitate the discrimination between arrested cells and separate, clumped cells. The cells were synchronised in early G1 with α-factor and released into nocodazole-containing media for 90 minutes

at the permissive temperature (25°C). Nocodazole is a spindle poison that prevents the polymerisation of spindle microtubules, thereby abolishing spindle forces and triggering the SAC. Once the G2/M arrest was confirmed by light microscopy, the cultures were shifted to the restrictive temperature (37°C) for 90 minutes. The cells were then fixed, and the dot-counting assay was performed as described in the methods. I find that 65% of G2/M-arrested *scc1-73 top2-4* double mutant cells retain tethered chromatids at 37°C, whereas only 21% of *scc1-73* single mutants do so, as evidenced by a single GFP dot (Figure 9A). The experiment was then repeated in a metaphase arrest with strains expressing a methionine-repressive version of the APC cofactor Cdc20 under the *MET3* promoter to assess the impact of spindle forces. Following synchronisation in G1, cells were released for 90 minutes at 25°C into methionine-containing YEP media + 2% glucose (YEPD), to which an additional 8mM methionine was added. After 60 minutes, an additional 4mM methionine was added. Upon confirmation of the metaphase arrest after 90 minutes, the cultures were shifted to 37°C for another 90 minutes. The cells were then fixed for fluorescent microscopy, and cohesion was measured. Nearly all cells, regardless of their genetic background, displayed split sister PeriCEN at 37°C (Figure 9B). Several conclusions can be made from these data. Firstly, it confirms that DNA catenation in chromosomes requires cohesin for protection against topoisomerase 2-mediated resolution *in vivo*. Secondly, since cohesin can still moderately hold sister chromatids under spindle forces without catenation but catenation cannot do so without cohesin, it

indicates that cohesion under spindle forces is first dependent on cohesin. Finally, it shows that DNA catenation alone exerts enough cohesive force to hold sisters together without spindle tension to some extent but fails to do so when tension is applied in metaphase. The last two points could be explained by the likely role of cohesin to prevent the sliding of catenation past pericentromere borders. Despite its self-evident nature, this implies that catenation cannot be the sole mechanism of cohesion in cells, which aligns with the overwhelming evidence of cohesin-mediated cohesion reported in the literature. Collectively, these results, together with our previous finding of cohesin's reliance on DNA catenation, provide, for the first time, definitive evidence of a cooperative cohesion mechanism mediated by both cohesin and DNA catenation.

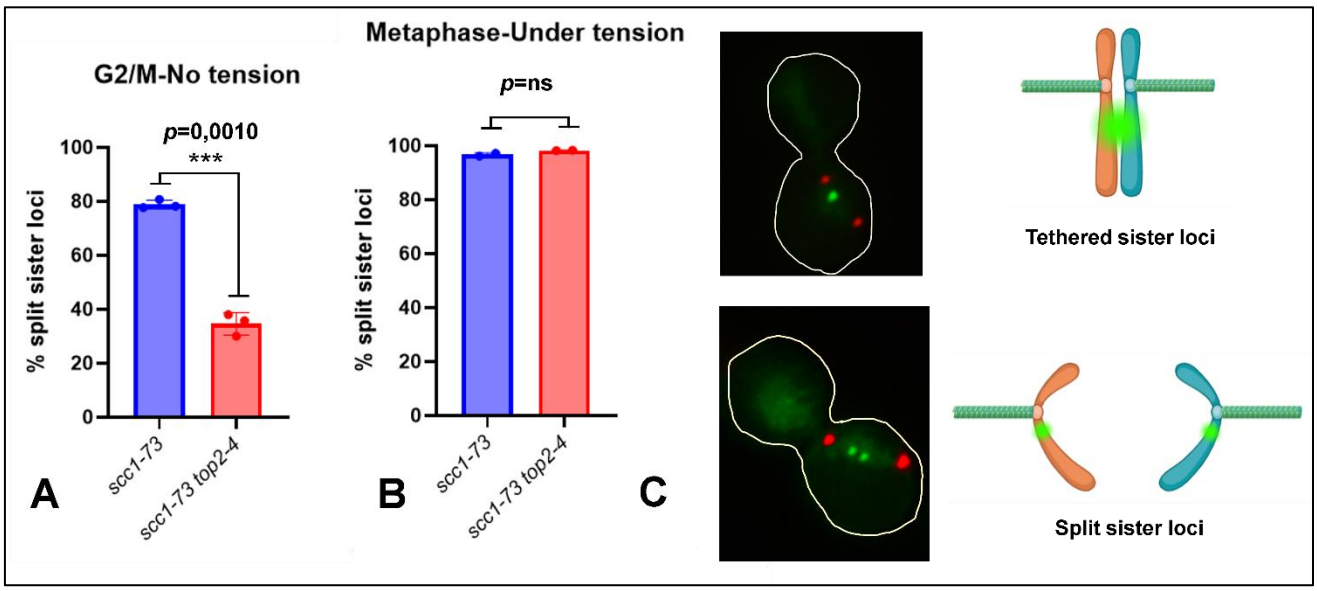

Figure 9. DNA catenation cannot hold sister loci under spindle tension without functional cohesin. Bar charts showing the difference in the percentage

of split sister loci between *scc1-73* and *scc1-73 top2-4* cells, **A** in the absence of spindle tension (Welch's t-test performed (p-value=0.0010)) (3 biological repeats, n=253 cells per repeat for *scc1-73*, n=268 cells per repeat for *scc1-73 top2-4*), and **B** under spindle tension (Welch's t-test performed (p-value=ns)) (2 biological repeats, n=210 cells per repeat for *scc1-73*, n=205 cells per repeat for *scc1-73 top2-4*). **C** Depiction of arrested cells displaying tethered (top) and split (bottom) GFP-tagged sister loci. Red dots represent TdTomato-tagged Spc42.

2.2 DNA knots in G1 are maintained by cohesin

Knowing the importance of DNA catenation in cohesion, I next aimed to study how they are generated and turned over. Previous experiments demonstrated that DNA catenation relies on cohesin to exist in chromatinized plasmids, a phenomenon we have previously extended to show that it also applies to chromosomal DNA catenation (Farcas et al., 2011). Nevertheless, how cohesin mediates this protection remains unknown. Broadly, there are four main cohesin populations in cells: soluble, dynamically DNA-binding, loop-extruding, and topologically entrapping complexes. It is plausible that cohesin could simply bind to DNA in a way that blocks the access of topoisomerase 2 to DNA catenation, whether by topological entrapment or non-topological binding, therefore inhibiting their resolution. However, loop extruding complexes could also impose physical constraints on topoisomerase 2 by means of rearranging the local topology of DNA. Farcas et al. revealed in 2011 that catenated fractions of a 26kb minichromosome are lost when yeast cells carrying the temperature-

sensitive *eco1-1* allele undergo replication at the restrictive temperature, concluding that cohesion is required for DNA catenation to exist (Farcas et al., 2011). However, our lab recently found that AID-mediated degradation of Pds5 does not significantly reduce the fraction of catenated DNA at centromeres in G2/M-arrested cells (unpublished data). Since Pds5 is essential to establish and maintain cohesion, this indicates that DNA catenation is maintained independently of Pds5 and, therefore, sister chromatid cohesion.

I decided to investigate this matter further by testing whether the same applied in G1 budding yeast cells, which naturally lack cohesion, as this phase precedes DNA replication and therefore sister chromatids have not yet been generated. The lack of sister chromatids also signifies that DNA catenation is absent in G1, in line with previous plasmid assays showing all DNA in G1 phase in monomeric form. Hence, I decided to employ DNA knots as a model to study DNA catenation in G1. In contrast to DNA catenation, knots are intramolecular entanglements, but both share a common turnover mechanism mediated by topoisomerase 2 and the geometry of their DNA crosses. Dyson et al. showed in 2021 how inactivating condensin results in increased knotted plasmid fractions, concluding that this protein is necessary for topoisomerase 2 to resolve DNA knots (Dyson et al., 2021). However, the role of cohesin and how SMC complexes are coordinated to mediate their turnover, maintenance and generation are not well understood.

For this experiment, I employed 2-dimensional agarose gel electrophoresis, which offers a way to analyse knots according to their shape and topological complexity, and differentiate them from other DNA fragments of similar size (Figure 10A). The process requires the nicking of the sample, whereby supercoiled DNA is relaxed to prevent its interference with the migration speed of the molecules, but the topologies are maintained (Valdés et al., 2017; Valdés et al., 2019). The first electrophoresis run is performed at a low voltage (25V), which allows the relaxed molecules to travel according to their volume, proportional to the number of strand crossings, with the more entangled molecules travelling fastest and the unknotted molecules travelling the slowest. The second dimension reveals the knotted molecules, as the linear DNA fragments in the sample with similar migration profiles in the first dimension now separate due to their increased gel mobility caused by the higher voltage (125V) employed in this dimension (Valdés et al., 2017; Valdés et al., 2019).

DNA knotting was studied in the CEN2 plasmid previously described. Two experimental strains were employed: one carrying the *scc1-73* allele and another a wild-type *scc1* (WT) strain, allowing the analysis of the role of cohesin in regulating the balance of DNA knots throughout the G1 phase. These strains also expressed a non-degradable version of Sic1 under the control of the *GAL1* promoter, which prevents entry into S phase. Cells were grown overnight in -TRP (tryptophan) media + 2% raffinose and synchronised in early G1 by the addition of α-factor for 150 minutes. At minute 60 of the arrest, the cells were shifted to YEP media + 2% GAL

(YEPgal) to induce the expression of non-degradable Sic1 for the remaining 90 minutes of α-factor-arrest induction. This allows the arrest of cells at the G1/S interphase. Once the α-factor arrest was confirmed, the synchronised cells were released by adding pronase (0.1mg/ml) at the permissive temperature for 90 minutes to allow Sic1-mediated G1/S arrest. The cells were then shifted to 37°C for 90 minutes. Analysis through gel electrophoresis and Southern blotting revealed a significant decrease in the knotted plasmid fraction upon inactivation of cohesin compared to WT (Figure 10B). This result validates the Pds5-depletion assay, corroborating cohesin's ability to maintain intra- and inter-chromosomal intertwines in a manner that does not require cohesion. This experiment, however, does not address the topological nature of the cohesin-DNA binding mechanism involved in mediating this function.

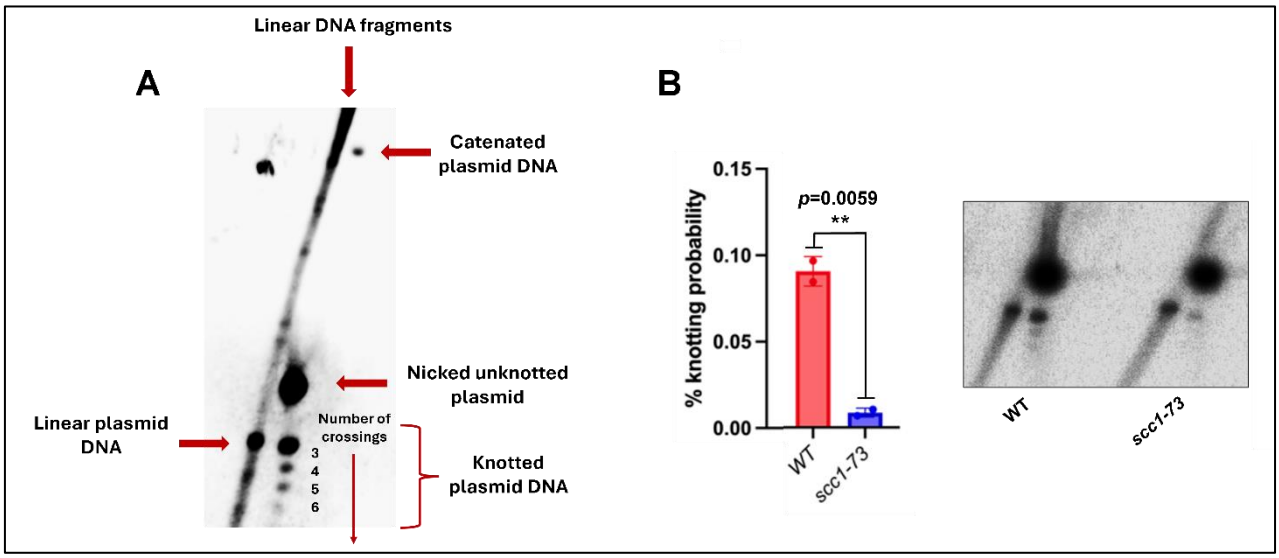

Figure 10. Cohesin protects DNA knots. A Example of 2-dimensional gel electrophoresis showing the different observable DNA species. **B** Bar chart and

Southern blot comparing the knotting probability of the CEN2 plasmid between the WT and *scc1-73* strains in 2 biological replicates (Welch's t-test performed (p-value *scc1-73* vs WT=0.0059)). The knotting probability was calculated with ImageJ by quantifying the signal intensity of the knotted minichromosome bands and normalising it to the total signal intensity of the nicked circular minichromosome DNA fraction.

2.3 Cohesin-mediated protection of DNA entanglements is antagonised by condensin-dependent topoisomerase 2 activity

Cohesin protects DNA catenation and knots, whereas condensin is instead required for their resolution. Nevertheless, there is much unknown about how these factors are coordinated in this context to determine when sister chromatids will be disentangled both inter- and intra-molecularly. To study the functional interplay between these proteins, I analysed the topology of the 9.3kbp CEN2 plasmid in G2/M-arrested cells. I employed the WT and *scc1-73* mutant yeast strains described above, in addition to a *smc2-8* mutant strain that allows the inactivation of condensin at 37°C. Cells were grown overnight in -TRP medium and then transferred to YEPD medium for the experiment the next day. The cell cultures were first synchronised with α-factor in early G1 and then released in the presence of 100mM nocodazole for 90 minutes at the permissive temperature. Once arrested in G2/M, the cells were shifted to an incubator at 37°C for 90 minutes before fixing them and extracting their DNA. 2D gel electrophoresis was then carried out for the three samples, and Southern blotting was performed to

visualise the distribution of plasmid topoisomers. Unfortunately, the area of the gel where the catenated plasmid fraction of the WT strain would have been observed was not included in the blot due to a mistake in the placement of the membrane for the transfer. Therefore, only the *scc1-73* and *smc2-8* strains were compared, which were expected to produce a decrease and an increase in the catenated DNA compared to the WT strain, respectively. In line with this, the inactivation of *scc1-73* cohesin showed a greatly decreased catenated plasmid fraction (8%) compared to the *smc2-8* strain (50.8%) (Figure 11A). To refine the results, I repeated the 2D gel and Southern blot. However, another misplacement of the membrane resulted in the uncatenated fraction of the smc2-8 strain sample being left out of the blot; therefore, the catenated fraction could not be quantified. Nevertheless, this blot confirmed my previous hypothesis, showing a higher level of catenated DNA in the WT (26.8%) strain compared to the scc1-73 strain (Figure 11B). An additional spot can be observed in both blots underneath the expected spot for the catenated minichromosome fraction, which corresponds to supercoiled species of this population. This spot resulted from the incomplete nicking of the DNA samples, and its signal was not included in the quantification. Collectively, these findings show that inactivation of condensin is enough to prevent the resolution and promote the accumulation of DNA catenation. Interestingly, the phenotypes of the strains in G1 are replicated in G2/M, showing the highest fractions of catenated and knotted plasmid in the *smc2-8* mutant, the lowest in the *scc1-73* single mutant. From these results, it can be concluded that a

conserved mechanism, driven by the constitutively opposing activities of cohesin and condensin, underpins the cell cycle-wide regulation of DNA knots and catenation.

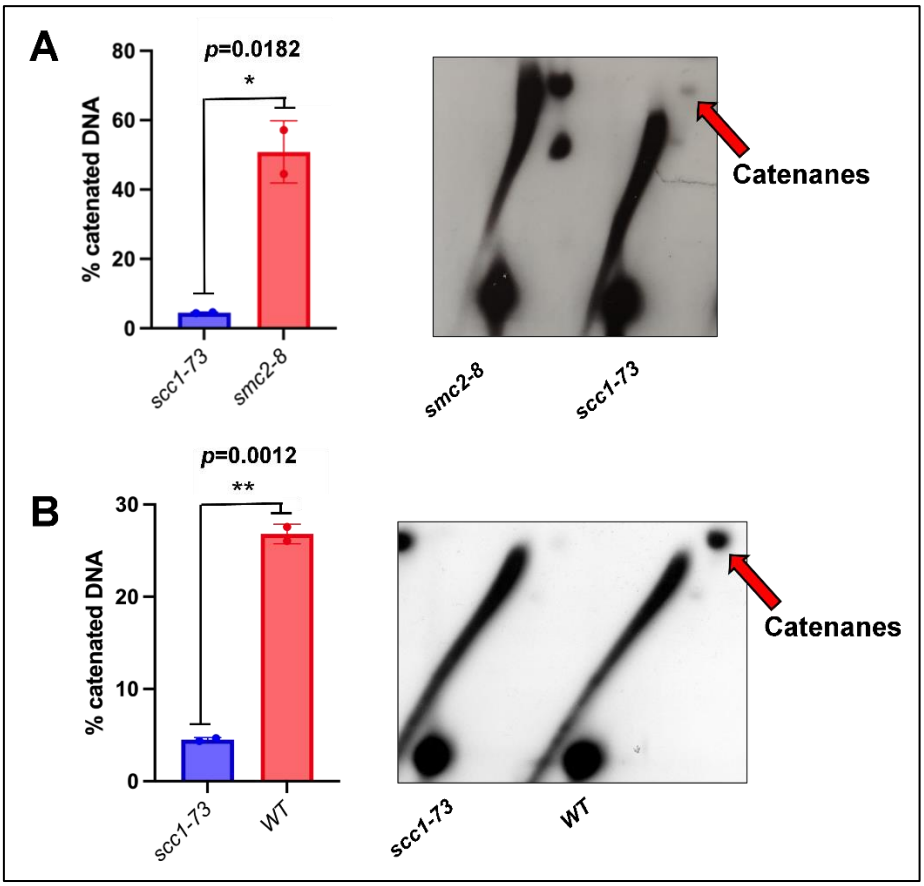

Figure 11. Cohesin and condensin have opposite roles in the regulation of DNA catenation. **A** Bar chart and Southern blot comparing the percentage of catenated CEN2 minichromosome between the *scc1-73* and *smc2-8* strains in 2 biological replicates (Welch's t-test performed (p-value= 0.0182)). **B** Bar chart and Southern blot comparing the percentage of catenated CEN2 minichromosome between the *scc1-73* and WT strains in 2 biological replicates (Welch's t-test performed (p-value= 0.0012)). The catenated minichromosome fraction of the *smc2-8* strain is shown for illustrative purposes but was not quantified.

2.4 Eco1 is not required for centromeric DNA catenation maintenance in G2/M

Since Pds5 is not required to protect DNA catenation, I extended this finding by studying the role of Eco1 in catenation maintenance. Eco1 is the acetyltransferase that acetylates the ATPase head of Smc3 to lock the cohesin ring around sister DNAs (Zhang et al., 2008). Pds5 and Eco1 are known to interact to regulate loop extrusion by cohesin (Dauban et al., 2020). Additionally, Pds5 facilitates and maintains Eco1-mediated acetylation of Smc3, thereby collaboratively influencing multiple cohesin functions (Chan et al., 2013). After several failed attempts to create a functional Eco1-AID strain, I instead decided to delete the *eco1* gene, which encodes Eco1. Since this deletion is lethal in budding yeast due to a complete loss of cohesion, I additionally deleted *wpl1*, which encodes the cohesin release factor Wpl1, whose absence partially rescues the viability of these cells. Deletion of *wpl1* alone causes a moderate cohesion defect, which is not yet understood, but is less pronounced than in *eco1Δwpl1Δ*. Comparing the amount of catenated DNA between *eco1Δwpl1Δ* and *wpl1Δ* cells could indicate whether Eco1 plays a role in promoting the maintenance of catenation on DNA. For this purpose, *eco1Δwpl1Δ* cells were first synchronised in early G1 by the addition of α-factor and subsequently released into YEP + 2% raffinose (YEPR) media containing nocodazole to 100μM to arrest them in the G2/M interphase. Galactose was then added

to make 2% of the total culture volume to induce the looping out of a 4kbp region of centromeric DNA of chromosome 3. One-dimensional gel electrophoresis followed by Southern blotting revealed little change in catenated DNA between *eco1Δwpl1Δ* and the *wpl1Δ* control strains, as evidenced by the similar band intensity shown in Figure 12. Although there is significantly less centromeric catenation in these strains than in WT (25-30%), that effect is almost completely driven by the deletion of *wpl1*, as simultaneously deleting *eco1* causes only a minimal extra loss. Eco1 has been reported to acetylate cohesin at several sites across the different subunits in addition to K112 and K113 for cohesion establishment, disruption of which results in variable levels of cohesion loss (Chao et al., 2017; Guacci et al., 2015). According to the finding reported here, not only does cohesin prescind of cohesion for protecting DNA catenation, but also largely of the acetylation events performed by Eco1, including those that precede cohesion establishment. These data also imply that any other function Eco1 performs, whether through its acetyltransferase activity or not, is not necessary in this context.

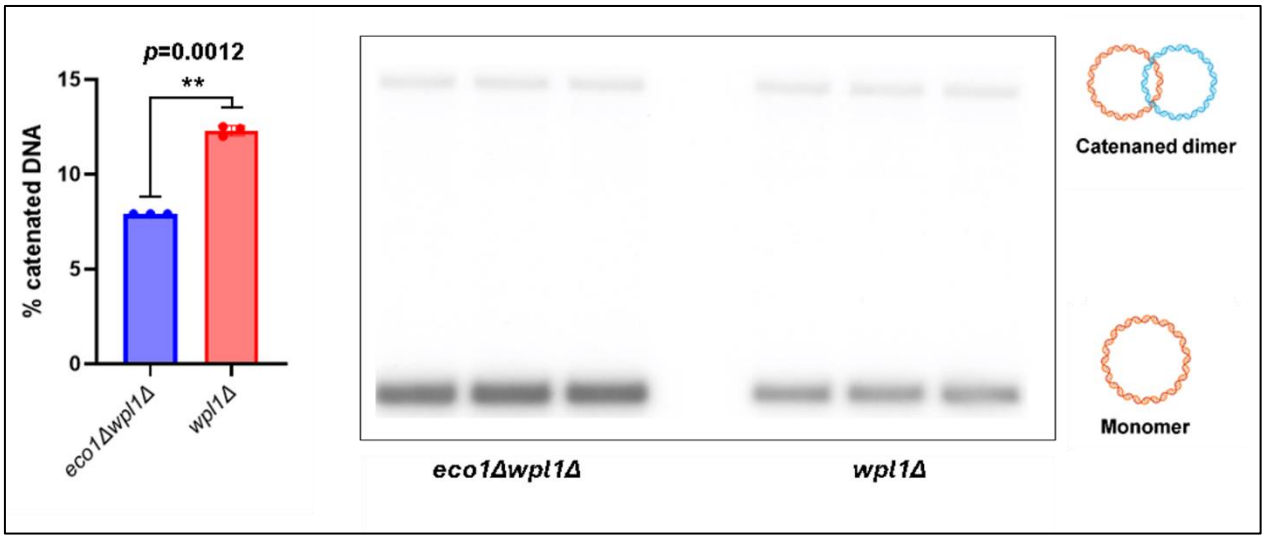

Figure 12. Deletion of *eco1* has a minimal effect on the fraction of catenated centromeric DNA in G2/M. (Left) Bar chart comparing the percentage of catenated centromeric DNA between *eco1Δwpl1Δ* and *wpl1Δ* cells in 3 biological replicates (Welch's t-test performed (p-value=0.0012)). (Right) Image of 1D agarose gel showing the difference in catenated centromeric loop-outs in *eco1Δwpl1Δ* and *wpl1Δ* cells. Note that the experiment was done in a *wpl1* deletion background to directly compare the effect of deleting *eco1*.

2.5 *eco1Δwpl1Δ* cells lose pericentric DNA catenation under spindle tension

The finding that depleting Pds5 results in the loss of pericentromeric DNA catenation from borders under spindle tension suggests that cohesin capable of co-entrapping sister chromatids, which is absent in these cells, is necessary to prevent this phenotype. This hypothesis prompted me to find a way to investigate this effect further. It is challenging to separate the cohesion-promoting function of Pds5 from the rest of its cohesin-specific

activities, as Pds5 mutations that abolish cohesion do so by disrupting its interaction with Scc1 (Muir et al., 2016; Lee et al., 2016). Therefore, I extended this result by assaying the effect of spindle forces on DNA catenation at the pericentromere borders in the absence of Eco1 using the *eco1Δwpl1Δ* genetic background. As opposed to Pds5-depleted cells, cohesin in *eco1Δwpl1Δ* cells is still able to co-entrap sister minichromosomes *in vivo*, although whether this applies to real chromatids is not clear (Srinivasan et al., 2018). Additionally, Eco1 is coordinated with Pds5 at many levels to promote and maintain cohesion and to regulate loop extrusion, making it an ideal next candidate to study (Panizza et al., 2000; Dauban et al., 2020). Importantly, both Pds5-depleted and *eco1Δwpl1Δ* cells preserve loop extruding cohesin (Petela et al., 2018; Dauban et al., 2020) and catenation within pericentromeres (unpublished data and Figure 12). However, Pds5-depleted cells are known to lack most cohesion at the pericentromere border, as shown using our lab setup (Figure 7B), whereas *eco1Δwpl1Δ* cells have been found to lack cohesion at several loci, including *LYS4*, *TRP1* and *URA3* (Guacci et al., 2015; Rowland et al., 2009). One caveat is that the distribution of the cohesion defect of *eco1Δwpl1Δ* cells across the chromosome is neither conserved nor understood. If *eco1Δwpl1Δ* cells preserve DNA catenation at borders under spindle forces, it could be because they retain the pool of cohesive cohesin at the border that is preventing their loss. If, in contrast, *eco1Δwpl1Δ* cells lose DNA catenation from the borders under spindle forces, it could be because cohesin in these cells may not be able to cohesively co-entrap

sister chromatids to prevent the sliding of catenation past the border. Because, as previously shown (Figure 9), cohesion under spindle forces is first dependent on cohesin, the first situation should be reflected by cohesion being maintained at the border, whereas the second situation should be reflected by cohesion being lost at the border.

For this matter, *eco1Δwpl1Δ* cells expressing Cdc20 under the *MET3* promoter were first synchronised in early G1 phase with α-factor for 2.5 hours and released by splitting the culture into two flasks. One flask contained YEPR media with an additional 8mM methionine to arrest cells under spindle forces by depleting Cdc20, and the other YEPR media with 100μM nocodazole to arrest them in the absence of spindles. The cells were left to grow for 90 minutes to arrest them in metaphase and G2/M, respectively. This allowed a direct comparison between the effect of present and absent spindle forces on catenated DNA. Galactose was then added to make up 2% of the culture volume to induce the looping-out of the pericentromere border region of chromosome 3 for 90 minutes, and the cells were harvested. Analysis through gel electrophoresis and Southern Blotting revealed that spindle forces in metaphase result in a major loss of catenated DNA at pericentromere borders in *eco1Δwpl1Δ* cells (Figure 13). In WT cells, DNA catenation contained within the pericentromere unavoidably slides to the borders under spindle tension (unpublished data), where it is stopped by cohesin (Figure 9). The net result is a redistribution of catenation that decreases at centromeres (from ~30% to ~5%) while it concomitantly increases at borders (from ~12% to 20%) (unpublished data).

This also means that under normal circumstances, DNA catenation at the border should be higher under spindle tension than in its absence. In contrast, *eco1Δwpl1Δ* cells show the opposite pattern, whereby DNA catenation at the border decreases when the kinetochores are subject to spindle tension (Figure 13). Cohesin is required to prevent the loss of catenation from the border (Figure 9), but which functional pool (cohesive or loop-extruding) is required for this event is unknown. These cells preserve loop extruding cohesin (Dauban et al., 2020), therefore raising the possibility that they may lack cohesive cohesin at the border, which could be the cause of this loss. As explained before, cohesion first depends on cohesin (Figure 9); therefore, the absence of cohesive cohesin co-entrapping sister chromatids in these cells could be reflected by the absence of cohesion at the border.

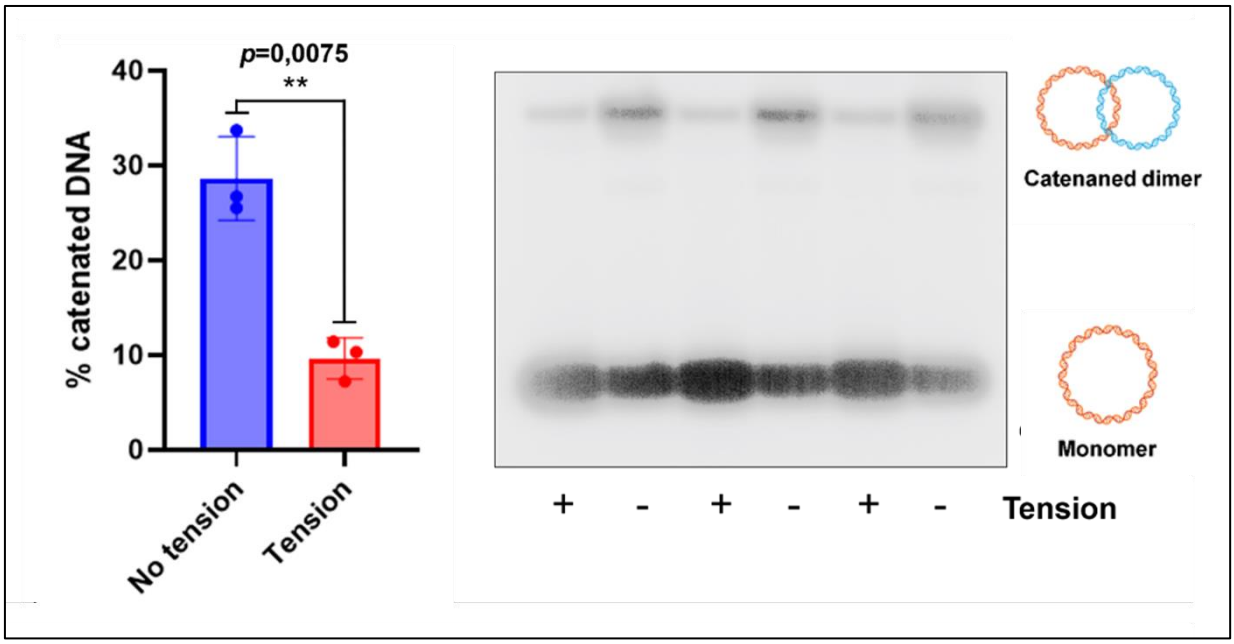

Figure 13. DNA catenation is lost from pericentromeric borders under spindle tension in *eco1Δwpl1Δ* cells. (Left) Bar chart comparing the percentage of catenated centromeric looped-out DNA in eco*1Δwpl1Δ* cells in the absence and presence of spindle tension in 3 biological replicates (p-value=0.0075). (Right) Image of 1D agarose gel showing the difference in catenated DNA loop-outs at the pericentromere border in *eco1Δwpl1Δ* cells.

2.6 *eco1Δwpl1Δ* cells present a significant cohesion defect at the PeriCEN

Cohesion in *eco1Δwpl1Δ* cells has been measured at centromeric proximal and distal loci, including *LYS4*, *TRP1* and *URA3*, revealing cohesion defects of up to 70% (Guacci et al., 2015; Rowland et al., 2009). It is nevertheless possible that these cells retain some degree of cohesion at other loci, which allows their survival. Since DNA catenation is lost from the pericentromere borders under spindle forces, I set out to investigate the

degree of cohesion preserved in this region. By knowing both parameters, it is possible to understand how cohesion and DNA catenation are coupled locally. To this end, I used fluorescence microscopy to track GFP-tagged sister PeriCEN (border locus) in *eco1Δwpl1Δ* cells under a G2/M arrest. As previously mentioned, this locus lies at the *SOK1-TRP1* intergenic region on chromosome 4. *SOK1* is one of the genes composing the right border of chromosome 4, and therefore, this setup allows the measurement of cohesion as close to the border as technically feasible with out setup. Since cohesion at *TRP1* was concluded to be only locally compromised (as measured by the distance between split GFP dots) (Guacci et al., 2015), it raises the possibility that other nearby regions may have a different degree of cohesion. The control strain employed for this experiment was *wpl1Δ,* which has been shown to exhibit a cohesion defect of 25-30% at the *TRP1* locus (Guacci et al., 2015). The historically observed differences in cohesion between *eco1Δwpl1Δ* and *wpl1Δ* result from the fact that Eco1 provides cohesion in a Wpl1-independent manner, and therefore the deletion of *wpl1* restores viability to *eco1Δ* cells without restoring cohesion (Guacci et al., 2015). As evidenced by the dot counting assay, PeriCEN sister loci in *eco1Δwpl1Δ* cells split at a rate of 70.2% (Figure 14), in line with the results obtained in previous studies (Guacci et al., 2015). In *wpl1Δ* cells, an unexpectedly low rate of cohesion loss of 10.25% was observed (Figure 14). For comparison, WT cells typically display a cohesion loss of ~5% when measured at the PeriCEN locus using this setup (unpublished data).

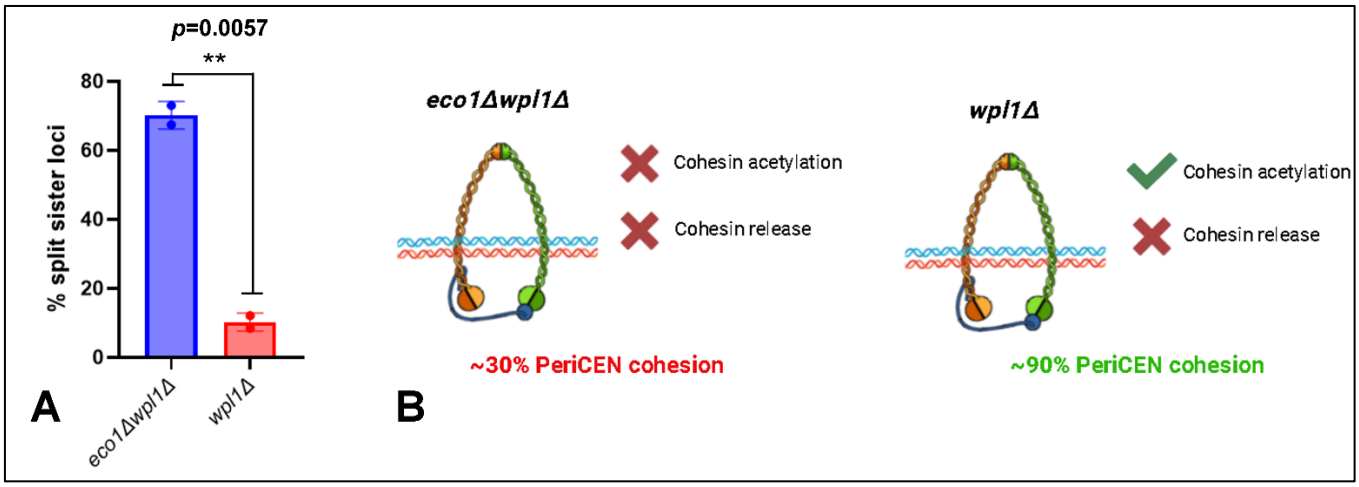

Figure 14. Cohesion is severely compromised in *eco1Δwpl1Δ* cells. A Bar chart comparing the percentage of split sister PeriCEN in *eco1Δwpl1Δ* and *wpl1Δ* cells arrested in metaphase in the absence of spindle forces (n=300 for each group). **B** Schematic summary of the results from the cohesion assay in the *eco1Δwpl1Δ* and *wpl1Δ* strains.

As previously shown (Figure 13), *eco1Δwpl1Δ* cells present a significant level of DNA catenation at pericentromere borders without spindle tension, yet under this condition, only 30% of cohesion is preserved (Figure 14). This is striking, since such a level of DNA catenation should be able to hold sister loci together to a much greater extent even without cohesin's assistance (Figure 9). Therefore, the cohesion provided by catenation appears to be compromised in *eco1Δwpl1Δ* cells, a phenomenon without explanation so far. Our lab has shown that cohesin can maintain nearly WT levels of cohesion in the absence of spindle forces, even when DNA catenation is artificially removed (Figure 7C right lane & unpublished data). Therefore, even if catenation-mediated cohesion was indeed compromised, cohesin-

mediated cohesion should still prevent the splitting of sister loci. This effect is not seen in the present experiment, indicating that these cells lack the cohesin pool capable of cohesively co-entrap sister chromatids. From these results, it can be concluded that the loss of DNA catenation from pericentromere borders under spindle forces is due to the loss of cohesive cohesin.

2.7 The C-terminal domain of *S. cerevisiae* topoisomerase 2 is required to prevent the premature resolution of sister chromatids

As previously explained, the overexpression of PBCV-1 topoisomerase 2 triggers a 50% loss of cohesion under spindle forces, arising exclusively from the decatenation of sister chromatids (Figure 7C & unpublished data). This unique capacity of this enzyme to produce such an effect, together with the fact that this is the only known topoisomerase 2 that naturally lacks a CTD, raises the following point. Although it is known that this protein possesses an intrinsically high decatenation rate, it is also possible that the lack of a C-terminal domain allows it to bypass the cohesin-mediated protection of DNA catenation to produce the aforementioned cohesion defect. Whether this lack of a CTD is part of the reason why cohesion is lost in cells overexpressing PBCV-1 topoisomerase 2 is a matter for further study. Nevertheless, it prompted me to investigate what would happen if the C-terminal domain of *S. cerevisiae* topoisomerase 2 were removed. To this end, I designed two truncated versions of yeast

topoisomerase 2 through PCR mutagenesis at residues 1166 (top2-1166) and 1220 (top2-1220) (Caron & Wang, 1994) and cloned them into a plasmid vector under the control of the *GAL1* promoter (Figure 15C and D). These proteins lack 262 and 208 residues at the C-terminus, respectively, mimicking the structure of PBCV-1 topoisomerase 2 to different extents. As a result of the truncations, top2-1166 completely lacks the C-terminal domain, whereas top2-1220 preserves only the first ~43 residues. Hence, this choice of enzymes allowed me to study the effect of a complete removal of the topoisomerase 2 CTD on the cohesion of sister chromatids, serving as a proxy for decatenation, and compare it with the effect of its partial truncation. The reason why I did not directly probe the effect of the truncations on decatenation was that the system our lab employs to assay decatenation *in vivo* is by overexpressing Cre to produce loop-outs (Figure 8A). Since this also requires galactose, Cre and the topoisomerase 2 truncations would have been expressed simultaneously, preventing the differentiation between decatenation happening on looped-out circles or on the chromosomal DNA.

Top2-1220 is the smallest truncation known to preserve decatenation and relaxation both *in vivo* and *in vitro,* whereas top2-1166 is the smallest truncation known to preserve DNA decatenation and relaxation activity *in vitro* (Caron & Wang, 1994). This is in part likely because top2-1166 lacks the nuclear localisation signal (NLS) of WT topoisomerase 2, which is thought to reside between residues 1227 and 1243 of the wild-type enzyme. Therefore, to ensure nuclear transport, I fused the NLS from the simian

vacuolating virus 40 (SV40) to the protein sequence. The assembled plasmids were transformed into a yeast strain expressing Cdc20 under the *MET3* promoter, which prevents its transcription in the presence of methionine, thereby arresting cells in metaphase. A GFP tag was also expressed at the PeriCEN in this strain, allowing the tracking of cohesion at PeriCEN sister loci through fluorescence microscopy. As a positive control, I employed the yeast strain carrying the plasmid expressing the PBCV-1 topoisomerase 2, whereas for negative controls, I employed a yeast strain with the empty plasmid vector and another one carrying the plasmid expressing wild-type yeast topoisomerase 2. All these strains carried the genetic markers necessary for the metaphase arrest and the fluorescent tags. The cells were grown overnight in -MET (methionine) + raffinose media and shifted to YEPR the next morning to induce α-factor arrest for 2.5 hours. The cells were then released for 90 minutes, and 8mM methionine was added to the culture, followed by the addition of 4mM methionine every hour for the rest of the experiment. Once the metaphase arrest was confirmed, galactose was added to 2% of the culture to induce the overexpression of the proteins for 90 minutes. The cells were then harvested and fixed for fluorescence microscopy. Cell samples were also taken under the metaphase arrest before and after the overexpression of the proteins for Western blotting (Figure 15B). The cohesion measurements at the PeriCEN showed that overexpression of PBCV-1 and wild-type topoisomerase 2 causes a 46.2% and 23% cohesion loss, respectively (Figure 15A). The strain carrying the empty plasmid vector displayed a

fraction of cohesion loss of 15%. Interestingly, overexpression of top2-1166 caused a 37.6% loss of cohesion, whereas a fraction of 24.3% was seen following top2-1220 overexpression. The results of this assay suggest that the CTD of yeast topoisomerase 2 governs the timely regulation of sister chromatid decatenation *in vivo*.

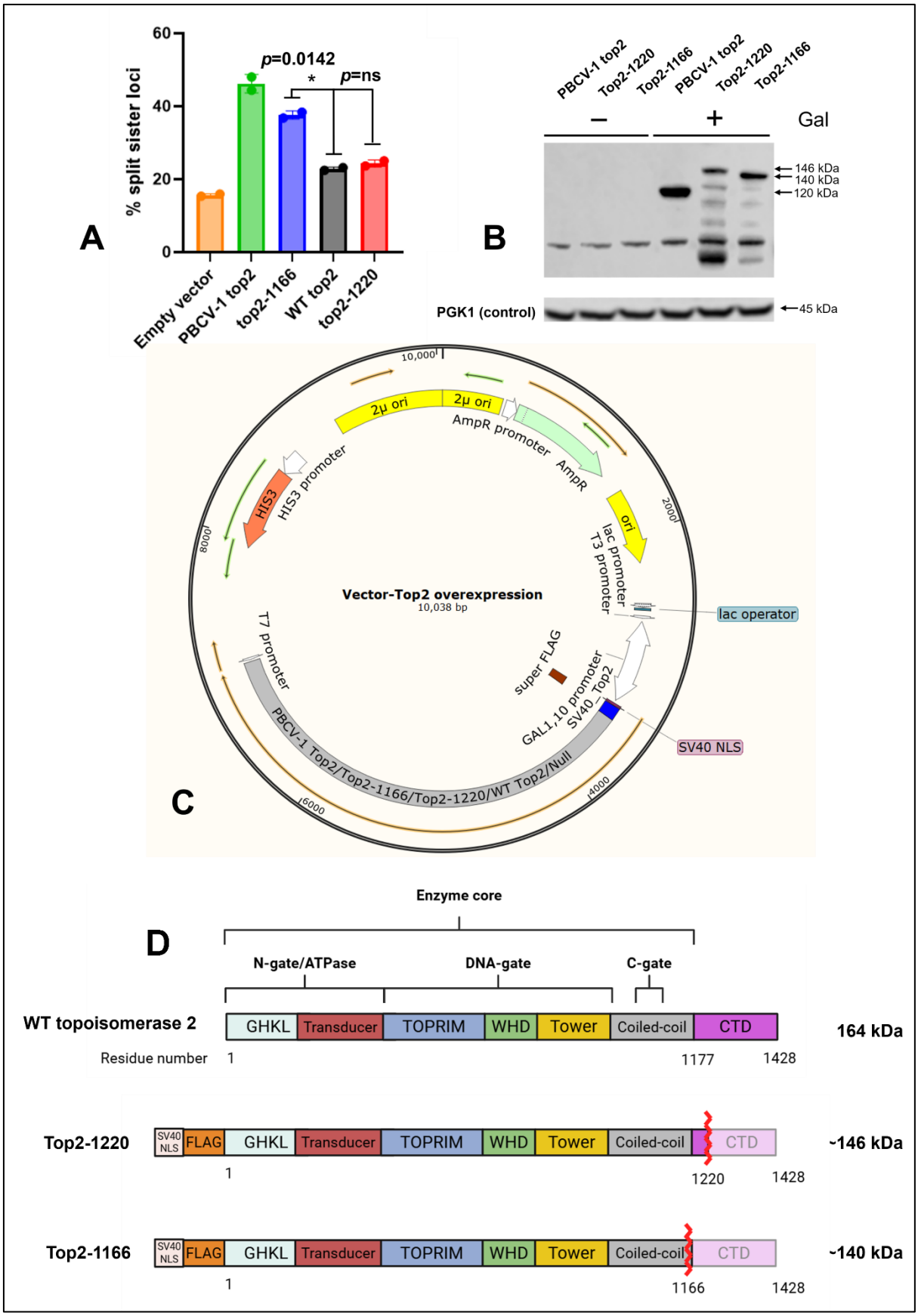
A
% split sister loci
60
40
20
0
p=0.0142
*
p=ns
Empty vector
PBCV-1 top2
top2-1166
WT top2
top2-1220
B
PBCV-1 top2
Top2-1220
Top2-1166
PBCV-1 top2
Top2-1220
Top2-1166
–
+
Gal
146 kDa
140 kDa
120 kDa
PGK1 (control)
45 kDa
C
10,000
2000
4000
6000
8000
2µ ori
2µ ori
AmpR promoter
AmpR
ori
lac promoter
T3 promoter
lac operator
SV40 NLS
GAL1,10 promoter
SV40_Top2
super FLAG
T7 promoter
HIS3
HIS3 promoter
Vector-Top2 overexpression
10,038 bp
PBCV-1 Top2/Top2-1166/Top2-1220/WT Top2/Null
D
Enzyme core
N-gate/ATPase
DNA-gate
C-gate
WT topoisomerase 2
GHKL
Transducer
TOPRIM
WHD
Tower
Coiled-coil
CTD
164 kDa
Residue number
1
1177
1428
Top2-1220
SV40 NLS
FLAG
~146 kDa
1220
Top2-1166
~140 kDa
1166

Figure 15. The C-terminus of *S. cerevisiae* topoisomerase 2 regulates the decatenation activity of the enzyme. A Bar chart comparing the percentage of split sister PeriCEN in the five experimental strains (Welch's t-test performed (p-value top2-166 vs WT top2=0.0142, p-value top2-1220 vs WT top2=ns)) (n=300 for each group). **B** Western blot showing bands for PBCV-1 top2 (120kDa), top2-1166 (140kDa) and top2-1220 (146kDa) following the addition of galactose. The proteins were blotted with the anti-FLAG M2 (F1804) primary antibody and the ECL anti-mouse IgG HRP (NA9310V) secondary antibody. **C** Plasmid employed for the assay, expressing either PBCV-1 top2, top2-1166, top2-1220, WT top2 or no protein, under the *GAL1* promoter. **D** Schematic view of the composition of the WT top2, top2-1220 and top2-1166 proteins employed in the experiment. Ori, Origin of replication. AmpR, Ampicillin-Resistance gene. SV40, Simian Vacuolating Virus 40. NLS, Nuclear Localisation Signal. FLAG, FLAG tag. GHKL, Gyrase-Hsp90-Histidine Kinase-MutL domain. TOPRIM, Topoisomerase/Primase domain. WHD, Winged-Helix Domain. CTD, C-Terminal Domain.

3. Discussion

3.1 DNA catenation is necessary for sister chromatid cohesion

The findings from the fluorescence microscopy cohesion assay in *scc1-73 top2-4* cells add the missing piece to the puzzle, finally revealing that DNA catenation does provide cohesion, but requires cohesin to do so under

spindle forces. Therefore, strongly suggesting that cohesin does not act alone to hold sister chromatids in metaphase, a theory that past experimental setups have been unable to challenge. For instance, Farcas et al. showed in 2011 that spindle forces dramatically reduced the catenated fraction of 26kbp sister minichromosomes while cohesin still maintained them cohesed (Farcas et al., 2011). While it is true that spindle forces likely promote sister DNA decatenation by topoisomerase 2, a significant amount of catenation necessarily remains on real chromosomes to tether sister chromatids (Figure 9 & unpublished data), evidencing the limitations of studying circular DNA molecules. Moreover, Sen et al. suggested in 2016 that cohesin is the sole entity mediating cohesion based on minichromosome catenation assays (Sen et al., 2016). In this paper, it is argued that catenation would never have sufficient time to provide cohesion, as it is dynamically formed and resolved throughout G2 and mitosis, and immediately eliminated following cohesin's removal from chromatin. This assumption, however, misses the fact that DNA catenation provides cohesion simultaneously to cohesin, even at the time sister chromatids are subjected to spindle forces, evidencing their interdependence (Figure 9 & Figure 7C).

There is at least one reasonable explanation for why *scc1-73 top2-4* cells completely lose cohesion under spindle forces at the restrictive temperature (37°C). My data suggest that cohesin is responsible for stopping the sliding of pericentromeric DNA catenation at borders when the spindle microtubules pull from the sister chromatids. Therefore, while DNA

catenation provides cohesion in the absence of these forces, cohesin in these cells is not functional, causing DNA catenation to slide down the chromosome arms and past pericentromere borders when spindle forces are applied. As a result, they are no longer able to accumulate and provide cohesion at the border. In WT cells, this could also be partly due to cohesin's protection of catenation, allowing the accumulation of the latter where they are safe from topoisomerase 2, that is, at the same loci as cohesin (the border). What aspect of the pericentromere borders allows cohesin to accumulate here and subsequently halt the sliding of DNA catenation at this same site is not fully understood. Recent data suggest that it is a combination of the transcription machinery progressing towards the centromeres (in the opposite direction to cohesin, which slides from centromeres towards chromosome arms under spindle forces) and high concentrations of DNA supercoils generated by convergent transcription (Paldi et al., 2020). The result is a high-energy barrier difficult for cohesin to bypass. Upon the eventual accumulation of catenation at the border, this barrier to cohesin could be further strengthened, creating a feedback loop that allows even more cohesin molecules to be recruited (Sun et al., 2013; Guo et al., 2021). This idea raises a new question regarding a possible interplay between DNA topology and cohesin that underpins the mechanistic details of cohesion.

Something that my results and those of the lab have been able to address is the past hypothesis that cohesin mediates cohesion both independently of DNA catenation and through it by guaranteeing its protection (Farcas et

al., 2011). The former is possible because presumably decatenated chromatids are still held together at a fraction of ~50% by cohesin, as shown in the PBCV-1 topoisomerase 2 decatenation assay, although some residual DNA catenation may also be driving this phenotype. The latter is challenged by the fact that even in *scc1-73 top2-4* cells, where catenation is not threatened, nearly all cohesion is lost. However, my results indicate that the intrinsic ability of DNA catenation to withstand spindle forces requires cohesin, and therefore, indirectly, also its protection from topoisomerase 2 under physiological conditions. DNA catenation-mediated cohesion might therefore rely on cohesin both for protection from topoisomerase 2 and to provide a meaningful force against the spindle.

3.2 An SMC-directed mechanism governs the timely formation and resolution of sister chromatid intertwining

The catenation of sister chromatids must be regulated across the cell cycle to allow cohesion onset and chromosome segregation. The findings presented here point to cohesin and condensin as the central regulators of this process. Cohesin protects DNA knots and catenation in situations in which cohesion is absent, suggesting this function is independent of sister chromatid co-entrapment. This could merely be mediated by the presence of cohesin, whereby topoisomerase 2 could be denied access to the DNA. Alternatively, and as previously explained, cohesin could bias topoisomerase 2 towards DNA catenation by maintaining segments of DNA in proximity, a

feature that has already been proven (Sen et al., 2016). Nevertheless, the results presented in section 2.2 show that the inactivation of cohesin in G1, when sister chromatid co-entrapment is absent, results in a marked loss of DNA knots (Figure 10). This perfectly aligns with the previous assay performed in our lab in which cells devoid of cohesive cohesin by depletion of Pds5 still preserved nearly WT levels of catenation (unpublished data). Due to the similarity between knots and catenation, it can be concluded that it is a non-cohesive cohesin pool that, likely through loop-extrusion, mediates the protection of both types of entanglements (Figure 16). Importantly, this mechanism is compatible with the mechanism postulated by Sen et al., meaning that cohesin could promote catenation simultaneously by bringing sisters in proximity and by extruding DNA loops. Additionally, and expanding from published results of condensin-promoted DNA unknotting, here I provide direct evidence of its role in decatenation *in vivo*. Hence, it is now evident that DNA knotting and catenation are linked through a common regulatory pathway governed by the antagonistic constraints that cohesin and condensin impose on topoisomerase 2 (Figure 16). Importantly, the decrease of DNA catenation and knots observed upon inactivation of cohesin, and their increase observed upon inactivation of condensin, carry significant implications (Figure 10 & Figure 11). Cohesin and condensin appear to constantly counteract each other throughout the cell cycle to determine the outcome of DNA entanglements. Whereas from S phase until mitotic entry, the balance is towards the preservation of DNA catenation, this quickly shifts once cells enter mitosis to allow the faithful

segregation of sister chromatids. Therefore, this mechanism must have a time-dependent trigger through which cohesin-mediated protection of DNA entanglements is overridden by condensin in metaphase. This switch, however, should not be dependent on the eviction of cohesin from chromatin by separase or Wpl1. The former is not feasible because separase only removes cohesin upon biorientation, and the set of experiments described herein is performed in the absence of spindle forces (Hauf et al., 2001; Hagting et al., 2002). The latter is unlikely because Wpl1 does not exhibit higher releasing activity during metaphase, and yeast cells lack a prophase pathway (Lopez-Serra et al., 2013; Kueng et al., 2006; Holzmann et al., 2019). While these results present cohesin, condensin and topoisomerase 2 as the core drivers of this regulation, the factors that control its fine-tuning remain unidentified. Nevertheless, the findings described here open a new frontier of investigation, in which the cell-cycle-wide modulation of DNA inter- and intra-molecular entanglements sits at the heart of SMC complexes.

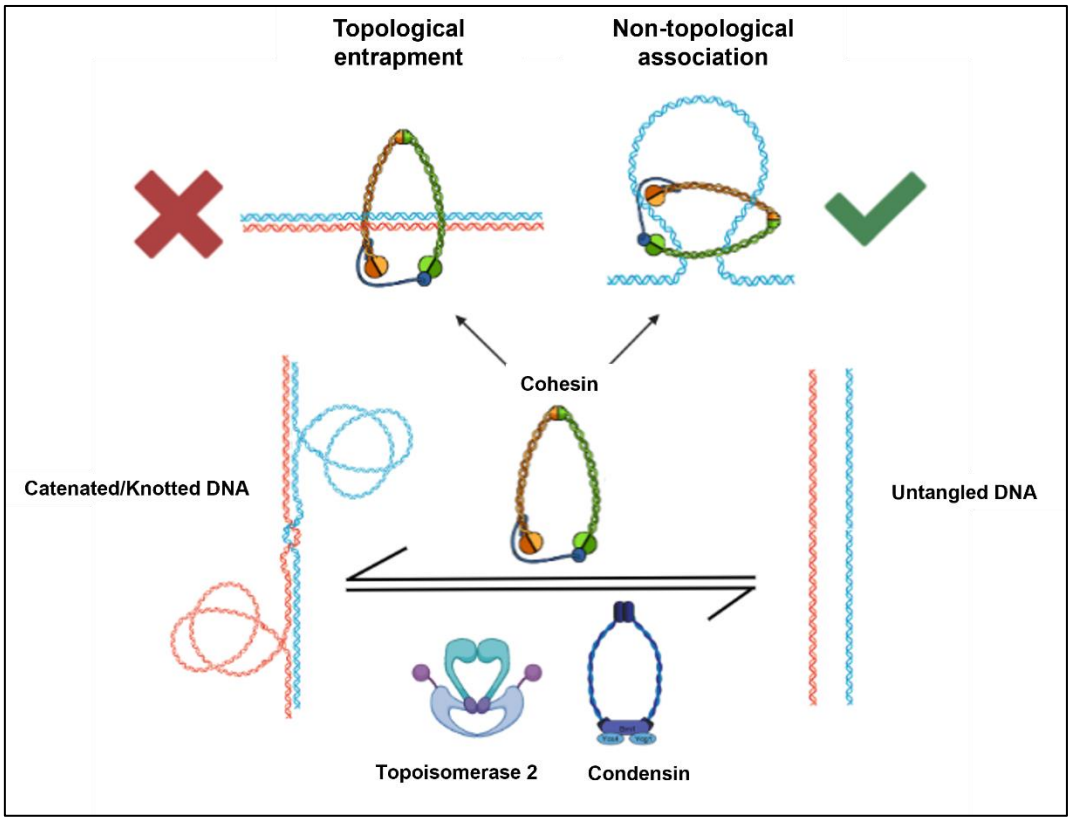

Figure 16. The regulation of DNA topology by cohesin and condensin.

Schematic representation of the roles of cohesin and condensin in regulating DNA knots and catenation. Cohesin protects DNA knots and catenation through non-topological associations with DNA. Conversely, condensin promotes their resolution through topoisomerase 2.

3.3 Cohesin-mediated cohesion underlies the retention of DNA catenation at pericentromere borders

Taking the pericentromere border region as an example, there seems to be a perfect correlation between cohesion and the amount of DNA catenation retained locally. This is not surprising, according to the finding that DNA catenation is an essential part of the cohesion mechanism. However, the

experimental setup I employed allowed me to go one step further and study how cohesin and DNA catenation are functionally coordinated to resist spindle tension. Cohesion at the pericentromere border in *eco1Δwpl1Δ* and Pds5-depleted cells is heavily compromised. This cohesion loss, however, is not reflected in the amount of catenation lost at borders in the absence of spindle forces (Dauban et al., 2020). The situation for *eco1Δwpl1Δ* cells is interesting, since compared to WT cells, their catenation at the centromere is very minimal, whereas at the border it is even higher. This suggests that part of the cohesion loss of *eco1Δwpl1Δ* cells could be driven by the altered configuration of catenation along the pericentromere, rendering them unable to tether sister chromatids even in the absence of spindle forces. However, this does not negate the fact that cohesin is not providing cohesion in these cells, since it should be able to maintain cohesion to WT levels even without the help provided by catenation. Hence, *eco1Δwpl1Δ* cells, just like Pds5-depleted cells, are missing the pool of cohesin capable of cohesively co-entrap sister chromatids. While cohesin in *eco1Δwpl1Δ* cells retains the capacity to co-entrap sister minichromosomes (Srinivasan et al., 2018), this capacity is either completely lost in real chromosomes or rendered inefficient in tethering sister chromatids in proximity.

Cohesin is required to protect DNA catenation from topoisomerase 2, a function I have shown to be performed by non-cohesive, presumably loop-extruding, cohesin. Importantly, Pds5-depleted and *eco1Δwpl1Δ* cells preserve this non-cohesive cohesin pool, allowing the protection of DNA

catenation at the border. Cohesin is additionally required to prevent the escape of DNA catenation from pericentromere borders under spindle forces in metaphase. However, this event is not observed in Pds5-depleted and *eco1Δwpl1Δ* cells, indicating that cohesive cohesin, missing in both strains, is fundamental for its accumulation at borders and the subsequent withstanding of spindle forces. Indirectly, the results of these experiments also indicate that Eco1 and Pds5 are crucial to the tension-resisting mechanism of cohesin and catenation. Interestingly, human Esco1 and Pds5A have recently been linked to the regulation of cohesin-mediated loop extrusion (van Ruiten et al., 2022). By acetylating Smc3, Esco1 promotes the binding of Pds5A to the cohesin complex, which has been proposed to inactivate ATPase activity at the SMC heads, thereby limiting further loop extension. Therefore, in both Pds5-depleted and *eco1ΔwplΔ* cells, this mechanism is likely severely affected, leading to significantly larger and displaced loops. It is thus tempting to propose that loop extrusion, apart from mediating the protection of DNA catenation, could have yet another essential role in cohesion, securing pericentromeric DNA catenation under spindle tension. This could also partially explain the similarity of the phenotypes resulting from the absence of Pds5 and Eco1. However, it also implies that both populations of cohesin, loop extruding and cohesive, interplay at pericentromere borders to create the resistance to spindle forces. This idea would be difficult to conceive with our current understanding of cohesin's mechanisms of action, through which it provides cohesion through co-entrapment and structures the genome through loop

extrusion. Nevertheless, the results described here pave the way for further investigation into the functional organisation of pericentromere borders by cohesin, which allows the regulation of sister chromatid segregation in metaphase.

3.4 A novel role of the CTD of eukaryotic topoisomerase 2

The CTD of topoisomerase 2 has remained relatively unexplored, mainly because its disordered nature precludes its structural characterisation. Nonetheless, the discovery that overexpressing top2-1166 causes a significant loss of cohesion unequivocally links this region to the regulation of sister chromatid segregation. It is important to note that, unlike PBCV-1 topoisomerase 2, the truncated protein does not possess an intrinsically high decatenation activity (Caron & Wang, 1994). This indicates that the observed phenotype results from an abolished regulatory mechanism that normally suppresses the activity of wild-type topoisomerase 2. One caveat in these assays is that they do not measure sister chromatid decatenation directly, but rather indirectly by measuring cohesion. It would be complicated to measure decatenation with our setup, since the system we employ to do so is by looping out chromosomal DNA, which also requires the overexpression of the Cre recombinase. Nevertheless, the results obtained have provided a framework that has thus far proven reliable to study the link between catenation and cohesion.

Importantly, the lack of a phenotype in cells overexpressing top2-1220 pinpoints the key region involved in this pathway between residues 1166 and 1220. This is further supported by the fact that the shortest known truncation that supports minimal viability in *TOP2* mutant yeast cells is top2-1220 (Caron & Wang, 1994). Hence, it would be valuable to screen for mutations in this region that produce a similar phenotype to top2-1166 cells, to narrow down the mechanism to specific key residues. Based on the data presented here, it is reasonable to hypothesise that the cohesin-mediated protection of DNA catenation depends, at least to some extent, on the key region. As shown by Chip-seq and Hi-C, human topoisomerase IIβ colocalises with cohesin and CTCF around TADs and is also thought to physically interact with cohesin (Uusküla-Reimand et al., 2016). However, whether the C-terminus of topoisomerase 2 is involved in any way is unknown. Consequently, identifying a human equivalent of top2-1166 and performing additional protein-protein interaction assays would be crucial to determine whether any of these features are affected by mutations in the key region and the biological consequences of such mutations. It would also shed light on any additional factors playing a role in the overall mechanism. Finally, it would be interesting to study decatenation by top2-1166 in strains carrying condensin-inactivating mutations, potentially elucidating whether top2-1166 still requires condensin's bias toward decatenation or if it can instead decatenate chromosomes independently. This experiment could determine whether the CTD of topoisomerase 2 hosts the key to the regulation of its directionality by both cohesin and

condensin. Together, these findings uncover a fundamental aspect of the cohesin-topoisomerase 2 interplay that governs the DNA catenation equilibrium, laying the groundwork for future studies to understand the molecular details of this mechanism.

4. Conclusion

Sister chromatid cohesion is ensured by the concomitant occurrence of several molecular events. Firstly, catenation must be maintained to fulfil the threshold of cohesion necessary for faithful chromosome segregation. As demonstrated in this work, this process is carefully managed across the cell cycle by cohesin and condensin through non-topological interactions with the underlying DNA. These SMC complexes differentially dictate the decatenation activity of topoisomerase 2, an aspect partially governed by its CTD. Secondly, DNA catenation must co-localise with cohesin at pericentromere borders to resist tension. Unlike the protection of DNA catenation, cohesin promotes this through its cohesive function. Overall, the work presented here, together with previous results from our lab, reveals novel insights into the cohesion mechanism, elucidating an intricate regulatory network that does not solely rely on sister chromatid co-entrapment by cohesin.

5. Materials and Methods

5.1 Yeast and bacterial cell culture

S. cerevisiae culture

YEPD (Yeast extract, Peptone and Dextrose) media was employed for *S.cerevisiae* culture except for experiments requiring specific growth conditions. Temperature-sensitive strains were grown at 25°C, whereas non-temperature-sensitive strains were preferably grown at 30°C, albeit this was dependent on the growth speed of the strain. Liquid cultures were shaken at 200 rpm. A spectrophotometer with a spectral correction factor of 0.5 was used to measure the optical density of the cultures at 600 nm wavelength (OD_{600}). Two methods were employed to arrest cells in G1: Sic1-mediated G1/S arrest by galactose-inducible expression of Sic1(Gal1-Sic1), or the addition of α-factor at a concentration of 1mg/L to liquid cultures every 30 minutes for 2 hours (early G1). Release of early G1-arrested cells was performed by adding pronase at a concentration of 0.1mg/ml. No releases from G1/S were performed in this project. G2 arrests were carried out by adding nocodazole at a concentration of at the time of G1 release. Metaphase arrests were performed by adding 8 mM methionine to sensitive

strains at the time of G1 release, followed by the addition of 4 mM methionine every 60 minutes. In both cases, cells were checked for arrest 2-3 hours after G1 release.

E. coli culture

DNA constructs made through Gibson assembly were transformed into the *E. coli* strain XL1-Blue for amplification before their introduction into *S. cerevisiae*. *E. coli* cells were incubated in liquid media containing 2xTY (tryptone-yeast extract) with ampicillin at a concentration of 100 µg/ml at 37°C while shaking at 250 rpm. Ampicillin as the choice of antibiotic stems from the presence of an ampicillin resistance gene within all DNA constructs employed.

5.2 Yeast and bacterial transformation

Yeast transformation

Yeast cells were inoculated in adequate media at the OD_{600} necessary to harvest them the following day at an OD_{600} of 0.6. Overnight yeast cultures were pelleted by centrifugation at 3500 rpm for 2 minutes in 50 mL Falcon tubes and washed twice with 25mL of 0.1M lithium acetate. The pellets were then resuspended in 300µL of 0.1M lithium acetate, and 50µL aliquots were made in new 1.5mL microfuge tubes from the mixture. The aliquots were incubated at 30°C for 30 minutes while salmon sperm DNA was sonicated, incubated at 95°C for 5 minutes and kept on ice for cooling

down. 350µL of transformation solution composed of 240µl of 50% (w/v) PEG, 35µl of 1M lithium acetate, 25µl of 1% (w/v) denatured salmon sperm DNA and 50µl of DNA for transformation were added to each aliquot. For transformation with plasmid DNA, 500ng were used, whereas for transformation with linear products, 1.5µg were used. The aliquots were incubated again at 30°C for 30 minutes. The cells were then heat-shocked for 45 minutes in a water bath at 42°C and centrifuged at 6000g for 3 minutes. The supernatant was discarded, and the cell pellet was resuspended in 300µl of YEPD. The cells were then incubated at 30°C for 90 minutes, plated onto appropriate selective agar media and left to grow for 48-72 hours. For DNA products containing antibiotic resistance markers, the cells were plated onto YEPD agar and left to grow overnight. The following day, these were replica plated onto agar plates containing the selective antibiotic and left to grow for another day. For linear DNA products, their correct integration in the host genome was confirmed by Sanger sequencing and agarose gel electrophoresis.

For transformation with linear DNA products, these were first amplified from the carrier vector (plasmid or genomic DNA) by PCR. This was done using primers designed to anneal to the vector sequence 250-500 bp upstream and downstream of the sequence containing the marker of interest. The PCR product was then purified, and the DNA was used for transformation, allowing its integration within the genomic DNA of the transformed strain by homologous recombination. If the construct was a circular plasmid vector for ectopic expression, the DNA was used directly for transformation.

E. coli transformation

A stock of -70 °C frozen competent XL1-Blue E. coli cells was warmed up at room temperature, and 100µL was transferred to a 1.5mL microfuge tube. 10-75ng of DNA were then added, and the mixture was left in an ice bucket for 20 minutes. The cells were then heat-shocked in a water bath at 42 °C for 1 minute and placed back on ice for 5 minutes. 600µL of 2xTY media was then added, and the cells were incubated in a heat block at 37°C for 45 minutes while shaking at 300 rpm. Cells were then plated in 100µL volumes onto 2xTY + Ampicillin agar plates for selection of colonies containing the Amp resistance marker carried in the vector DNA and grown for 24 hours at 37°C.

5.3 Sample preparation techniques

E. coli plasmid DNA extraction (miniprep)

Individual colonies from transformed cells were picked using a pipette and inoculated in 25ml flasks containing 10ml of 2xTY + Ampicillin at 100µg/mL. Cells were grown at 37 °C for 12-16 hours while shaking at 180 rpm and harvested by centrifugation at 3,500 rpm for 3 minutes. The cell pellet was resuspended in 250µL of buffer P1 (10mM EDTA, 50mM Tris-Cl, 100µg/mL RNase A) and transferred to a 1.5ml microfuge tube. 250µl of buffer P2 (lysis buffer) (200nM NaCl, 1% SDS) were then added, and the tube was inverted 6 times. 350µL of buffer N3 (neutralisation buffer) (3M KOAc) was then added, and the tube was inverted 6 times. The tube was centrifuged

for 10 minutes at 13,000 rpm, and 800µL of the supernatant was transferred into a QIAprep 2.0 Spin Column inserted into a collection tube with a pipette. The tube was centrifuged for 45 seconds at 13,300 rpm, and the flow-through was discarded. 750µL of buffer PE was then added to wash the column, and the tube was centrifuged for 45 seconds at 13,300 rpm. The flow-through was discarded, and the empty tube was centrifuged at 13,300 rpm for 1 minute to remove residual liquid. The collection tube was discarded, and the column was inserted into a clean 1.5mL microfuge tube, after which 40-50µL of elution buffer (10mM Tris-HCl) was added to the centre of the column. After 3 minutes of incubation at room temperature, the tube was centrifuged for 1 minute at 13,300 rpm to collect the purified DNA and the column was discarded.

S. cerevisiae whole cell extract collection and protein isolation

Fresh patches of *S. cerevisiae* strains were used to make 100 ml liquid cultures with YEPD media at the desired OD_{600} (variable depending on the strain used), which were incubated overnight at 25°C while shaking at 200 rpm. The OD_{600} of the cultures was measured. If the cultures had an OD600 of ~0.6, the cells were harvested; otherwise, the cultures were diluted to an OD_{600} of 0.3 or left to grow directly until they reached the desired OD_{600}. The harvested cells were centrifuged at 3500 rpm for 2 minutes, and most of the supernatant was discarded. The pellet was resuspended in the remaining supernatant and transferred to a 1.5 ml tube. Following a 30-second centrifugation at 13,300g, the supernatant was

discarded and 700 ul of HEPES lysis buffer (5 mM HEPES, 100 mM KCl, 0.05% w/v NP-40, 2.5 mM MgCl2, 1 mM BME, 1mM PMSF, 0.25% Triton X-100, 1 tablet of protease inhibitor (Roche). Glass beads were added to the tube until full, and the tubes loaded onto the FastPrep-24 bead beater. The cells were lysed at 4°C in three 1-minute rounds at 6.5 m/s with 5-minute intervals in between, during which the samples were left on ice. A flame-heated needle was used to punch a hole at the bottom of the tubes, which were then placed inside 4 ml FACS tubes and centrifuged at 3500 rpm for 2 minutes. The collected lysate was transferred to a 1.5 mL tube and centrifuged at 13,300g, after which the supernatant was collected in a new 1.5 mL tube.

The protein concentration of the sample was evaluated with a Bradford assay. Spectrophotometry cuvettes containing 2, 4, 6, 8, 10 and 12µL of 1mg/mL BSA plus 1mL of 1:4 diluted 5X Bradford Reagent (Bio-Rad) were measured for their OD_{595} to plot a standard curve. The OD_{595} of 1ul of sample+1mL of Bradford Reagent was then measured using 2µL EbX lysis buffer+1 1mL of Bradford Reagent as blank. This was then compared to the standard curve to estimate the protein concentration.

Yeast genomic DNA extraction

Yeast cell pellets from overnight liquid or agar plate cultures were transferred to a 1.5 ml tube containing 200µL of SCE buffer (1M sorbitol, 0.1 M sodium citrate, 50 mM EDTA, 0.1 M β-mercaptoethanol, 1 mg/mL zymolyase) and incubated for 1 hour at 37°C in a heat block while shaking

at 300 rpm. 200µL of lysis buffer (0.1 M Tris pH 8.8 25 mM EDTA 1% w/v SDS) was then added and the tube was incubated at 65°C for 20 minutes. Following the incubation, 200µL of 5 M potassium acetate was added to the mixture, and the tube was placed in an ice bucket for 30 minutes. The sample was centrifuged at 13,300 rpm and 4°C for 10 minutes. The supernatant from the tube was then transferred into a 2 mL microcentrifuge tube containing 200µL of 3 M sodium acetate, and 1 mL of 70% isopropanol was added to pellet the DNA. Following a 1-minute centrifugation at 2,300g, the supernatant was discarded, and 700µL of 70% ethanol at 4°C was added. The sample was centrifuged at 13,300 rpm and 4°C for 5 minutes, and the ethanol was discarded. To remove residual ethanol from the tube, these were tapped on a tissue paper and left to dry at 37°C for 30 minutes to 1 hour, after which 100µL of elution buffer and 0.15mg/mL of RNase A were added and the tubes placed back at 37°C for another 1 hour. The DNA samples were collected, and the concentration was measured using a NanoDrop spectrophotometer device.

Yeast cell fixing

Yeast cells were fixed following the experimental protocol for the extraction of their genetic material or for fluorescence microscopy analysis. For the former, yeast cell cultures were collected in 20mL volumes in a 50mL Falcon tube and mixed with 20mL of 100% ethanol and 800µL of 0.5M EDTA before freezing them at -20 °C until DNA extraction. For fluorescence microscopy analysis, 3mL of formaldehyde was added to 20mL volumes of

yeast culture and incubated at room temperature for 2 hours in a roller mixer device (Stuart). 3mL of 2M glycine was then added, and the tubes were centrifuged at 3500 rpm for 2 minutes. The supernatant was discarded, and 20mL of 1X PBS was added before mixing and centrifuging as described above. This washing step was repeated, and once the supernatant was discarded, 10 mL of 1X Phosphate-sorbitol (1:1 ratio) was added. The tubes were stored at 4°C.

Cell plating onto solid agar

Cells in suspension were plated onto agar in volumes of 100µL per plate. ~9 glass beads were then added onto the agar, and the plate was closed to allow for shaking. The beads were discarded once the liquid on the agar was visibly distributed across its surface.

5.4 Molecular biology techniques

PCR reaction for DNA amplification

Primers for PCR were designed to stretch 23-40 bp, have a GC content of 40-50%, and a melting temperature of 56-65°C, with a difference no greater than 5°C between each other. For PCR products intended for Gibson assembly, melting temperatures of up to 75°C were used. PCR reactions had a total volume of 25µL or 50µL, and contained 50-200ng of template DNA, 0.5µM of forward primer, 0.5µM of reverse primer, 1X dilution of 2X Phanta Flash Master Mix Dye Plus (Vazyme), which contained 800µM of

dNTPs in equal proportions and Phanta Flash Super-Fidelity DNA Polymerase. The PCR programme consisted of the following steps: denaturation at 98°C for 2 minutes, followed by 98°C for 20 seconds; primer annealing for 20 seconds at 56-65°C according to melting temperatures; extension at 72°C for 30 seconds per kb. These steps were repeated in order 30 times, after which a final extension step at 72°C for 2 minutes and a pause at 16°C were performed.

Plasmid building with Gibson assembly

Primers for PCR products intended for fusion through Gibson assembly were designed to stretch 50-65bp and contain a 3' 20-45bp sequence homologous to the template DNA (homology sequence) and a 5' 20-30bp sequence overlapping with the adjacent sequence to be joined (overlap sequence). PCR reactions were carried out as described above, considering only the melting temperature of the homology sequence, which was 60-67°C. Once the insert fragments were amplified through PCR and purified, 50-100ng of each were mixed in equal volumes in 100µL tubes and 2X CE Mix (Vazyme) was added to 1X the volume. The tube was then placed in the PCR Thermal Cycler and incubated at 50°C for 20-30 minutes. The correct assembly of the construct was confirmed through Whole Plasmid Sequencing (GENEWIZ).

DNA sample nicking prior to agarose gel electrophoresis

Nicking reactions were carried out in volumes of 20-30 µL. The nicking enzymes employed (all supplied by New England Biolabs (NEB)) were

chosen according to the DNA sample to be digested. Reactions were prepared to contain 2-6 µg of DNA and 15-45 enzyme units (~7.5 units/µg of DNA), equivalent to 1.5-4.5 µL of 10 units/µL enzyme stock. The samples were gently mixed and transferred to a heating block at the optimal temperature for digestion with the selected enzyme (as recommended by NEB) for 5 hours without shaking. The samples were then collected, and 1X DNA loading dye (0.08% SDS) was added to the samples before reducing their volume to ~10µL using a speed vacuum concentrator. For enzymes requiring heat-inactivation (as recommended by NEB), the loading dye was added, and the tubes were transferred to a heat block at 80°C for 20 minutes before reducing their volume. The samples were then gently mixed and loaded into an agarose gel.

1D (1-dimensional) Agarose gel electrophoresis for DNA samples

Agarose gels were made by mixing 0.8-1.0% (w/v) solid agarose powder with 1X TAE (Tris-acetate-EDTA) buffer and microwaving the mixture for ~2 minutes until boiling. The mixture was stirred until it cooled down. 1.5µg/mL ethidium bromide was added right before pouring it onto a gel tray into which 0.8-1.5 mm well combs were attached. Once solid, the tray was placed inside an electrophoresis tank, subsequently filled with TAE 1X buffer, after which the well combs were carefully removed. 1X DNA loading dye was added to the samples, and these were spun down prior to loading into the gel. The DNA loading dye contained SDS at a concentration of 0.08% for DNA ligation products. For PCR products, no extra loading dye

was added as this was contained within the PCR master mix. Depending on the purpose, sample volumes between 5 and 30µL were loaded alongside 5µL of 1kb DNA ladder with markers between 10kb and 0.5kb. Electrophoresis was performed at 120-150V for 30-60 minutes except for 22-hour gels, which were run at 45V. For confirmatory gels, a Bio-Rad GelDoc XR UV filter imager was employed to expose the DNA bands. If the DNA was to be retrieved, a micro-UV imaging screen was used to reveal the bands for excision with a scalpel.

Extraction of DNA from agarose gel bands

Excised agarose gel bands were incubated at 55°C with ~700µL of Agarose Dissolving Buffer. Once visibly dissolved, the samples were transferred to a Zymo-Spin™ Column in a collection tube and spun down for 35 seconds at 13,300 rpm. The flow-through was discarded, and the column was washed with 700µL of DNA wash buffer twice for 30 seconds, followed by a wash with 400µL of the same buffer for 1 minute at 13,300 rpm. The empty column was then centrifuged as previously described to remove residual wash buffer. Afterwards, it was transferred to a 1.5mL microcentrifuge tube, and 17µL of elution buffer was applied to the centre of the column. After 5 minutes, the column was centrifuged at 13,300 rpm for 45 seconds, and the DNA concentration and purity were measured with a nanodrop device.

2D (2-dimensional) Agarose gel electrophoresis for DNA samples

Agarose gels were made by mixing 0.4% (w/v) solid agarose powder with 1X TBE (Tris-borate-EDTA) buffer and microwaving the mixture for ~2 minutes

until boiling. The mixture was stirred until it cooled down. Ethidium bromide was added at a concentration of 1.5µg/mL right before pouring it onto a glass tray into which 0.8-1.5 mm well combs were attached. For 2D gel electrophoresis, an additional 2% gel without ethidium bromide was made to serve as a bed for the main gel. This prevented the main gel from sticking to the tank tray, allowing its safe handling. Once solid, the tray was placed inside an electrophoresis tank, subsequently filled with TBE 1X buffer, after which the well combs were carefully removed. 1X DNA loading dye was added to the samples, and these were spun down before loading into the gel. 2D gels were run for 42 hours at 25V, after which the gel tray was taken out, turned by 90°C and placed back inside the tank for an additional 3-hour run at 125V.

Southern Blotting

2D gels and 22-hour 1D gels were analysed through Southern Blotting following their respective running programmes. The gel was first taken out of the tank and carefully slid into a plastic tray. For the first wash, the tray was filled with 500 mL of depurination solution containing 0.2 M HCl and gently shaken for 10 minutes. The tray was then emptied, and the gel was further washed twice with 500mL of ddH20 for 2 minutes. The tray was emptied, and the last two washes were performed with denaturation solution (0.5 M NaOH, 1.5 M NaCl), the first for 20 minutes and the second for 15 minutes. Following the washes, a new plastic tray was employed to assemble the transfer of the DNA samples onto an Amersham

Hybond™ N+ nitrocellulose membrane (provided by Cytiva). This tray was filled with 3 litres of denaturation solution, and a rectangular glass platform was placed covering the tray. Onto this platform, a sheet of whatmann filter paper wetted with denaturation solution, was placed in a way that its sides were in contact with the denaturation solution contained in the tray. The gel was placed on top of the filter paper, and the nitrocellulose membrane was placed over the gel, removing any bubbles in between the two. Three more whatmann paper sheets, previously soaked in denaturation solution, were placed on top of the membrane. Finally, a pile of tissue paper and a metal weight were placed on top of the assembly. The transfer was performed overnight. The following day, the membrane was taken from the assembly and rinsed in 5X SSC pH 7.0 (0.75 M NaCl, 0.075 M sodium citrate) to neutralise its pH before baking it at 65°C in between two whatmann paper sheets in an incubator for 2.5 hours. Single-stranded salmon sperm DNA was denatured at 95°C for 5 minutes, cooled down on ice for 5 minutes, and 150µL was added to 25mL of pre-hybridisation solution (20% dextran, 2% SLS, 11.2X SSC) pre-warmed at 65°C. The 25mL of pre-hybridisation solution was poured into a hybridisation tube, and the membrane was fitted inside, making sure no air bubbles remained between the membrane and the wall of the tube. The signal detection probe was prepared by mixing 2µL of linear template DNA 10ng/µL, 10µL of 9mer (primer mixture) solution from Agilent, 22µL of ddH_2O and boiling the mixture at 95°C for 5 minutes to denature the DNA. The mixture was then left on ice to allow random primer annealing, and 10µL of dATP mix, 1µL of Klenow fragment

polymerase and 5µL of P-32 dATP were added, and the mixture was incubated at 37°C for 10 minutes. This allows the extension of the annealed primers with radiolabelled nucleotides. The mixture was then filtered by applying it to a Q15 column (Amersham) and pouring 300mL of TE 1X buffer to wash off unattached nucleotides. 500mL of TE 1X buffer was then added to elute and collect the radiolabelled DNA probe. This was denatured once more for 4 minutes at 95°C, left on ice for cooling down and added to the tube containing the pre-hybridisation solution with the membrane. The tube was incubated overnight in a roller inside a 65°C oven, and the following day, the hybridisation buffer was discarded. The tube was then washed three times in the 65°C roller for 20 minutes using 200mL of wash buffer (1% SDS, 2X SSC) each time. The membrane was then dried and placed on a glass platform. The following steps were all performed in a dark room. 4mL of detection reagent 1 and 4 mL of detection reagent 2 from the ECL DIRECT Nucleic Acid Labelling and Detection kit (Cytiva) were mixed in a Falcon tube and added by pipetting onto the membrane. After waiting for 2 minutes, excess liquid was gently removed before placing the membrane inside a transparent plastic film, and this was placed inside an imaging cassette (FUJIFILM). Two high-performance chemiluminescence films (Cytiva) and an autoradiography intensifying screen were placed on top of the film, and the cassette was closed and incubated overnight at -80°C. The following day, the films were developed using the Konica Minolta SRX-101A film processor.

Sodium dodecyl sulfate-polyacrylamide gel electrophoresis (SDS-PAGE) followed by western blotting

2X NuPAGE loading dye and whole cell extracts were added in equal amounts in a tube and heated at 95°C for 5 minutes. A 4-12% Bis-Tris SDS gel was inserted in the gel tank and submerged in 500ml of 1:20 diluted 20X MOPS SDS Running buffer (Gel and buffer provided by NuPAGE). The gel was then loaded with the samples and a molecular weight ladder and run at 150V until the bands from the loading dye escaped from the gel. The gel was then embedded in Trans-Blot Turbo Mini 0.2 µm Nitrocellulose Transfer Pack (Bio-Rad) layers. A Trans-blot Turbo transfer system (Bio-Rad) was employed to transfer the proteins and ladder from the gel to the nitrocellulose membrane provided in the pack. The membrane was then washed in PBS-T (1:1 PBS+TWEEN) and stained with Ponceau S Staining Solution (Thermo Fisher Scientific). Another wash with PBS-T was carried out before blocking the membrane with 5% skimmed milk powder w/v for 30 minutes. The membrane was then cut in half, ensuring both halves contained all protein samples. Both halves were incubated for 1 hour in primary antibody (mixed in PBS-T+5% milk), one being the control. The membranes were washed in PBS-T 3 times for 5 minutes each. The membranes were then transferred to the tube containing the secondary antibody (mixed in PBS-T+5% milk) and incubated for 45 minutes. The membranes were washed as before, 3 times for 5 minutes in PBS-T and dried before adding the chemiluminescent HRP substrate (Amersham

Solution A and B in a 1:1 ratio). After 10 seconds, the membrane was exposed with the LI-COR Odyssey Fc imaging device.

5.5 Image analysis and fluorescence microscopy

Southern blotting signal intensity analysis

The quantification of signal intensity of Southern blots from 1D and 2D agarose gels was carried out using ImageJ image processing software.

Fluorescence microscopy sample and slide preparation

A 100µL aliquot of fixed cells was made in a new 1.5mL microfuge tube. The tube was centrifuged at 13,300 rpm for 1 minute, and 50µL of the supernatant was discarded. The pellet was resuspended in the remaining supernatant, and the tube was placed in an ice bucket and kept as a stock to prepare the slides. 3µL of cell suspension was pipetted onto a microscope slide, and a borosilicate glass cover slip was placed on top. A brushstroke of halogen-free, low fluorescence immersion oil for fluorescence microscopy (Immersol™ 518F) provided by ZEISS was added on top of the cover slip to lubricate the contact with the oil immersion objective lens of the ZEISS Axio Observer. Z1 microscope. The slide was loaded onto the 63X objective lens, and the cells were imaged using the ZEN Pro programme within the ZEN 3.3 application. The cells were exposed to light from wavelengths appropriate to visualise GFP and TdTomato, with exposure times of 1000-3500 ms. Images were taken with the ZEISS Axiocam MRm camera

and saved as RGB 3-slice stacks. The fluorescent dots were counted throughout the procedure as images were taken.

5.6 S. cerevisiae genetics

Yeast strain crossing

Yeast strains were selected based on their genotype and mating type (α or a) to create new strains with the genetic features of interest. One strain was first streaked on a YEPD plate, making a patch onto which another strain of the opposite mating type was streaked. The cells were gently mixed to induce mating and left to grow. After 1 day, the cells were harvested and streaked onto plates containing media selective for one of the strains and left to grow for 1 day. The process was repeated employing media selective for the other strain crossed, minimising the survival of haploid cells. The cells were then patched onto a meiosis-inducing sporulation plate and left to grow for 1-2 days. Incubation temperatures would have been 25°C for temperature-sensitive strains or 30°C for non-temperature-sensitive strains.

Tetrad dissection

A suspension consisting of 2M sorbitol, 1mg/mL zymolyase and H_2O was prepared to digest the ascus wall that sticks together the spores of a tetrad from the sporulation plate. A sterile toothpick was employed to harvest cells from the plate and mix them gently in the solution. The mixture was

then incubated at 30°C for 1 hour. 7uL of the mixture was then pipetted onto the side of a YEPD plate, which was gently tilted to distribute the cells along a straight line and left to dry for 5 minutes. The MSM 300 Singer Instruments micro-manipulator was used to separate the spores of the tetrads for individual growth on the same plate, employing the device's needle to collect and drop the spores on the agar. The spores were plated using a 9x9 digital grid as a framework, allowing their analysis. The plate was then incubated for 2-4 days at an adequate temperature.

Replica plating

Plates containing agar selective for the genetic markers of the parent strains were left at room temperature overnight before replica plating. The colonies from dissected spores were transferred onto a sterile velvet by gently pressing the agar-containing side of the plate onto it. The subsequent transfer of the spores from the velvet to the selection plates was carried out in the same way. To confirm the mating type of the spores, standardised strains of mating types a and α were plated onto nutrient-depleted minimal agar plates and stamped onto the velvet following the same procedure. The replicated plates were incubated at an adequate temperature for 1-2 days before scoring the strains for survival on the different media. The standardised strains possess all necessary resistance markers for survival on minimal agar; therefore, only strains able to mate with them could proliferate, revealing their mating type.

Table1. *S. cerevisiae* strains employed. All the strains below derive from W303 (699).

Strain number	**Genotype**	**Description and purpose**	**Creator**
699	MATa, ade2-1, trp1-1, can1-100, leu2-3,112,his3-11,15, ura3, GAL, psi+	WT Mat a	Kim Nasmyth
700	MATalpha,ade2-1,trp1-1,can1-100,leu2-3,112,his3-11,15, ura3,GAL,psi+	WT Mat α	Kim Nasmyth
30484	MATa, ade2-1, leu2-3, ura3, trp1-1,his3-11,15, can1-100, GAL,psi+ MET-CDC20::URA3 Spc42-tdTomato::NAT leu2::PURA3::tetR-GFP::LEU2 tetOx224-URA3 (tetOs~11.5kb to right of CEN4, OUTSIDE	Control strain for the truncated topoisomerase 2 cohesion assay carrying an empty pRS423 plasmid vector. CDC20 is expressed under the methionine-repressive *MET3* promoter, allowing the arrest in metaphase in the presence of	Aditi Kaushik

	the boundary) pRS423::His	methionine. The spindle pole body protein Spc42 is tagged with the TdTomato red tag to allow its tracking through fluorescence microscopy. 224 copies of the tetracycline operator are arrayed in tandem (tetOx224) and integrated into the PeriCEN of chromosome 4. This allows the binding of the tet repressor-GFP fusion protein (tetR-GFP) expressed in this strain to visualise the PeriCEN through fluorescence microscopy.	

30489	MATa, ade2-1, leu2-3, ura3, trp1-1,his3-11,15, can1-100, GAL,psi+ MET-CDC20::URA3 Spc42-tdTomato::NAT leu2::PURA3::tetR-GFP::LEU2 tetOx224-URA3 (tetOs~11.5kb to right of CEN4, OUTSIDE the boundary) pRS423-Gal-Top2::His	Control strain for the truncated topoisomerase 2 cohesion assay carrying the pRS423 plasmid vector expressing wild-type yeast topoisomerase 2 under the *GAL1* promoter. CDC20 is expressed under the methionine-repressive *MET3* promoter, allowing the arrest in metaphase in the presence of methionine. The spindle pole body protein Spc42 is tagged with the TdTomato red tag to allow its tracking through fluorescence microscopy. 224 copies of the tetracycline operator are arrayed in tandem (tetOx224) and integrated into the PeriCEN of	Aditi Kaushik

		chromosome 4. This allows the binding of the tet repressor-GFP fusion protein (tetR-GFP) expressed in this strain to visualise the PeriCEN through fluorescence microscopy.	
30548	MATa, ade2-1, leu2-3, ura3, trp1-1,his3-11,15, can1-100, GAL,psi+ MET-CDC20::URA3 Spc42-tdTomato::NAT leu2::PURA3::tetR-GFP::LEU2 tetOx224-URA3 (tetOs~11.5kb to right of CEN4, OUTSIDE the boundary) pRS423::His	Control strain for the truncated topoisomerase 2 cohesion assay carrying the pRS423 plasmid vector expressing PBCV1 topoisomerase 2 under the *GAL1* promoter. CDC20 is expressed under the methionine-repressive *MET3* promoter, allowing the arrest in metaphase in the presence of methionine. The spindle	Aditi Kaushik

		pole body protein Spc42 is tagged with the TdTomato red tag to allow its tracking through fluorescence microscopy. 224 copies of the tetracycline operator are arrayed in tandem (tetOx224) and integrated into the PeriCEN of chromosome 4. This allows the binding of the tet repressor-GFP fusion protein (tetR-GFP) expressed in this strain to visualise the PeriCEN through fluorescence microscopy.	

31001	MATa, ade2-1, leu2-3, ura3, trp1-1,his3-11,15, can1-100, GAL,psi+ scc1-73::HIS MX MET-CDC20::URA3 Spc42-tdTomato::NAT leu2::PURA3::tetR-GFP::LEU2 tetOx224-URA3 (tetOs~11.5kb to right of CEN4, OUTSIDE the boundary	Strain expressing the *scc1-73* thermosensitive allele, which allows the inactivation of cohesin at 37℃. CDC20 is expressed under the methionine-repressive *MET3* promoter, allowing the arrest in metaphase in the presence of methionine. The spindle pole body protein Spc42 is tagged with the TdTomato red tag to allow its tracking through fluorescence microscopy. 224 copies of the tetracycline operator are arrayed in tandem (tetOx224) and integrated into the PeriCEN of chromosome 4. This allows the binding of the tet repressor-GFP fusion	Aditi Kaushik

		protein (tetR-GFP) expressed in this strain to visualise the PeriCEN through fluorescence microscopy.	
31044	MATa, ade2-1, leu2-3, ura3, trp1-1,his3-11,15, can1-100, GAL,psi+ scc1-73::HIS MX Top2-4::Trp MET-CDC20::URA3 Spc42-tdTomato::NAT leu2::PURA3::tetR-GFP::LEU2 tetOx224-URA3 (tetOs~11.5kb to right of CEN4, OUTSIDE the boundary)	Strain expressing the *scc1-73 and top2-4* thermosensitive alleles, which allow the inactivation of cohesin and topoisomerase 2 at 37℃. CDC20 is expressed under the methionine-repressive *MET3* promoter, allowing the arrest in metaphase in the presence of methionine. The spindle pole body protein Spc42 is tagged	Alejandro Mateos Martin

		with the TdTomato red tag to allow its tracking through fluorescence microscopy. 224 copies of the tetracycline operator are arrayed in tandem (tetOx224) and integrated into the PeriCEN of chromosome 4. This allows the binding of the tet repressor-GFP fusion protein (tetR-GFP) expressed in this strain to visualise the PeriCEN through fluorescence microscopy.	

31454	MATa Scc1(S525N)::His3MX6 (scc1-73) leu2::Gal1p-Sic1(9m)/His3p-Gal1/His3p-Gal2/Gal1p-Gal4:: Leu2 (single copy) Cen2 PeriCen2 TRP1 ARS1 9.3 KB Plasmid	Strain expressing the *scc1-73* thermosensitive allele which allow the inactivation of cohesin at 37℃. A non-degradable version of Sic1 is expressed under the *GAL1* promoter, allowing its expression in the presence of galactose to arrest cells at the G1/S interphase. This strain carries the plasmid spanning the centromere and 9.3kbp into the right arm of chromosome 2 of *S. cerevisiae*, employed for plasmid knotting and catenation assays.	Alejandro Mateos Martin

31456	MATalpha leu2::Gal1p-Sic1(9m)/His3p-Gal1/His3p-Gal2/Gal1p-Gal4:: Leu2 (single copy) Cen2 PeriCen2 TRP1 ARS1 9.3 KB Plasmid	WT scc1 strain. A non-degradable version of Sic1 is expressed under the *GAL1* promoter, allowing its expression in the presence of galactose to arrest cells at the G1/S interphase. This strain carries the plasmid spanning the centromere and 9.3kbp into the right arm of chromosome 2 of *S. cerevisiae*, employed for plasmid knotting and catenation assays.	Alejandro Mateos Martin
31457	MAT A leu2::Gal1p-Sic1(9m)/His3p-Gal1/His3p-Gal2/Gal1p-Gal4:: Leu2 (single copy) Cen2 PeriCen2 TRP1 ARS1 9.3 KB Plasmid	WT scc1 strain. A non-degradable version of Sic1 is expressed under the *GAL1* promoter, allowing its expression in the presence of galactose to arrest cells at the G1/S interphase. This strain	Alejandro Mateos Martin

		carries the plasmid spanning the centromere and 9.3kbp into the right arm of chromosome 2 of *S. cerevisiae*, employed for plasmid knotting and catenation assays.	
31465	MAT A leu2::Gal1p-Sic1(9m)/His3p-Gal1/His3p-Gal2/Gal1p-Gal4:: Leu2 (single copy) Cen2 PeriCen2 TRP1 ARS1 9.3 KB Plasmid	WT strain. A non-degradable version of Sic1 is expressed under the *GAL1* promoter, allowing its expression in the presence of galactose to arrest cells at the G1/S interphase. This strain carries the plasmid spanning the centromere and 9.3kbp into the right arm of chromosome 2 of *S. cerevisiae*, employed for plasmid knotting and catenation assays.	Alejandro Mateos Martin

31467	MAT A Scc1(S525N)::His3MX6 (scc1-73) leu2::Gal1p-Sic1(9m)/His3p-Gal1/His3p-Gal2/Gal1p-Gal4:: Leu2 (single copy) Cen2 PeriCen2 TRP1 ARS1 9.3 KB Plasmid	Strain expressing the *scc1-73* thermosensitive allele which allow the inactivation of cohesin at 37℃. A non-degradable version of Sic1 is expressed under the *GAL1* promoter, allowing its expression in the presence of galactose to arrest cells at the G1/S interphase. This strain carries the plasmid spanning the centromere and 9.3kbp into the right arm of chromosome 2 of *S. cerevisiae*, employed for plasmid knotting and catenation assays.	Alejandro Mateos Martin

31496	MAT A smc2-8 leu2::Gal1p-Sic1(9m)/His3p-Gal1/His3p-Gal2/Gal1p-Gal4:: Leu2 (single copy) Cen2 PeriCen2 TRP1 ARS1 9.3 KB Plasmid	Strain expressing the *smc2-8* thermosensitive allele, which allows the inactivation of condensin at 37℃. A non-degradable version of Sic1 is expressed under the *GAL1* promoter, allowing its expression in the presence of galactose to arrest cells at the G1/S interphase. This strain carries the plasmid spanning the centromere and 9.3kbp into the right arm of chromosome 2 of *S. cerevisiae*, employed for plasmid knotting and catenation assays.	Alejandro Mateos Martin

31501	MATa eco1::NatMX4 rad61::hphMX4 LoxP CEN III LoxP ::HIS3MX ura3::Gal CRE::URA3 CEN IIIflanked by LoxP LoxP Upstream of YCL001W-A and downstream of YCR001W :HIS3MX	*eco1Δwpl1Δ* strain employed for the centromeric DNA catenation loop-out assay. LoxP sites are inserted at the edges of the *CEN* locus of chromosome 3. The Cre recombinase is expressed under the *GAL1* promoter, allowing its expression upon the addition of galactose and the subsequent circularisation of the DNA flanked by LoxP sites	Alejandro Mateos Martin
31504	MATalpha rad61::hphMX4 LoxP CEN III LoxP ::HIS3MX ura3::Gal CRE::URA3 CEN IIIflanked by LoxP LoxP Upstream of YCL001W-A and downstream of YCR001W :HIS3MX	*wpl1Δ* strain employed for the centromeric DNA catenation loop-out assay. LoxP sites are inserted at the edges of the *CEN* locus of chromosome 3. The Cre recombinase is expressed under the *GAL1*	Alejandro Mateos Martin

		promoter, allowing its expression upon the addition of galactose and the subsequent circularisation of the DNA flanked by LoxP sites	
31870	MATa 30 eco1::NatMX4 rad61::hphMX4 *MET3*-CDC20::LEU2 loxP pericenIII loxP::Trp ura3::Gal CRE::URA3	*eco1Δwpl1Δ* strain employed for the pericentromere border DNA catenation loop-out assay. CDC20 is expressed under the methionine-repressive *MET3* promoter, allowing the arrest in metaphase in the presence of methionine. LoxP sites are inserted at the edges of the pericentromere border of chromosome 3. The Cre recombinase is expressed under the *GAL1*	Aditi Kaushik

		promoter, allowing its expression upon the addition of galactose and the subsequent circularisation of the DNA flanked by LoxP sites	
32079	MATa, ade2-1, leu2-3, ura3, trp1-1,his3-11,15, can1-100, GAL,psi+ MET-CDC20::URA3 Spc42-tdTomato::NAT leu2::PURA3::tetR-GFP::LEU2 tetOx224-URA3 (tetOs~11.5kb to right of CEN4, OUTSIDE the boundary) Gal-Top2 truncation 1166aa::His	Strain carrying the plasmid expressing the topoisomerase 2 C-terminus truncation at amino acid 1166. CDC20 is expressed under the methionine-repressive *MET3* promoter, allowing the arrest in metaphase in the presence of methionine. The spindle pole body protein Spc42 is tagged with the TdTomato red tag to allow its tracking through fluorescence microscopy.	Alejandro Mateos Martin

		224 copies of the tetracycline operator are arrayed in tandem (tetOx224) and integrated into the PeriCEN of chromosome 4. This allows the binding of the tet repressor-GFP fusion protein (tetR-GFP) expressed in this strain to visualise the PeriCEN through fluorescence microscopy.	
32080	MATa, ade2-1, leu2-3, ura3, trp1-1,his3-11,15, can1-100, GAL,psi+ MET-CDC20::URA3 Spc42-tdTomato::NAT leu2::PURA3::tetR-GFP::LEU2 tetOx224-URA3 (tetOs~11.5kb to right of CEN4, OUTSIDE	Strain carrying the plasmid expressing the topoisomerase 2 C-terminus truncation at amino acid 1220. CDC20 is expressed under the methionine-repressive *MET3* promoter, allowing the arrest in metaphase in the presence of	Alejandro Mateos Martin

	the boundary) Gal-Top2 truncation 1220aa::His	methionine. The spindle pole body protein Spc42 is tagged with the TdTomato red tag to allow its tracking through fluorescence microscopy. 224 copies of the tetracycline operator are arrayed in tandem (tetOx224) and integrated into the PeriCEN of chromosome 4. This allows the binding of the tet repressor-GFP fusion protein (tetR-GFP) expressed in this strain to visualise the PeriCEN through fluorescence microscopy.	

32100	MATa, ade2-1, leu2-3, ura3, trp1-1,his3-11,15, can1-100, GAL,psi+ eco1::NatMX4 rad61::hphMX4 Spc42-tdTomato::NAT leu2::PURA3::tetR-GFP::LEU2 tetOx224-URA3 (tetOs~11.5kb to right of CEN4, OUTSIDE the boundary)	*eco1Δwpl1Δ* strain employed for the cohesion assay. CDC20 is expressed under the methionine-repressive *MET3* promoter, allowing the arrest in metaphase in the presence of methionine. The spindle pole body protein Spc42 is tagged with the TdTomato red tag to allow its tracking through fluorescence microscopy. 224 copies of the tetracycline operator are arrayed in tandem (tetOx224) and integrated into the PeriCEN of chromosome 4. This allows the binding of the tet repressor-GFP fusion protein (tetR-GFP)	Alejandro Mateos Martin

		expressed in this strain to visualise the PeriCEN through fluorescence microscopy.	
32101	MATa, ade2-1, leu2-3, ura3, trp1-1,his3-11,15, can1-100, GAL,psi+ rad61::hphMX4 Spc42-tdTomato::NAT leu2::PURA3::tetR-GFP::LEU2 tetOx224-URA3 (tetOs~11.5kb to right of CEN4, OUTSIDE the boundary)	*wpl1Δ* strain employed for the cohesion assay. The spindle pole body protein Spc42 is tagged with the TdTomato red tag to allow its tracking through fluorescence microscopy. 224 copies of the tetracycline operator are arrayed in tandem (tetOx224) and integrated into the PeriCEN of chromosome 4. This allows the binding of the tet repressor-GFP fusion	Alejandro Mateos Martin

		protein (tetR-GFP) expressed in this strain to visualise the PeriCEN through fluorescence microscopy.	

Table 2. Plasmids employed

Name	Origin	Description and purpose	Creator
7686	Cen2 PeriCen2 TRP1 ARS1 10.9 KB Plasmid	Plasmid employed for the DNA catenation and knotting assays in G1 and G2/M spanning 9.3kbp of pericentromeric chromatin of chromosome 2 of *S. cerevisiae*. Shortened from 10.9 KB to 9.3 KB through enzymatic digestion.	Alejandro Mateos Martin
7689	pRS423 vector. Gal-Top2 truncation 1166aa::His	Plasmid expressing a version of *S. cerevisiae* topoisomerase 2 truncated at residue 1166 under the *GAL1* promoter	Alejandro Mateos Martin

7690	pRS423 vector. Gal-Top2 truncation 1220aa::His	Plasmid expressing a version of *S. cerevisiae* topoisomerase 2 truncated at residue 1220 under the *GAL1* promoter	Alejandro Mateos Martin

Table 3. Antibodies employed

Name	Origin	Purpose	Provider
Anti-PGK1 (ab113687)	Mouse	Western blot	Abcam
Anti-FLAG M2 (F1804)	Mouse	Western blot	Sigma Aldrich
ECL Anti-mouse IgG HRP (NA9310V)	Sheep	Western blot	Cytiva

6. References

(1-180)

1. Mitosis. Nature Education. 2014.

2. Abremski K, Hoess R. Bacteriophage P1 site-specific recombination. Purification and properties of the Cre recombinase protein. J Biol Chem. 1984;259(3):1509-14.

3. Alberts B JA, Lewis J, et al. The Structure and Function of DNA. In: Science G, editor. Molecular Biology of the Cell. 4th Edition ed. National Library of Medicine: National Library of Medicine; 2002.

4. Alberts B JA, Lewis J, et al. Cytokinesis. Molecular Biology of the Cell. 2002;4th Edition.

5. Anderson DE, Losada A, Erickson HP, Hirano T. Condensin and cohesin display different arm conformations with characteristic hinge angles. Journal of Cell Biology. 2002;156(3):419-24.

6. Andrade MA, Petosa C, O'Donoghue SI, Müller CW, Bork P. Comparison of ARM and HEAT protein repeats11Edited by P. E. Wright. Journal of Molecular Biology. 2001;309(1):1-18.

7. Anjur-Dietrich MI, Kelleher CP, Needleman DJ. Mechanical Mechanisms of Chromosome Segregation. Cells. 2021;10(2).

8. Baird CL, Gordon MS, Andrenyak DM, Marecek JF, Lindsley JE. The ATPase Reaction Cycle of Yeast DNA Topoisomerase II: SLOW RATES OF ATP RESYNTHESIS AND PiRELEASE*. Journal of Biological Chemistry. 2001;276(30):27893-8.

9. Baird CL, Harkins TT, Morris SK, Lindsley JE. Topoisomerase II drives DNA transport by hydrolyzing one ATP. Proceedings of the National Academy of Sciences. 1999;96(24):13685-90.

10. Baldi MI, Benedetti P, Mattoccia E, Tocchini-Valentini GP. In vitro catenation and decatenation of DNA and a novel eucaryotic ATP-dependent topoisomerase. Cell. 1980;20(2):461-7.

11. Bauer DL, Marie R, Rasmussen KH, Kristensen A, Mir KU. DNA catenation maintains structure of human metaphase chromosomes. Nucleic Acids Res. 2012;40(22):11428-34.

12. Baxter J, Aragón L. Physical linkages between sister chromatids and their removal during yeast chromosome segregation. Cold Spring Harb Symp Quant Biol. 2010;75:389-94.

13. Bendich AJ, Drlica K. Prokaryotic and eukaryotic chromosomes: what's the difference? Bioessays. 2000;22(5):481-6.

14. Bermejo R, Lai Mong S, Foiani M. Preventing Replication Stress to Maintain Genome Stability: Resolving Conflicts between Replication and Transcription. Molecular Cell. 2012;45(6):710-8.

15. Blat Y, Kleckner N. Cohesins Bind to Preferential Sites along Yeast Chromosome III, with Differential Regulation along Arms versus the Centric Region. Cell. 1999;98(2):249-59.

16. Boettcher B, Barral Y. The cell biology of open and closed mitosis. Nucleus. 2013;4(3):160-5.

17. Bürmann F, Löwe J. Structural biology of SMC complexes across the tree of life. Current Opinion in Structural Biology. 2023;80:102598.

18. Bürmann F, Shin H-C, Basquin J, Soh Y-M, Giménez-Oya V, Kim Y-G, et al. An asymmetric SMC–kleisin bridge in prokaryotic condensin. Nature Structural & Molecular Biology. 2013;20(3):371-9.

19. Capranico G, Marinello J, Chillemi G. Type I DNA Topoisomerases. Journal of Medicinal Chemistry. 2017;60(6):2169-92.

20. Caron PR, Watt P, Wang JC. The C-terminal domain of Saccharomyces cerevisiae DNA topoisomerase II. Mol Cell Biol. 1994;14(5):3197-207.

21. Chan K-L, Roig Maurici B, Hu B, Beckouët F, Metson J, Nasmyth K. Cohesin’s DNA Exit Gate Is Distinct from Its Entrance Gate and Is Regulated by Acetylation. Cell. 2012;150(5):961-74.

22. Chan KL, Gligoris T, Upcher W, Kato Y, Shirahige K, Nasmyth K, et al. Pds5 promotes and protects cohesin acetylation. Proc Natl Acad Sci U S A. 2013;110(32):13020-5.

23. Chao William CH, Murayama Y, Muñoz S, Costa A, Uhlmann F, Singleton Martin R. Structural Studies Reveal the Functional Modularity of the Scc2-Scc4 Cohesin Loader. Cell Reports. 2015;12(5):719-25.

24. Chao WCH, Wade BO, Bouchoux C, Jones AW, Purkiss AG, Federico S, et al. Structural Basis of Eco1-Mediated Cohesin Acetylation. Scientific Reports. 2017;7(1):44313.

25. Charbin A, Bouchoux C, Uhlmann F. Condensin aids sister chromatid decatenation by topoisomerase II. Nucleic Acids Research. 2013;42(1):340-8.

26. Chu L, Zhang Z, Mukhina M, Zickler D, Kleckner N. Sister chromatids separate during anaphase in a three-stage program as directed by interaxis bridges. Proc Natl Acad Sci U S A. 2022;119(10):e2123363119.

27. Cohen-Fix O, Peters JM, Kirschner MW, Koshland D. Anaphase initiation in Saccharomyces cerevisiae is controlled by the APC-dependent

degradation of the anaphase inhibitor Pds1p. Genes Dev. 1996;10(24):3081-93.

28. Corbett KD, Berger JM. Structure, Molecular Mechanisms, and Evolutionary Relationships in DNA Topoisomerases. Annual Review of Biophysics. 2004;33(Volume 33, 2004):95-118.

29. Costantino L, Hsieh TS, Lamothe R, Darzacq X, Koshland D. Cohesin residency determines chromatin loop patterns. Elife. 2020;9.

30. D'Ambrosio C, Kelly G, Shirahige K, Uhlmann F. Condensin-Dependent rDNA Decatenation Introduces a Temporal Pattern to Chromosome Segregation. Current Biology. 2008;18(14):1084-9.

31. Dabney J, Knapp M, Glocke I, Gansauge MT, Weihmann A, Nickel B, et al. Complete mitochondrial genome sequence of a Middle Pleistocene cave bear reconstructed from ultrashort DNA fragments. Proc Natl Acad Sci U S A. 2013;110(39):15758-63.

32. Dauban L, Montagne R, Thierry A, Lazar-Stefanita L, Bastié N, Gadal O, et al. Regulation of Cohesin-Mediated Chromosome Folding by Eco1 and Other Partners. Mol Cell. 2020;77(6):1279-93.e4.

33. Davidson IF, Bauer B, Goetz D, Tang W, Wutz G, Peters J-M. DNA loop extrusion by human cohesin. Science. 2019;366(6471):1338-45.

34. Delvaux de Fenffe CM, Govers J, Mattiroli F. Always on the Move: Overview on Chromatin Dynamics within Nuclear Processes. Biochemistry. 2025;64(10):2138-53.

35. Denker A, de Laat W. The second decade of 3C technologies: detailed insights into nuclear organization. Genes Dev. 2016;30(12):1357-82.

36. Deweese JE, Osheroff MA, Osheroff N. DNA Topology and Topoisomerases: Teaching a "Knotty" Subject. Biochem Mol Biol Educ. 2008;37(1):2-10.

37. Dong KC, Berger JM. Structural basis for gate-DNA recognition and bending by type IIA topoisomerases. Nature. 2007;450(7173):1201-5.

38. Dougherty AC, Hawaz MG, Hoang KG, Trac J, Keck JM, Ayes C, et al. Exploration of the Role of the C-Terminal Domain of Human DNA Topoisomerase IIα in Catalytic Activity. ACS Omega. 2021;6(40):25892-903.

39. Dröge P, Cozzarelli NR. [6] Topological structure of DNA knots and catenanes. Methods in Enzymology. 212: Academic Press; 1992. p. 120-30.

40. Dyson S, Segura J, Martínez-García B, Valdés A, Roca J. Condensin minimizes topoisomerase II-mediated entanglements of DNA in vivo. Embo j. 2021;40(1):e105393.

41. Fang G, Yu H, Kirschner MW. Direct Binding of CDC20 Protein Family Members Activates the Anaphase-Promoting Complex in Mitosis and G1. Molecular Cell. 1998;2(2):163-71.

42. Fennell-Fezzie R, Gradia SD, Akey D, Berger JM. The MukF subunit of Escherichia coli condensin: architecture and functional relationship to kleisins. The EMBO Journal. 2005;24(11):1921-30-30.

43. Fernández X, Díaz-Ingelmo O, Martínez-García B, Roca J. Chromatin regulates DNA torsional energy via topoisomerase II-mediated relaxation of positive supercoils. The EMBO Journal. 2014;33(13):1492-501.

44. Fischer M, Dang CV, DeCaprio JA. Chapter 17 - Control of Cell Division. In: Hoffman R, Benz EJ, Silberstein LE, Heslop HE, Weitz JI,

Anastasi J, et al., editors. Hematology (Seventh Edition): Elsevier; 2018. p. 176-85.

45. Flemming W. Zellsubstanz, kern und zelltheilung: Vogel; 1882.

46. Gaikwad M, Konkimalla VB, Salunke-Gawali S. Metal complexes as topoisomerase inhibitors. Inorganica Chimica Acta. 2022;542:121089.

47. Gilbert N, Allan J. Supercoiling in DNA and chromatin. Current Opinion in Genetics & Development. 2014;25:15-21.

48. Gligoris T, Löwe J. Structural Insights into Ring Formation of Cohesin and Related Smc Complexes. Trends in Cell Biology. 2016;26(9):680-93.

49. Gligoris TG, Scheinost JC, Bürmann F, Petela N, Chan KL, Uluocak P, et al. Closing the cohesin ring: structure and function of its Smc3-kleisin interface. Science. 2014;346(6212):963-7.

50. Gloyd M, Ghirlando R, Guarné A. The Role of MukE in Assembling a Functional MukBEF Complex. Journal of Molecular Biology. 2011;412(4):578-90.

51. GM C. The Origin and Evolution of Cells. In: Associates S, editor. The Cell: A Molecular Approach 2nd edition. 2nd Edition ed. National Library of Medicine: National Library of Medicine; 2000.

52. GM C. Cell Proliferation in Development and Differentiation. The Cell: A Molecular Approach. 2000.

53. GM. C. The Eukaryotic Cell Cycle. In: Associates S, editor. The Cell: A Molecular Approach. 2nd Edition ed. National Library of Medicine: National Library of Medicine; 2000.

54. Gottlieb SF GA, Tegay DH. Genetics, Meiosis. StatPearls Publishing. 2023.

55. Gruber S, Arumugam P, Katou Y, Kuglitsch D, Helmhart W, Shirahige K, et al. Evidence that Loading of Cohesin Onto Chromosomes Involves Opening of Its SMC Hinge. Cell. 2006;127(3):523-37.

56. Guacci V, Koshland D. Cohesin-independent segregation of sister chromatids in budding yeast. Mol Biol Cell. 2012;23(4):729-39.

57. Guacci V, Koshland D, Strunnikov A. A direct link between sister chromatid cohesion and chromosome condensation revealed through the analysis of MCD1 in S. cerevisiae. Cell. 1997;91(1):47-57.

58. Guacci V, Stricklin J, Bloom MS, Guō X, Bhatter M, Koshland D. A novel mechanism for the establishment of sister chromatid cohesion by the ECO1 acetyltransferase. Mol Biol Cell. 2015;26(1):117-33.

59. Guo MS, Kawamura R, Littlehale ML, Marko JF, Laub MT. High-resolution, genome-wide mapping of positive supercoiling in chromosomes. eLife. 2021;10:e67236.

60. Haering CH, Farcas A-M, Arumugam P, Metson J, Nasmyth K. The cohesin ring concatenates sister DNA molecules. Nature. 2008;454(7202):297-301.

61. Haering CH, Löwe J, Hochwagen A, Nasmyth K. Molecular Architecture of SMC Proteins and the Yeast Cohesin Complex. Molecular Cell. 2002;9(4):773-88.

62. Haering CH, Schoffnegger D, Nishino T, Helmhart W, Nasmyth K, Löwe J. Structure and Stability of Cohesin's Smc1-Kleisin Interaction. Molecular Cell. 2004;15(6):951-64.

63. Hagting A, Den Elzen N, Vodermaier HC, Waizenegger IC, Peters JM, Pines J. Human securin proteolysis is controlled by the spindle checkpoint and reveals when the APC/C switches from activation by Cdc20 to Cdh1. J Cell Biol. 2002;157(7):1125-37.

64. Hartman T, Stead K, Koshland D, Guacci V. Pds5p is an essential chromosomal protein required for both sister chromatid cohesion and condensation in Saccharomyces cerevisiae. J Cell Biol. 2000;151(3):613-26.

65. Hauf S, Roitinger E, Koch B, Dittrich CM, Mechtler K, Peters J-M. Dissociation of Cohesin from Chromosome Arms and Loss of Arm Cohesion during Early Mitosis Depends on Phosphorylation of SA2. PLOS Biology. 2005;3(3):e69.

66. Hauf S, Waizenegger IC, Peters J-M. Cohesin Cleavage by Separase Required for Anaphase and Cytokinesis in Human Cells. Science. 2001;293(5533):1320-3.

67. Hirano M, Hirano T. Opening Closed Arms: Long-Distance Activation of SMC ATPase by Hinge-DNA Interactions. Molecular Cell. 2006;21(2):175-86.

68. Hirano T, Kobayashi R, Hirano M. Condensins, Chromosome Condensation Protein Complexes Containing XCAP-C, XCAP-E and a Xenopus Homolog of the Drosophila Barren Protein. Cell. 1997;89(4):511-21.

69. Hirano T, Mitchison TJ. A heterodimeric coiled-coil protein required for mitotic chromosome condensation in vitro. Cell. 1994;79(3):449-58.

70. Hoess RH, Ziese M, Sternberg N. P1 site-specific recombination: nucleotide sequence of the recombining sites. Proc Natl Acad Sci U S A. 1982;79(11):3398-402.

71. Holzmann J, Politi AZ, Nagasaka K, Hantsche-Grininger M, Walther N, Koch B, et al. Absolute quantification of cohesin, CTCF and their regulators in human cells. Elife. 2019;8.

72. Hu B, Itoh T, Mishra A, Katoh Y, Chan KL, Upcher W, et al. ATP hydrolysis is required for relocating cohesin from sites occupied by its Scc2/4 loading complex. Curr Biol. 2011;21(1):12-24.

73. Hu B, Petela N, Kurze A, Chan KL, Chapard C, Nasmyth K. Biological chromodynamics: a general method for measuring protein occupancy across the genome by calibrating ChIP-seq. Nucleic Acids Res. 2015;43(20):e132.

74. Hudson B, Vinograd J. Catenated Circular DNA Molecules in HeLa Cell Mitochondria. Nature. 1967;216(5116):647-52.

75. Icard P, Fournel L, Wu Z, Alifano M, Lincet H. Interconnection between Metabolism and Cell Cycle in Cancer. Trends in Biochemical Sciences. 2019;44(6):490-501.

76. Irniger S, Piatti S, Michaelis C, Nasmyth K. Genes involved in sister chromatid separation are needed for b-type cyclin proteolysis in budding yeast. Cell. 1995;81(2):269-77.

77. Ivanov D, Schleiffer A, Eisenhaber F, Mechtler K, Haering CH, Nasmyth K. Eco1 Is a Novel Acetyltransferase that Can Acetylate Proteins Involved in Cohesion. Current Biology. 2002;12(4):323-8.

78. Jallepalli PV, Lengauer C. Chromosome segregation and cancer: cutting through the mystery. Nature Reviews Cancer. 2001;1(2):109-17.

79. Johnson LF. G1 events and the regulation of genes for S-phase enzymes. Current Opinion in Cell Biology. 1992;4(2):149-54.

80. Kim E, Gonzalez AM, Pradhan B, van der Torre J, Dekker C. Condensin-driven loop extrusion on supercoiled DNA. Nature Structural & Molecular Biology. 2022;29(7):719-27.

81. Kreuzer KN, Cozzarelli NR. Formation and resolution of DNA catenanes by DNA gyrase. Cell. 1980;20(1):245-54.

82. Kueng S, Hegemann B, Peters BH, Lipp JJ, Schleiffer A, Mechtler K, et al. Wapl Controls the Dynamic Association of Cohesin with Chromatin. Cell. 2006;127(5):955-67.

83. Lavrukhin OV, Fortune JM, Wood TG, Burbank DE, Van Etten JL, Osheroff N, et al. Topoisomerase II from Chlorella Virus PBCV-1: CHARACTERIZATION OF THE SMALLEST KNOWN TYPE II TOPOISOMERASE *. Journal of Biological Chemistry. 2000;275(10):6915-21.

84. Lee B-G, Roig Maurici B, Jansma M, Petela N, Metson J, Nasmyth K, et al. Crystal Structure of the Cohesin Gatekeeper Pds5 and in Complex with Kleisin Scc1. Cell Reports. 2016;14(9):2108-15.

85. Lengronne A, Katou Y, Mori S, Yokobayashi S, Kelly GP, Itoh T, et al. Cohesin relocation from sites of chromosomal loading to places of convergent transcription. Nature. 2004;430(6999):573-8.

86. Lengronne A, McIntyre J, Katou Y, Kanoh Y, Hopfner K-P, Shirahige K, et al. Establishment of Sister Chromatid Cohesion at the S. cerevisiae Replication Fork. Molecular Cell. 2006;23(6):787-99.

87. Li S, Yue Z, Tanaka TU. Smc3 Deacetylation by Hos1 Facilitates Efficient Dissolution of Sister Chromatid Cohesion during Early Anaphase. Mol Cell. 2017;68(3):605-14.e4.

88. Liu LF, Liu C-C, Alberts BM. T4 DNA topoisomerase: a new ATP-dependent enzyme essential for initiation of T4 bacteriophage DNA replication. Nature. 1979;281(5731):456-61.

89. Liu LF, Liu C-C, Alberts BM. Type II DNA topoisomerases: Enzymes that can unknot a topologically knotted DNA molecule via a reversible double-strand break. Cell. 1980;19(3):697-707.

90. Lopez-Serra L, Kelly G, Patel H, Stewart A, Uhlmann F. The Scc2-Scc4 complex acts in sister chromatid cohesion and transcriptional regulation by maintaining nucleosome-free regions. Nat Genet. 2014;46(10):1147-51.

91. Lopez-Serra L, Lengronne A, Borges V, Kelly G, Uhlmann F. Budding Yeast Wapl Controls Sister Chromatid Cohesion Maintenance and Chromosome Condensation. Current Biology. 2013;23(1):64-9.

92. Losada A, Yokochi T, Kobayashi R, Hirano T. Identification and characterization of SA/Scc3p subunits in the Xenopus and human cohesin complexes. J Cell Biol. 2000;150(3):405-16.

93. Lotz C, Lamour V. The interplay between DNA topoisomerase 2α post-translational modifications and drug resistance. Cancer Drug Resist. 2020;3(2):149-60.

94. Lyons NA, Morgan DO. Cdk1-dependent destruction of Eco1 prevents cohesion establishment after S phase. Mol Cell. 2011;42(3):378-89.

95. Ma J, Bai L, Wang MD. Transcription under torsion. Science. 2013;340(6140):1580-3.

96. Magnan D, Bates D. Regulation of DNA Replication Initiation by Chromosome Structure. J Bacteriol. 2015;197(21):3370-7.

97. Mäkelä J, Sherratt DJ. Organization of the Escherichia coli Chromosome by a MukBEF Axial Core. Mol Cell. 2020;78(2):250-60.e5.

98. Marko JF, De Los Rios P, Barducci A, Gruber S. DNA-segment-capture model for loop extrusion by structural maintenance of chromosome (SMC) protein complexes. Nucleic Acids Res. 2019;47(13):6956-72.

99. Marko JF, Siggia ED. Statistical mechanics of supercoiled DNA. Physical Review E. 1995;52(3):2912-38.

100. Marston AL, Amon A. Meiosis: cell-cycle controls shuffle and deal. Nature Reviews Molecular Cell Biology. 2004;5(12):983-97.

101. Martínez-García B, Fernández X, Díaz-Ingelmo O, Rodríguez-Campos A, Manichanh C, Roca J. Topoisomerase II minimizes DNA entanglements by

proofreading DNA topology after DNA strand passage. Nucleic Acids Res. 2014;42(3):1821-30.

102. McIntosh JR. Mitosis. Cold Spring Harb Perspect Biol. 2016;8(9).

103. Mori R, Oliferenko S. Cell Biology: An Open Solution for Closed Mitosis. Current Biology. 2020;30(16):R942-R4.

104. Morozova NE, Potysyeva AS, Vedyaykin AD. Organization and Role of Bacterial SMC, MukBEF, MksBEF, Wadjet, and RecN Complexes. Cell and Tissue Biology. 2024;18(2):115-27.

105. Muir Kyle W, Kschonsak M, Li Y, Metz J, Haering Christian H, Panne D. Structure of the Pds5-Scc1 Complex and Implications for Cohesin Function. Cell Reports. 2016;14(9):2116-26.

106. Muñoz S, Minamino M, Casas-Delucchi CS, Patel H, Uhlmann F. A Role for Chromatin Remodeling in Cohesin Loading onto Chromosomes. Mol Cell. 2019;74(4):664-73.e5.

107. Nasmyth K, Peters J-M, Uhlmann F. Splitting the Chromosome: Cutting the Ties That Bind Sister Chromatids. Science. 2000;288(5470):1379-84.

108. Naughton C, Avlonitis N, Corless S, Prendergast JG, Mati IK, Eijk PP, et al. Transcription forms and remodels supercoiling domains unfolding large-scale chromatin structures. Nature Structural & Molecular Biology. 2013;20(3):387-95.

109. Neuwald AF, Hirano T. HEAT Repeats Associated with Condensins, Cohesins, and Other Complexes Involved in Chromosome-Related Functions. Genome Research. 2000;10(10):1445-52.

110. Nudler E. RNA polymerase backtracking in gene regulation and genome instability. Cell. 2012;149(7):1438-45.

111. O'Connor C. Cell Division: Stages of Mitosis. Nature Education. 2008;1(1).

112. Ohkura H. Meiosis: an overview of key differences from mitosis. Cold Spring Harb Perspect Biol. 2015;7(5).

113. Onn I, Guacci V, Koshland DE. The zinc finger of Eco1 enhances its acetyltransferase activity during sister chromatid cohesion. Nucleic Acids Res. 2009;37(18):6126-34.

114. Palecek JJ, Gruber S. Kite Proteins: a Superfamily of SMC/Kleisin Partners Conserved Across Bacteria, Archaea, and Eukaryotes. Structure. 2015;23(12):2183-90.

115. Panizza S, Tanaka T, Hochwagen A, Eisenhaber F, Nasmyth K. Pds5 cooperates with cohesin in maintaining sister chromatid cohesion. Current Biology. 2000;10(24):1557-64.

116. Peng XP, Zhao X. The multi-functional Smc5/6 complex in genome protection and disease. Nature Structural & Molecular Biology. 2023;30(6):724-34.

117. Petela NJ, Gligoris TG, Metson J, Lee BG, Voulgaris M, Hu B, et al. Scc2 Is a Potent Activator of Cohesin's ATPase that Promotes Loading by Binding Scc1 without Pds5. Mol Cell. 2018;70(6):1134-48.e7.

118. Piskadlo E, Tavares A, Oliveira RA. Metaphase chromosome structure is dynamically maintained by condensin I-directed DNA (de)catenation. eLife. 2017;6:e26120.

119. Portugal J, Rodríguez-Campos A. T7 RNA Polymerase Cannot Transcribe Through a Highly Knotted DNA Template. Nucleic Acids Research. 1996;24(24):4890-4.

120. Pradhan B, Barth R, Kim E, Davidson IF, Bauer B, van Laar T, et al. SMC complexes can traverse physical roadblocks bigger than their ring size. Cell Reports. 2022;41(3).

121. Pradhan B, Kanno T, Umeda Igarashi M, Loke MS, Baaske MD, Wong JSK, et al. The Smc5/6 complex is a DNA loop-extruding motor. Nature. 2023;616(7958):843-8.

122. Roca J, Berger JM, Harrison SC, Wang JC. DNA transport by a type II topoisomerase: direct evidence for a two-gate mechanism. Proceedings of the National Academy of Sciences. 1996;93(9):4057-62.

123. Roca J, Wang JC. The capture of a DNA double helix by an ATP-dependent protein clamp: A key step in DNA transport by type II DNA topoisomerases. Cell. 1992;71(5):833-40.

124. Roca J, Wang JC. DNA transport by a type II DNA topoisomerase: Evidence in favor of a two-gate mechanism. Cell. 1994;77(4):609-16.

125. Rodríguez-Campos A. DNA Knotting Abolishes in Vitro Chromatin Assembly*. Journal of Biological Chemistry. 1996;271(24):14150-5.

126. Rosenberg LE, Rosenberg DD. Chapter 16 - The Genetics of Cancer. In: Rosenberg LE, Rosenberg DD, editors. Human Genes and Genomes. San Diego: Academic Press; 2012. p. 259-88.

127. Rowland BD, Roig MB, Nishino T, Kurze A, Uluocak P, Mishra A, et al. Building Sister Chromatid Cohesion: Smc3 Acetylation Counteracts an Antiestablishment Activity. Molecular Cell. 2009;33(6):763-74.

128. Rybenkov VV, Ullsperger C, Vologodskii AV, Cozzarelli NR. Simplification of DNA Topology Below Equilibrium Values by Type II Topoisomerases. Science. 1997;277(5326):690-3.

129. Sansam CL, Pezza RJ. Connecting by breaking and repairing: mechanisms of DNA strand exchange in meiotic recombination. Febs j. 2015;282(13):2444-57.

130. Sarkar R, Petrushenko ZM, Dawson DS, Rybenkov VV. Ycs4 Subunit of Saccharomyces cerevisiae Condensin Binds DNA and Modulates the Enzyme Turnover. Biochemistry. 2021;60(45):3385-97.

131. Sazer S, Lynch M, Needleman D. Deciphering the evolutionary history of open and closed mitosis. Curr Biol. 2014;24(22):R1099-103.

132. Schalbetter SA, Mansoubi S, Chambers AL, Downs JA, Baxter J. Fork rotation and DNA precatenation are restricted during DNA replication to prevent chromosomal instability. Proceedings of the National Academy of Sciences. 2015;112(33):E4565-E70.

133. Schalch T, Steiner FA. Structure of centromere chromatin: from nucleosome to chromosomal architecture. Chromosoma. 2017;126(4):443-55.

134. Schleiffer A, Kaitna S, Maurer-Stroh S, Glotzer M, Nasmyth K, Eisenhaber F. Kleisins: A Superfamily of Bacterial and Eukaryotic SMC Protein Partners. Molecular Cell. 2003;11(3):571-5.

135. Schmidt BH, Osheroff N, Berger JM. Structure of a topoisomerase II–DNA–nucleotide complex reveals a new control mechanism for ATPase activity. Nature Structural & Molecular Biology. 2012;19(11):1147-54.

136. Schmitt AD, Hu M, Ren B. Genome-wide mapping and analysis of chromosome architecture. Nature Reviews Molecular Cell Biology. 2016;17(12):743-55.

137. Schvartzman JB, Hernández P, Krimer DB, Dorier J, Stasiak A. Closing the DNA replication cycle: from simple circular molecules to supercoiled and knotted DNA catenanes. Nucleic Acids Res. 2019;47(14):7182-98.

138. Sen N, Leonard J, Torres R, Garcia-Luis J, Palou-Marin G, Aragón L. Physical Proximity of Sister Chromatids Promotes Top2-Dependent Intertwining. Molecular Cell. 2016;64(1):134-47.

139. Shishido K, Komiyama N, Ikawa S. Increased production of a knotted form of plasmid pBR322 DNA in Escherichia coli DNA topoisomerase mutants. Journal of Molecular Biology. 1987;195(1):215-8.

140. Sieber B, Coronas-Serna JM, Martin SG. A focus on yeast mating: From pheromone signaling to cell-cell fusion. Seminars in Cell & Developmental Biology. 2023;133:83-95.

141. Sogo JM, Stasiak A, Martínez-Robles MaL, Krimer DB, Hernández P, Schvartzman JB. Formation of knots in partially replicated DNA molecules11Edited by M. Yaniv. Journal of Molecular Biology. 1999;286(3):637-43.

142. Srinivasan M, Scheinost JC, Petela NJ, Gligoris TG, Wissler M, Ogushi S, et al. The Cohesin Ring Uses Its Hinge to Organize DNA Using Non-

topological as well as Topological Mechanisms. Cell. 2018;173(6):1508-19.e18.

143. Sternberg N, Hamilton D. Bacteriophage P1 site-specific recombination. I. Recombination between loxP sites. J Mol Biol. 1981;150(4):467-86.

144. Sun M, Nishino T, Marko JF. The SMC1-SMC3 cohesin heterodimer structures DNA through supercoiling-dependent loop formation. Nucleic Acids Research. 2013;41(12):6149-60.

145. Sundin O, Varshavsky A. Terminal stages of SV40 DNA replication proceed via multiply intertwined catenated dimers. Cell. 1980;21(1):103-14.

146. Sutani T, Kawaguchi T, Kanno R, Itoh T, Shirahige K. Budding Yeast Wpl1(Rad61)-Pds5 Complex Counteracts Sister Chromatid Cohesion-Establishing Reaction. Current Biology. 2009;19(6):492-7.

147. Takeda DY, Dutta A. DNA replication and progression through S phase. Oncogene. 2005;24(17):2827-43.

148. Tanaka T, Cosma MP, Wirth K, Nasmyth K. Identification of Cohesin Association Sites at Centromeres and along Chromosome Arms. Cell. 1999;98(6):847-58.

149. Tanaka T, Fuchs J, Loidl J, Nasmyth K. Cohesin ensures bipolar attachment of microtubules to sister centromeres and resists their precocious separation. Nature Cell Biology. 2000;2(8):492-9.

150. Timsit Y, Duplantier B, Jannink G, Sikorav J-L. Symmetry and chirality in topoisomerase II-DNA crossover recognition11Edited by T. Richmond. Journal of Molecular Biology. 1998;284(5):1289-99.

151. Tóth A, Ciosk R, Uhlmann F, Galova M, Schleiffer A, Nasmyth K. Yeast cohesin complex requires a conserved protein, Eco1p(Ctf7), to establish cohesion between sister chromatids during DNA replication. Genes Dev. 1999;13(3):320-33.

152. Uemura T, Ohkura H, Adachi Y, Morino K, Shiozaki K, Yanagida M. DNA topoisomerase II is required for condensation and separation of mitotic chromosomes in S. pombe. Cell. 1987;50(6):917-25.

153. Uhlmann F. Chromosome cohesion and segregation in mitosis and meiosis. Current Opinion in Cell Biology. 2001;13(6):754-61.

154. Uhlmann F, Lottspeich F, Nasmyth K. Sister-chromatid separation at anaphase onset is promoted by cleavage of the cohesin subunit Scc1. Nature. 1999;400(6739):37-42.

155. Uhlmann F, Nasmyth K. Cohesion between sister chromatids must be established during DNA replication. Current Biology. 1998;8(20):1095-102.

156. Uhlmann F, Wernic D, Poupart M-A, Koonin EV, Nasmyth K. Cleavage of Cohesin by the CD Clan Protease Separin Triggers Anaphase in Yeast. Cell. 2000;103(3):375-86.

157. Uusküla-Reimand L, Hou H, Samavarchi-Tehrani P, Rudan MV, Liang M, Medina-Rivera A, et al. Topoisomerase II beta interacts with cohesin and CTCF at topological domain borders. Genome Biol. 2016;17(1):182.

158. Uzbekov R, Prigent C. A Journey through Time on the Discovery of Cell Cycle Regulation. Cells. 2022;11(4).

159. Valdés A, Coronel L, Martínez-García B, Segura J, Dyson S, Díaz-Ingelmo O, et al. Transcriptional supercoiling boosts topoisomerase II-

mediated knotting of intracellular DNA. Nucleic Acids Res. 2019;47(13):6946-55.

160. Valdés A, Segura J, Dyson S, Martínez-García B, Roca J. DNA knots occur in intracellular chromatin. Nucleic Acids Res. 2018;46(2):650-60.

161. van Ruiten MS, van Gent D, Sedeño Cacciatore Á, Fauster A, Willems L, Hekkelman ML, et al. The cohesin acetylation cycle controls chromatin loop length through a PDS5A brake mechanism. Nature Structural & Molecular Biology. 2022;29(6):586-91.

162. Vondrova L, Kolesar P, Adamus M, Nociar M, Oliver AW, Palecek JJ. A role of the Nse4 kleisin and Nse1/Nse3 KITE subunits in the ATPase cycle of SMC5/6. Scientific Reports. 2020;10(1):9694.

163. Waizenegger IC, Hauf S, Meinke A, Peters J-M. Two Distinct Pathways Remove Mammalian Cohesin from Chromosome Arms in Prophase and from Centromeres in Anaphase. Cell. 2000;103(3):399-410.

164. Wang H-Z, Yang S-H, Li G-Y, Cao X. Subunits of human condensins are potential therapeutic targets for cancers. Cell Division. 2018;13(1):2.

165. Wang JC. Superhelical DNA. Trends in Biochemical Sciences. 1980;5(8):219-21.

166. Wang JC. DNA TOPOISOMERASES. Annual Review of Biochemistry. 1985;54(Volume 54, 1985):665-97.

167. Wang M, Robertson D, Zou J, Spanos C, Rappsilber J, Marston AL. Molecular mechanism targeting condensin for chromosome condensation. Embo j. 2025;44(3):705-35.

168. Wang Q, Mordukhova EA, Edwards AL, Rybenkov VV. Chromosome condensation in the absence of the non-SMC subunits of MukBEF. Journal of Bacteriology. 2006;188(12):4431-41.

169. Wang Y, Ji P, Liu J, Broaddus RR, Xue F, Zhang W. Centrosome-associated regulators of the G2/M checkpoint as targets for cancer therapy. Molecular Cancer. 2009;8(1):8.

170. Watson JD, Crick FHC. Molecular Structure of Nucleic Acids: A Structure for Deoxyribose Nucleic Acid. Nature. 1953;171(4356):737-8.

171. Weber SA, Gerton JL, Polancic JE, DeRisi JL, Koshland D, Megee PC. The kinetochore is an enhancer of pericentric cohesin binding. PLoS Biol. 2004;2(9):E260.

172. Wells JN, Gligoris TG, Nasmyth KA, Marsh JA. Evolution of condensin and cohesin complexes driven by replacement of Kite by Hawk proteins. Current Biology. 2017;27(1):R17-R8.

173. Worland ST, Wang JC. Inducible overexpression, purification, and active site mapping of DNA topoisomerase II from the yeast Saccharomyces cerevisiae. Journal of Biological Chemistry. 1989;264(8):4412-6.

174. Wutz G, Várnai C, Nagasaka K, Cisneros DA, Stocsits RR, Tang W, et al. Topologically associating domains and chromatin loops depend on cohesin and are regulated by CTCF, WAPL, and PDS5 proteins. Embo j. 2017;36(24):3573-99.

175. Xiong B, Lu S, Gerton JL. Hos1 Is a Lysine Deacetylase for the Smc3 Subunit of Cohesin. Current Biology. 2010;20(18):1660-5.

176. Yamamoto A, Guacci V, Koshland D. Pds1p, an inhibitor of anaphase in budding yeast, plays a critical role in the APC and checkpoint pathway(s). Journal of Cell Biology. 1996;133(1):99-110.

177. Zawadzka K, Zawadzki P, Baker R, Rajasekar KV, Wagner F, Sherratt DJ, et al. MukB ATPases are regulated independently by the N- and C-terminal domains of MukF kleisin. eLife. 2018;7:e31522.

178. Zhang H, Shi Z, Banigan EJ, Kim Y, Yu H, Bai X-c, et al. CTCF and R-loops are boundaries of cohesin-mediated DNA looping. Molecular Cell. 2023;83(16):2856-71.e8.

179. Zhang J, Shi X, Li Y, Kim B-J, Jia J, Huang Z, et al. Acetylation of Smc3 by Eco1 Is Required for S Phase Sister Chromatid Cohesion in Both Human and Yeast. Molecular Cell. 2008;31(1):143-51.

180. Zhou M. DNA sliding and loop formation by E. coli SMC complex: MukBEF. Biochem Biophys Rep. 2022;31:101297.